

DYNAMIC SEISMIC RESPONSE OF SKEWED AND CURVED INTEGRAL BRIDGES

Thesis Submitted by

SUBHAJIT PAUL

(M.E. Civil Engineering)

(University Roll no. - 002210402004)

(Examination Roll no. - M4CIV24004)

In partial fulfillment of the requirements for the award of degree of

MASTER OF ENGINEERING

IN

CIVIL ENGINEERING

Specialization:

STRUCTURAL ENGINEERING

Under the guidance of

Dr. Dipankar Chakravorty

DEPARTMENT OF CIVIL ENGINEERING

JADAVPUR UNIVERSITY

WEST BENGAL, KOLKATA – 700032

DEPARTMENT OF CIVIL ENGINEERING
FACULTY OF ENGINEERING AND TECHNOLOGY
JADAVPUR UNIVERSITY
KOLKATA – 700 032

CERTIFICATE OF RECOMMENDATION

This is to certify that the thesis entitled, “**DYNAMIC SEISMIC RESPONSE OF SKEWED AND CURVED INTEGRAL BRIDGES**” submitted by **Subhajit Paul**, Class Roll No. 002210402004, Registration No. 163457 of 2022-2023 in partial fulfilment of the requirements for the award of Master of Engineering degree in Civil Engineering with specialization in “**Structural Engineering**” at Jadavpur University, Kolkata is an authentic work carried out by him under my supervision and guidance.

I hereby recommend that the thesis be accepted in partial fulfilment of the requirements for awarding the degree of “**Master of Engineering in Civil Engineering**”.

Supervisor

(Dr. Dipankar Chakravorty)
Professor
Civil Engineering Department
Jadavpur University, Kolkata

Head of the Department

(Dr. Partha Bhattacharya)
Professor
Civil Engineering Department
Jadavpur University, Kolkata

Dean, FET

Prof. Dipak Laha
Jadavpur University, Kolkata

DEPARTMENT OF CIVIL ENGINEERING
FACULTY OF ENGINEERING AND TECHNOLOGY
JADAVPUR UNIVERSITY
KOLKATA, INDIA

CERTIFICATE OF APPROVAL

This thesis paper is hereby approved as a credible study of an engineering subject carried out and presented in a manner satisfactorily to warrant its acceptance as a pre-requisite for the degree for which it has been submitted. It is understood that, by this approval, the undersigned do not necessarily endorse or approve any statement made, opinion expressed or conclusion drawn therein but approved the thesis paper only for the purpose for which it is submitted.

Committee of Thesis Paper Examiners

Signature of Examiner

Signature of Examiner

DECLARATION

I, Subhajit Paul, Master of Engineering in Civil Engineering (Structure Engineering), Jadavpur University, Faculty of Engineering and Technology, hereby declare that the work being presented in the thesis work titled, “Dynamic Seismic Response of Skewed and Curved Integral Bridges”, is an authentic record of work that has been carried out in the Department of Civil Engineering, Jadavpur University, Kolkata under the guidance of Dr. Dipankar Chakravorty. The work contained in this thesis has not yet been submitted in parts or full to any other university or institute or professional body for award of any degree or diploma or any fellowship.

Place: Kolkata

Date:

Subhajit Paul
Roll No.: 002210402004
Registration no.: 163457 of 2022-2023

ACKNOWLEDGEMENT

I gratefully acknowledge the resourceful guidance, active supervision and constant encouragement of our reverent Professor **Dr. Dipankar Chakravorty** of the Department of Civil Engineering, Jadavpur University, Kolkata, who despite his other commitments could find time to help me in bringing this thesis to its present shape. I do convey my sincere thanks and gratitude to him.

I also thankfully acknowledge my gratefulness to all Professors and staff of the Civil Engineering Department, Jadavpur University, Kolkata, for extending all facilities to carry out the present study.

I also thankfully acknowledge the assistance and encouragement received from my family members, friends and others during the preparation of this Thesis.

.....

SUBHAJIT PAUL
ROLL NO - 002210402004
M.E. CIVIL ENGINEERING
Specialization: STRUCTURAL ENGINEERING
JADAVPUR UNIVERSITY
KOLKATA- 700032

CONTENTS

Chapter – 1: Introduction.....	13
1.1 General	13
1.2 History of bridge engineering.....	13
1.3 Importance of bridge	13
1.4 Bridge geometry	14
1.5 Curvature in bridge.....	14
1.6 Skewed bridge	15
1.7 Integral bridge	15
1.8 Integral bridge practices in various parts of the world	15
1.9 Integral bridge characteristics.....	16
1.10 Behavior of integral bridges under earthquake loads and soil structure interaction	17
Chapter– 2: Literature review.....	19
2.1 Literature review on straight integral bridges.....	19
2.2 Literature review on skewed integral bridges.....	22
2.3 Literature review on curved integral bridges.....	25
2.4 Critical discussion	27
2.5 Scope of the present study	28
Chapter – 3: Modelling and analysis	30
3.1 Flowchart of methodology.....	30
3.2 Finite element modelling.....	30
3.3 Modelling the structure.....	31
3.4 Element type and properties in Midas Civil	33
3.5 Soil properties and springs	36
3.6 Dynamic analysis.....	38
3.7 Eigenvalue analysis	38
3.8 Time history analysis.....	38
Chapter – 4: Results and discussion	40
4.1 Benchmark validation.....	40
4.1.1 Model validation.....	40
4.2 Numerical study of author’s own problems.....	41
4.2.1 Variation of dead load.....	42
4.2.2 Variation of time period	44
4.2.3 Variation of base reaction	46
4.2.4 Variation of the moment at abutment in longitudinal seismic condition.....	52
4.2.5 Variation of the moment at bent columns in longitudinal seismic condition	58
4.2.6 Variation of the moment at abutment in transverse seismic condition.....	65
4.2.7 Variation of the moment at bent columns in transverse seismic condition	71
Chapter – 5: Conclusions.....	78
5.1 General	78
5.1.1 Time period.....	78
5.1.2 Base reaction	79

5.1.3	Moment and torsion of abutment	80
5.1.4	Moment and torsion of bent columns.....	81
5.2	Future scope of study.....	83
References	84

List of Figures

Fig. 1.	Curved bridge	14
Fig. 2.	3D Types of skew deck.	15
Fig. 3.	Elevation of integral bridge	16
Fig. 4.	Elevation fundamental differences between conventional bridge (left) and integral bridge construction (right)	16
Fig. 5.	Idealization of integral bridge	16
Fig. 6.	Abutment wall: active and passive states (Alizadeh, et al., 2010)	17
Fig. 7.	Soil spring idealization of the integral bridge.	18
Fig. 8.	Winkler spring approach.	18
Fig. 9.	Flow chart of the study.	31
Fig. 10.	Elevation of the bridge.	32
Fig. 11.	Section of the superstructure	32
Fig. 12.	3D view of straight integral bridge.	33
Fig. 13.	Elevation of straight integral bridge.	34
Fig. 14.	3D view of skewed integral bridge.	34
Fig. 15.	Elevation of skewed integral bridge.	35
Fig. 16.	3D view of curved integral bridge.	35
Fig. 17.	Elevation of curved integral bridge.	36
Fig. 18.	Pile spring.	37
Fig. 19.	Pile spring in Midas Civil.	37
Fig. 20.	Time history graph longitudinal direction.	39
Fig. 21.	Time history graph transverse direction.	39
Fig. 22.	Cross section of benchmarking bridge.	40
Fig. 23.	Natural time period vs sa/g.	79

List of Graphs

Variation of dead load

Graph 1.	Variation of dead load with respect to skew angle for bridge with open foundation.	43
Graph 2.	Variation of dead load with respect to skew angle for bridge with pile foundation.	43
Graph 3.	Variation of dead load with respect to curvature for bridge with pile foundation.	44
Graph 4.	Variation of dead load with respect to curvature for bridge with open foundation.	44

Variation of time period

Graph 5.	Comparison on variation of time period w.r.t. skew for bridge with pile foundation and with and without earth behind abutment.	45
Graph 6.	Comparison on variation of time period w.r.t. skew for bridge with open foundation and with and without earth behind abutment.	45
Graph 7.	Comparison on variation of time period w.r.t. curvature for bridge with pile foundation and with and without earth behind abutment.	45
Graph 8.	Comparison on variation of time period w.r.t. curvature for bridge with open foundation and with and without earth behind abutment.	45

Variation of base reaction

Graph 9.	Comparison on longitudinal base shear w.r.t. skew with pile foundation and with or without earth behind abutment.	46
Graph 10.	Comparison on longitudinal base shear/Vertical reaction w.r.t. skew with pile foundation and with or without earth behind abutment.	46

Graph 11. Comparison on transverse base shear w.r.t. skew with pile foundation and with or without earth behind abutment.	46
Graph 12. Comparison on transverse base shear/vertical reaction w.r.t. skew with pile foundation and with or without earth behind abutment.	46
Graph 13. Comparison on longitudinal base shear w.r.t. skew with open foundation and with or without earth behind abutment.	47
Graph 14. Comparison on longitudinal/vertical base shear w.r.t. skew with open foundation and with or without earth behind abutment.	47
Graph 15. Comparison on transverse base shear w.r.t. skew with open foundation and with or without earth behind abutment.	47
Graph 16. Comparison on transverse/vertical base shear w.r.t. skew with open foundation and with or without earth behind abutment.	47
Graph 17. Variation on longitudinal base shear w.r.t. skew with pile foundation and with or without earth behind abutment.	47
Graph 18. Variation on longitudinal base shear/vertical base shear w.r.t. skew with pile foundation and with or without earth behind abutment.	47
Graph 19. Variation on transverse base shear w.r.t. skew with pile foundation and with or without earth behind abutment.	48
Graph 20. Variation on transverse base shear/vertical base shear w.r.t. skew with pile foundation and with or without earth behind abutment.	48
Graph 21. Variation on longitudinal base shear w.r.t. skew with open foundation and with or without earth behind abutment.	48
Graph 22. Variation on longitudinal base shear/vertical base shear w.r.t. skew with open foundation and with or without earth behind abutment.	48
Graph 23. Variation on transverse base shear w.r.t. skew with open foundation and with or without earth behind abutment.	48
Graph 24. Variation on transverse base shear/vertical base shear w.r.t. skew with open foundation and with or without earth behind abutment.	48
Graph 25. Variation on longitudinal base shear w.r.t. curvature with pile foundation and with or without earth behind abutment.	49
Graph 26. Variation on longitudinal base shear/vertical base shear w.r.t. curvature with pile foundation and with or without earth behind abutment.	49
Graph 27. Variation on transverse base shear w.r.t. curvature with pile foundation and with or without earth behind abutment.	49
Graph 28. Variation on transverse base shear/vertical base shear w.r.t. curvature with pile foundation and with or without earth behind abutment.	49
Graph 29. Variation on longitudinal base shear w.r.t. curvature with open foundation and with or without earth behind abutment.	49
Graph 30. Variation on longitudinal base shear/vertical base shear w.r.t. curvature with open foundation and with or without earth behind abutment.	49
Graph 31. Variation on transverse base shear w.r.t. curvature with open and open foundation and with or without earth behind abutment.	50
Graph 32. Variation on transverse base shear /vertical base shear w.r.t. curvature with open foundation and with or without earth behind abutment.	50
Graph 33. Variation on longitudinal base shear/vertical base shear w.r.t. curvature with pile foundation and with or without earth behind abutment.	50
Graph 34. Variation on transverse base shear/vertical base shear w.r.t. curvature with pile foundation and with or without earth behind abutment.	50
Graph 35. Variation on longitudinal base shear/vertical base shear w.r.t. curvature with open foundation and with or without earth behind abutment.	51
Graph 36. Variation on transverse base shear/vertical base shear w.r.t. curvature with open foundation and with or without earth behind abutment.	51

Variation of the moment at abutment in longitudinal seismic condition

Graph 37. Variation of longitudinal moment at top of abutment w.r.t. skew with pile foundation with or with earth behind abutment.	52
Graph 38. Variation of longitudinal moment at top of abutment w.r.t. skew with open foundation with or without earth behind abutment.	52

Graph 39. Variation of longitudinal moment at top of abutment w.r.t. curvature with pile foundation with or with earth behind abutment.	52
Graph 40. Variation of longitudinal moment at top of abutment w.r.t. curvature with open foundation with or without earth behind abutment.	52
Graph 41. Variation of transverse moment at top of abutment w.r.t. skew with pile foundation with or with earth behind abutment.	53
Graph 42. Variation of transverse moment at top of abutment w.r.t. skew with open foundation with or without earth behind abutment.	53
Graph 43. Variation of transverse moment at top of abutment w.r.t. curvature with pile foundation with or with earth behind abutment.	53
Graph 44. Variation of transverse moment at top of abutment w.r.t. curvature with open foundation with or without earth behind abutment.	53
Graph 45. Variation of torsion at top of abutment w.r.t. skew with pile foundation with or with earth behind abutment.	54
Graph 46. Variation of torsion at top of abutment w.r.t. skew with open foundation with or without earth behind abutment.	54
Graph 47. Variation of torsion at top of abutment w.r.t. curvature with pile foundation with or with earth behind abutment.	54
Graph 48. Variation of torsion at top of abutment w.r.t. curvature with open foundation with or without earth behind abutment.	54
Graph 49. Variation of longitudinal moment at bottom of abutment w.r.t. skew with pile foundation with or with earth behind abutment.	55
Graph 50. Variation of longitudinal moment at bottom of abutment w.r.t. skew with open foundation with or without earth behind abutment.	55
Graph 51. Variation of longitudinal moment at bottom of abutment w.r.t. curvature with pile foundation with or with earth behind abutment.	55
Graph 52. Variation of longitudinal moment at bottom of abutment w.r.t. curvature with open foundation with or without earth behind abutment.	55
Graph 53. Variation of transverse moment at bottom of abutment w.r.t. skew with pile foundation with or with earth behind abutment.	56
Graph 54. Variation of transverse moment at bottom of abutment w.r.t. skew with open foundation with or without earth behind abutment.	56
Graph 55. Variation of transverse moment at bottom of abutment w.r.t. curvature with pile foundation with or with earth behind abutment.	56
Graph 56. Variation of transverse moment at bottom of abutment w.r.t. curvature with open foundation with or without earth behind abutment.	56
Graph 57. Variation of torsion at bottom of abutment w.r.t. skew with pile foundation with or with earth behind abutment.	57
Graph 58. Variation of torsion at bottom of abutment w.r.t. skew with open foundation with or without earth behind abutment.	57
Graph 59. Variation of torsion at bottom of abutment w.r.t. curvature with pile foundation with or with earth behind abutment.	57
Graph 60. Variation of torsion at bottom of abutment w.r.t. curvature with open foundation with or without earth behind abutment.	57

Variation of the moment at bent columns in longitudinal seismic condition

Graph 61. Variation of longitudinal moment at top of bent columns w.r.t. skew with pile foundation with or with earth behind abutment.	58
Graph 62. Variation of longitudinal moment at top of bent columns w.r.t. skew with open foundation with or without earth behind abutment.	58
Graph 63. Variation of longitudinal moment at top of bent columns w.r.t. curvature with pile foundation with or with earth behind abutment.	59
Graph 64. Variation of longitudinal moment at top of bent columns w.r.t. curvature with open foundation with or without earth behind abutment.	59
Graph 65. Variation of transverse moment at top of bent columns w.r.t. skew with pile foundation with or with earth behind abutment.	59
Graph 66. Variation of transverse moment at top of bent columns w.r.t. skew with open foundation with or without earth behind abutment.	59

Graph 67. Variation of transverse moment at top of bent columns w.r.t. curvature with pile foundation with or with earth behind abutment.	60
Graph 68. Variation of transverse moment at top of bent columns w.r.t. curvature with open foundation with or without earth behind abutment.	60
Graph 69. Variation of torsion at top of bent columns w.r.t. skew with pile foundation with or with earth behind abutment.	60
Graph 70. Variation of torsion at top of bent columns w.r.t. skew with open foundation with or without earth behind abutment.	60
Graph 71. Variation of torsion at top of bent columns w.r.t. curvature with pile foundation with or with earth behind abutment.	61
Graph 72. Variation of torsion at top of bent columns w.r.t. curvature with open foundation with or without earth behind abutment.	61
Graph 73. Variation of longitudinal moment at bottom of bent columns w.r.t. skew with pile foundation with or with earth behind abutment.	61
Graph 74. Variation of longitudinal moment at bottom of bent columns w.r.t. skew with open foundation with or without earth behind abutment.	61
Graph 75. Variation of longitudinal moment at bottom of bent columns w.r.t. curvature with pile foundation with or with earth behind abutment.	62
Graph 76. Variation of longitudinal moment at bottom of bent columns w.r.t. curvature with open foundation with or without earth behind abutment.	62
Graph 77. Variation of transverse moment at bottom of bent columns w.r.t. skew with pile foundation with or with earth behind abutment.	62
Graph 78. Variation of transverse moment at bottom of bent columns w.r.t. skew with open foundation with or without earth behind abutment.	62
Graph 79. Variation of transverse moment at bottom of bent columns w.r.t. curvature with pile foundation with or with earth behind abutment.	63
Graph 80. Variation of transverse moment at bottom of bent columns w.r.t. curvature with open foundation with or without earth behind abutment.	63
Graph 81. Variation of torsion at bottom of bent columns w.r.t. skew with pile foundation with or with earth behind abutment.	63
Graph 82. Variation of torsion at bottom of bent columns w.r.t. skew with open foundation with or without earth behind abutment.	63
Graph 83. Variation of torsion at bottom of bent columns w.r.t. curvature with pile foundation with or with earth behind abutment.	64
Graph 84. Variation of torsion at bottom of bent columns w.r.t. curvature with open foundation with or without earth behind abutment.	64

Variation of the moment at abutment in transverse seismic condition

Graph 85. Variation of longitudinal moment at top of abutment w.r.t. skew with pile foundation with or with earth behind abutment.	65
Graph 86. Variation of longitudinal moment at top of abutment w.r.t. skew with open foundation with or without earth behind abutment.	65
Graph 87. Variation of longitudinal moment at top of abutment w.r.t. curvature with pile foundation with or with earth behind abutment.	65
Graph 88. Variation of longitudinal moment at top of abutment w.r.t. curvature with open foundation with or without earth behind abutment.	65
Graph 89. Variation of transverse moment at top of abutment w.r.t. skew with pile foundation with or with earth behind abutment.	66
Graph 90. Variation of transverse moment at top of abutment w.r.t. skew with open foundation with or without earth behind abutment.	66
Graph 91. Variation of transverse moment at top of abutment w.r.t. curvature with pile foundation with or with earth behind abutment.	66
Graph 92. Variation of transverse moment at top of abutment w.r.t. curvature with open foundation with or without earth behind abutment.	66
Graph 93. Variation of torsion at top of abutment w.r.t. skew with pile foundation with or with earth behind abutment.	67
Graph 94. Variation of torsion at top of abutment w.r.t. skew with open foundation with or without earth behind abutment.	67

Graph 95. Variation of torsion at top of abutment w.r.t. curvature with pile foundation with or with earth behind abutment.	67
Graph 96. Variation of torsion at top of abutment w.r.t. curvature with pile foundation with open foundation with or without earth.	67
Graph 97. Variation of longitudinal moment at bottom of abutment w.r.t. skew with pile foundation with or with earth behind abutment.	68
Graph 98. Variation of longitudinal moment at bottom of abutment w.r.t. skew with open foundation with or without earth behind abutment.	68
Graph 99. Variation of longitudinal moment at bottom of abutment w.r.t. curvature with pile foundation with or with earth behind abutment.	68
Graph 100. Variation of longitudinal moment at bottom of abutment w.r.t. curvature with open foundation with or without earth behind abutment.	68
Graph 101. Variation of transverse moment at bottom of abutment w.r.t. skew with pile foundation with or with earth behind abutment.	69
Graph 102. Variation of transverse moment at bottom of abutment w.r.t. skew with open foundation with or without earth behind abutment.	69
Graph 103. Variation of transverse moment at bottom of abutment w.r.t. curvature with pile foundation with or with earth behind abutment.	69
Graph 104. Variation of transverse moment at bottom of abutment w.r.t. curvature with open foundation with or without earth behind abutment.	69
Graph 105. Variation of torsion at bottom of abutment w.r.t. skew with pile foundation with or with earth behind abutment.	70
Graph 106. Variation of torsion at bottom of abutment w.r.t. skew with open foundation with or without earth behind abutment.	70
Graph 107. Variation of torsion at bottom of abutment w.r.t. curvature with pile foundation with or with earth behind abutment.	70
Graph 108. Variation of torsion at bottom of abutment w.r.t. curvature with open foundation with or without earth behind abutment.	70

Variation of the moment at bent columns in transverse seismic condition

Graph 109. Variation of longitudinal moment at top of bent columns w.r.t. skew with pile foundation with or with earth behind abutment.	71
Graph 110. Variation of longitudinal moment at top of bent columns w.r.t. skew with open foundation with or without earth behind abutment.	71
Graph 111. Variation of longitudinal moment at top of bent columns w.r.t. curvature with pile foundation with or with earth behind abutment.	72
Graph 112. Variation of longitudinal moment at top of bent columns w.r.t. curvature with open foundation with or without earth behind abutment.	72
Graph 113. Variation of transverse moment at top of bent columns w.r.t. skew with pile foundation with or with earth behind abutment.	72
Graph 114. Variation of transverse moment at top of bent columns w.r.t. skew with open foundation with or without earth behind abutment.	72
Graph 115. Variation of transverse moment at top of bent columns w.r.t. curvature with pile foundation with or with earth behind abutment.	73
Graph 116. Variation of transverse moment at top of bent columns w.r.t. curvature with open foundation with or without earth behind abutment.	73
Graph 117. Variation of torsion at top of bent columns w.r.t. skew with pile foundation with or with earth behind abutment.	73
Graph 118. Variation of torsion at top of bent columns w.r.t. skew with open foundation with or without earth behind abutment.	73
Graph 119. Variation of torsion at top of bent columns w.r.t. curvature with pile foundation with or with earth behind abutment.	74
Graph 120. Variation of torsion at top of bent columns w.r.t. curvature with open foundation with or without earth behind abutment.	74
Graph 121. Variation of longitudinal moment at bottom of bent columns w.r.t. skew with pile foundation with or with earth behind abutment.	74
Graph 122. Variation of longitudinal moment at bottom of bent columns w.r.t. skew with open foundation with or without earth behind abutment.	74

Graph 123. Variation of longitudinal moment at bottom of bent columns w.r.t. curvature with pile foundation with or with earth behind abutment.	75
Graph 124. Variation of longitudinal moment at bottom of bent columns w.r.t. curvature with open foundation with or without earth behind abutment.	75
Graph 125. Variation of transverse moment at bottom of bent columns w.r.t. skew with pile foundation with or with earth behind abutment.	75
Graph 126. Variation of transverse moment at bottom of bent columns w.r.t. skew with open foundation with or without earth behind abutment.	75
Graph 127. Variation of transverse moment at bottom of bent columns w.r.t. curvature with pile foundation with or with earth behind abutment.	76
Graph 128. Variation of transverse moment at bottom of bent columns w.r.t. curvature with open foundation with or without earth behind abutment.	76
Graph 129. Variation of torsion at bottom of bent columns w.r.t. skew with pile foundation with or with earth behind abutment.	76
Graph 130. Variation of torsion at bottom of bent columns w.r.t. skew with open foundation with or without earth behind abutment.	76
Graph 131. Variation of torsion at bottom of bent columns w.r.t. curvature with pile foundation with or with earth behind abutment.	77
Graph 132. Variation of torsion at bottom of bent columns w.r.t. curvature with open foundation with or without earth behind abutment.	77

List of Tables

Table 1. Benchmarking results comparison.	41
Table 2. List of analysis models.	42

ABSTRACT

Road alignment, including bridge geometry in the plan, is influenced by multiple factors such as vehicle speed, existing road alignment, land availability, budget constraints, and more. These practical considerations often lead to the design and construction of skewed and curved bridges. Ensuring the seismic performance of bridges is vital for maintaining uninterrupted traffic flow over their considerable lifespan. Bridge construction involves specialized skills, significant costs, and labour-intensive processes, making it imperative to ensure their longevity for economic reasons. Integral bridges, known as lightweight and stable structures, are recommended by IRC: SP: 114 – 2018 for regions prone to high seismic activity.

While numerous analytical and experimental studies exist on straight integral bridges, research on skewed and curved integral bridges is limited. Therefore, this study aims to investigate the impact of various parameters such as central angle, radius of curvature for curved bridges, and skew angle for skewed bridges on crucial design parameters like time period, bending moment, torsional moment, and support reactions. Numerical analysis results generated using Midas Civil software are interpreted from a practical engineering perspective to derive meaningful recommendation which would help in design of curved and skewed integral bridges. An indication is also provided that codal recommendation of restricting skewness to 30° might be over-conservative. Thus, this study aims at proposing design guidelines for abutment and bents in integral bridges considering the cases where there is no backfill and when backfill exists. Additionally, the study outlines future research possibilities in this area.

INTRODUCTION

1.1 General

A bridge serves as a vital structure facilitating the passage of roads, paths, railways, and other transportation routes over obstacles such as rivers, water bodies, valleys, or roads without impeding the flow beneath. Its primary function is to provide a seamless traversal over hindrances that would otherwise pose significant challenges or barriers to crossing. Bridges come in diverse designs tailored to specific purposes and adaptable to varying conditions. Their shapes, sizes, and materials are determined by factors including the bridge's intended function, the topography of its location, the construction materials utilized, and the financial resources allocated for its construction.

Bridges are categorized under various terms:

- A structure carrying road or railway traffic, or a pipeline over a channel or valley is referred to simply as a bridge.
- If it carries traffic or a pipeline over a communication system such as roads or railways, it is termed a flyover or over-bridge.
- A viaduct is constructed over a busy locality, valley, dry or wetland, or as a flyover to accommodate vehicular traffic across multiple small spans.

1.2 History of Bridge Engineering

The history of bridge engineering is intricately linked with the progression of human civilization spanning over millennia. The earliest known bridge dates back to approximately 4000 B.C., attributed to the lake dwellers of Switzerland, who pioneered timber trestle construction for river crossings. Among the oldest surviving bridges is a pedestrian stone slab structure, over 2800 years old, spanning the Meles River in Smyrna, Turkey. Many ancient bridges were constructed by armies, with records indicating the use of floating bridges made from inflated skins as early as 800 B.C. One such bridge was built by King Cyrus in 556 B.C.

Around 320 B.C., Alexander the Great utilized floating bridges during his conquest of the East. India introduced wooden cantilever bridges in the Himalayas, employing planks of wood anchored by heavy stones at the banks, progressively extending towards the mid-stream.

From 200 B.C. to 260 A.D., Romans widely employed stone arches supported by massive piers. Following the decline of Rome, bridge construction in Europe was primarily driven by religious orders. Notable bridges from this period include the Pont d'Avignon over the river Rhone and the old London Bridge across the Thames.

During the medieval period, bridges were adorned with decorative and defensive elements, such as towers, chapels, and shops. The Rialto Bridge in Venice, built in 1591, exemplifies Renaissance-era bridge architecture. In the Middle Ages, numerous bridges were erected in European cities like London, Florence, and Venice. The first treatise on bridge engineering was published in 1714 by the French Engineer, Robert Guiter, marking the beginning of systematic bridge design.

The 19th century saw significant advancements in bridge engineering due to the production of alloy steel, cement, and heavy-load lifting equipment. Reinforced concrete bridges gained prominence in the 20th century for their construction versatility, economy, and low maintenance. These bridges can be moulded on-site to meet architectural requirements and utilize locally available materials, reducing transportation costs. The development of prestressed concrete further enhanced the capabilities of reinforced concrete bridges, leading to the construction of long-span bridges such as extra-dosed and cable-stayed bridges.

1.3 Importance of bridge

Bridges play a vital role in facilitating connectivity and accessibility across geographical barriers such as rivers, mountains, and other obstacles. They serve as crucial transportation infrastructure, enabling the efficient

movement of people and vehicles between different locations. By providing safe and efficient passage, bridges contribute to improved transportation networks, enhancing accessibility and connectivity for communities. Moreover, bridges are integral to the transportation sector, enabling buses, trains, and other vehicles to traverse distances swiftly and securely. This not only enhances transportation efficiency but also supports economic activities by facilitating the movement of goods and services, thereby reducing traffic congestion and improving overall logistics.

Furthermore, bridges hold significant importance for tourism and recreational activities, often serving as iconic landmarks that attract visitors and enhance the aesthetic appeal of an area. Their architectural beauty and functionality make them appealing destinations for both tourists and local residents alike.

From an economic standpoint, bridges are instrumental in driving economic growth and development in the regions they serve. They stimulate commerce, trade, and tourism, thus contributing to local economies and fostering regional development. Additionally, bridges play a crucial role in shaping social and political dynamics by connecting communities, fostering cultural exchange, and promoting unity and cohesion among diverse populations.

In summary, bridges hold multifaceted significance, encompassing economic, social, and political dimensions. Their role in facilitating transportation, promoting tourism, and driving economic activity underscores their importance as essential infrastructure for modern societies.

1.4 Bridge geometry

The establishment of bridge geometry is intricately tied to the alignment of roadways, a task overseen by roadway geometric designers. These professionals meticulously consider various factors to optimize roadway functionality and ensure user safety within the constraints of the site. The complexity of bridge geometry can range from relatively simple for straightforward grade separations to highly intricate for congested urban interchanges.

Modern traffic demands often dictate the need for alignments to accommodate fast-moving traffic, leading to the utilization of skewed crossings or curved bridges. Overcoming these geometric challenges has spurred a growing interest in the construction of skewed-curved Integral bridges, driven by both economic and aesthetic considerations.

1.5 Curvature in Bridge

As a consequence of intricate geometrical considerations, limited right-of-way availability, and the need for traffic management, horizontally curved bridges are increasingly common in highway interchanges and urban expressways.

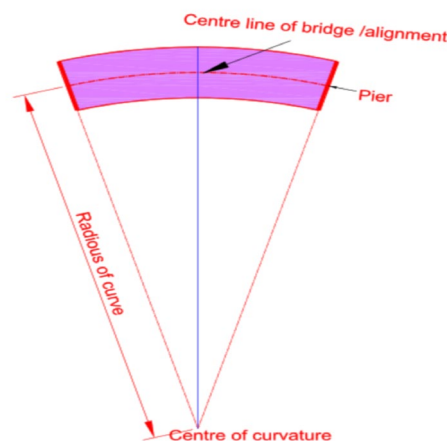


Fig. 1. Curved bridge

When the axis of the bridge girder system exhibits curvature in the plan (as depicted in Fig. 1), the bridge is referred to as a curved bridge. The degree of curvature for a particular span is measured by its central angle. Curvature in a girder can be achieved either through a single curve or by connecting small straight beam elements.

1.6 Skewed Bridge

A bridge constructed diagonally between abutments or piers is referred to as a skewed bridge. The skew angle is defined as the angle between the normal to the centerline of the bridge and the centerline of the abutments or piers, or alternatively, the angle between the traffic direction and the normal to the abutments or piers. A clockwise rotation of the bridge abutment normal in relation to the traffic direction is indicated as positive skew (θ_1 and θ_2), whereas a counterclockwise rotation signifies negative skew (θ_3 and θ_4), as illustrated in Fig. 2.

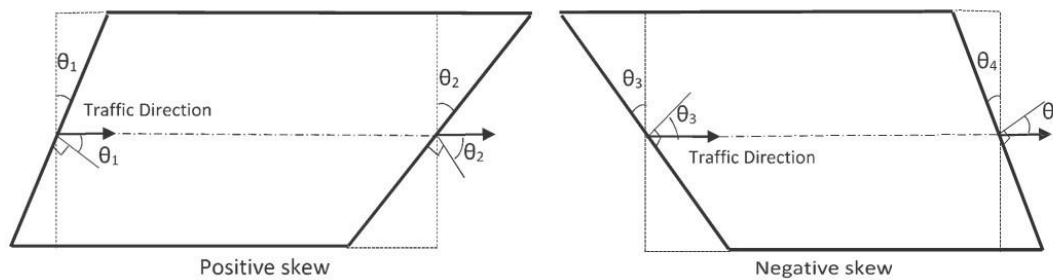


Fig. 2. 3D Types of skew deck

1.7 Integral Bridge

An Integral Bridge (IB) is characterized by its absence of bearings over the abutments and the lack of expansion joints in the superstructure. Unlike traditional bridge constructions, where the superstructure is supported by bearings, an IB features a monolithic connection between the superstructure and the substructure (piers and abutments). In traditional bridges, expansion joints and bearings allow for movement and rotation of the bridge deck without transferring any force to the abutment, pier, or foundation, accommodating thermal, creep, and shrinkage-induced movements. However, in IBs, the deck facilitates the movement of the deck to the abutment as well as to the backfill soil behind the abutment. The approach slab between the bridge end and the pavements is designed to accommodate these necessary movements, fostering a robust soil-structure interaction. Integral bridges have been recommended as preferred option in IRC:SP:115-2018.

1.8 Integral bridge practices in various parts of the world

The construction of integral bridges in the United States dates back to the late 1930s and early 1940s, with Ohio, South Dakota, and Oregon being among the first states to routinely employ continuous construction with integral abutments. California followed suit in the 1950s, while Tennessee and other states began adopting integral bridges in the 1960s. New Zealand initiated its experience with joint-less bridges in the 1930s, with standardized design drawings for concrete bridges of this type developed by the New Zealand Ministry of Works and Development (NZMWD) as early as the 1950s.

In the 1970s, Britain commenced research on integral bridges, and currently in the UK, bridges with span lengths less than 60 meters and a skew not exceeding 30 degrees are generally required to be continuous over intermediate piers and integral at abutments. The thermally induced cyclic movement at each abutment is restricted to ± 20 mm in the case of integral bridges, as per the British Advisory Note.

Japan built its first integral bridge in 1996, with integral bridge length generally restricted to 30 meters. Australia has been practising integral bridge construction since 1975, led by the Queensland Main Roads Department (QMRD). China started building integral bridges in the 1990s.

European experience with integral bridges dates back to the 1960s, with positive outcomes leading to an increasing trend of integral bridges in newly constructed bridges across Europe. Switzerland, for example, saw the construction of many integral bridges on the national motorway network between 1960 and 1985. The long-term experiences with these structures have been overwhelmingly positive, both in terms of construction and

maintenance. Over 40% of the existing bridges on the FEDRO (Federal Roads Office of Switzerland) network are integral or semi-integral structures. Scientists at EPFL (Ecole Polytechnique Federale de Lausanne) are currently conducting research programs on the abutment and approach slab construction techniques, aiming to build long-span bridges with integral concepts (i.e., bridges of length >200 meters). A sample elevation of an integral bridge is depicted in Fig. 3.

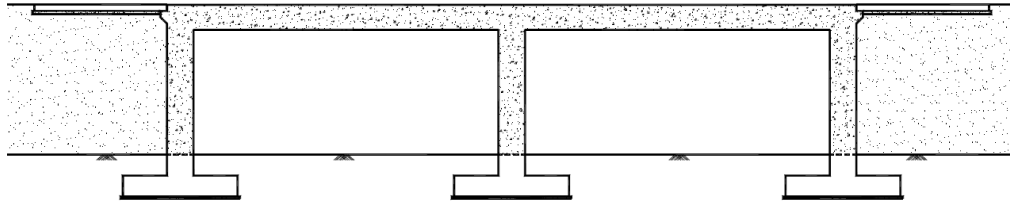


Fig. 3. Elevation of integral bridge

1.9 Integral bridge characteristics

There are notable distinctions between integral and conventional bridges, with perhaps the most significant being the rigidity of integral bridges compared to the flexibility of conventional ones. These differences are depicted in Fig. 4.

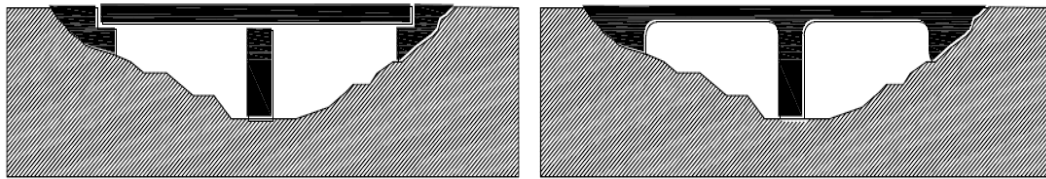
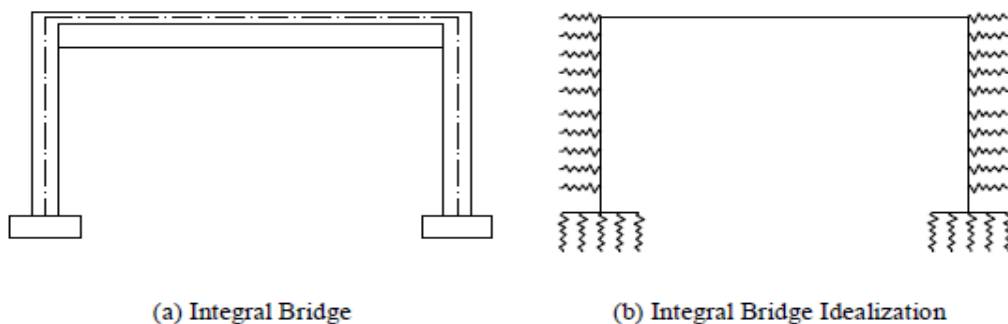


Fig. 4. Elevation fundamental differences between conventional bridge (left) and integral bridge construction (right)

Conventional bridges incorporate expansion joints and bearings within their structure, whereas integral bridges are constructed monolithically without the need for bearings or expansion joints. The simplified representation of a bridge is depicted in Fig. 5. Such bridges are ideal for small to medium-length spans, where the use of bearings and expansion joints can be minimized or eliminated entirely. With continuous decks that are monolithically connected to the abutments, these bridges function as unified structures. This design approach has demonstrated initial cost savings and efficient material usage, along with reduced maintenance requirements. The absence of expansion joints at the abutment and bridge deck contributes to lower construction and maintenance expenses. Engineers are increasingly inclined towards utilizing integral bridges, despite ongoing challenges such as soil-structure interaction and issues related to cracking. In Fig. 5, the soil is represented as a series of springs providing horizontal and vertical support to the structure.



(a) Integral Bridge

(b) Integral Bridge Idealization

Fig. 5. Idealization of integral bridge

1.10 Behavior of integral bridges under earthquake loads and soil structure interaction

The fundamental distinction between integral and conventional bridges lies in the integration of the superstructure, substructure, and surrounding soil into a unified structural model. In integral bridges, the superstructure directly influences the substructure and thus must be modelled as a cohesive unit. It is essential to incorporate the impact of the backfill behind the abutments into the structural model, considering the substructure's interaction with the surrounding soil. This interaction, known as soil-structure interaction, is crucial in the design of integral bridges due to their rigid nature.

Integral bridges, particularly those with long main spans, experience longitudinal displacements caused by daily and seasonal temperature variations. These displacements, commonly manifested as bridge expansion and contraction, are constrained by the abutment backfill and interactive substructure, as depicted in Fig. 6.

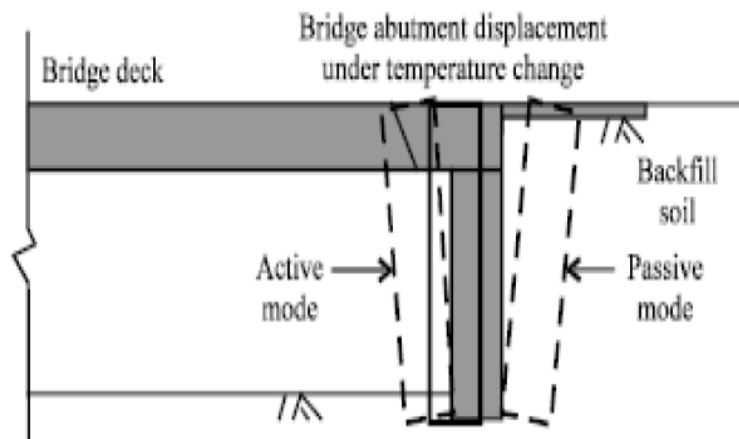


Fig. 6. Abutment wall: active and passive states (Alizadeh, et al., 2010)

Fig. 6 illustrates the phenomenon of bridge length fluctuations resulting from temperature variations. When temperatures rise, the bridge expands, causing the backfill soil to become denser. Conversely, during contraction, the abutment moves away from the backfill soil, potentially reducing its density and leading to sliding over the wall, thereby generating active earth pressure behind the abutment wall.

In instances where external forces, such as seismic activity, affect these systems, the displacements of both the structure and the ground are interdependent. This reciprocal relationship, where the soil's response influences the structure's motion and vice versa, exemplifies soil-structure interaction. As the structure applies stresses and forces to the ground, it incurs additional force and deformation in return, perpetuating this process until both the structure and the soil reach equilibrium or failure under excessive loading and deformation.

However, structural analysis typically simplifies soil behavior, while geotechnical analysis simplifies structural behavior. Lateral earth pressure, predominantly influenced by soil properties and responses, plays a significant role. The modelling of soil is crucial in analyzing integral bridges, as their performance is notably influenced by the interaction between the backfill soil and the abutment, as depicted in Fig. 7. This interaction involves relative displacement and soil stress-strain behavior due to lateral earth pressure. Consequently, employing a reasonable soil constitutive model becomes imperative to accurately represent soil properties in the analysis. Soil constitutive models serve as drastic idealizations of soil characteristics, essential for practical applications.

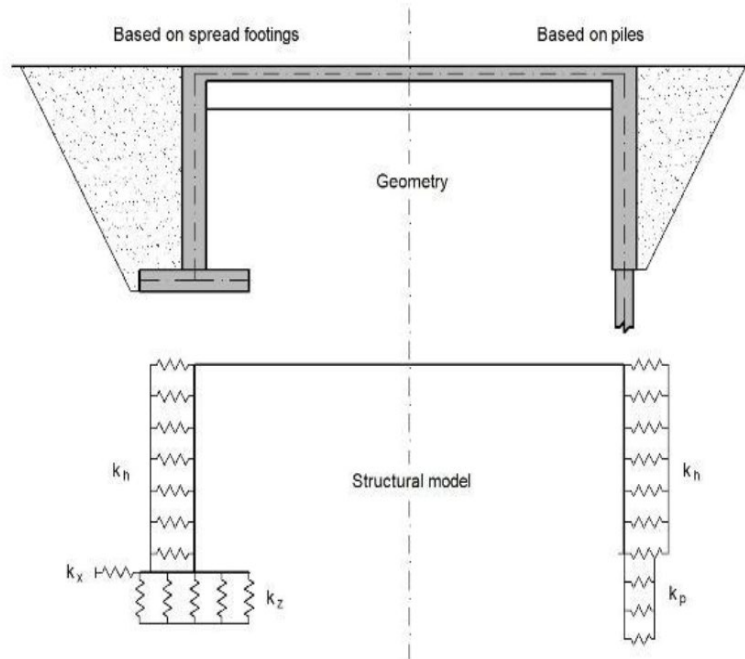


Fig. 7. Soil spring idealization of the integral bridge

Furthermore, accounting for the soil-structure interaction effect enhances the effective damping ratio of the system. The smooth idealization of the design spectrum suggests a smaller seismic response with increased natural periods and effective damping ratio, attributed to soil-structure interaction. Traditionally, it was assumed that neglecting soil-structure interaction could lead to conservative designs, as it simplifies the analysis of structures and reduces complexity significantly, tempting designers to overlook its effects.

However, since integral abutment analysis inherently involves soil-structure interaction, a realistic and reliable modelling approach is essential. The selected approach must yield accurate and dependable analysis results.

The pursuit of a physically close and mathematically simple model to represent soil media in soil-structure interaction problems has resulted in two classic approaches: the Winklerian and the Continuum approaches. The Winkler method, originating from Winkler's mathematical idealization of the foundation medium, assumes a linear load versus settlement relation. This model, depicted in Fig. 8, represents a finite soil layer atop basement rock using a family of linear springs resting on a rigid base. In the Winkler model, only one parameter, the elastic spring constant, is required. Several researchers have modified this original model to enhance realism, introducing additional parameters and resulting in modified models known as two-parameter elastic models.

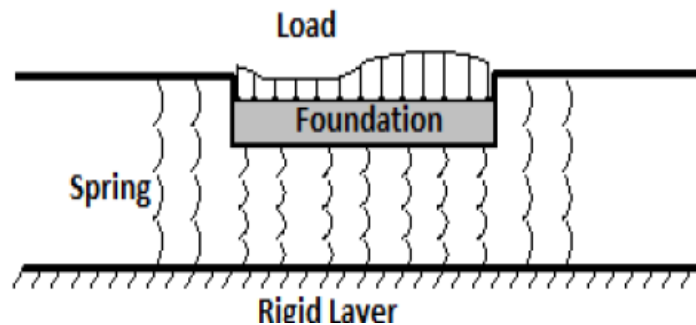


Fig. 8. Winkler spring approach

LITERATURE REVIEW

To understand the seismic behavior of skewed and curved integral bridges, a thorough knowledge of the work done so far in this area is a prerequisite. Hence the volume of literature on integral bridges reported in the last 25 years is studied and presented in the action to follow.

2.1 Literature review on straight integral bridges

Several researchers have investigated skewed integral bridges, and their findings are summarized below-

Faraji et al. (2001) conducted a study on the non-linear analysis of integral bridges using the finite element method. They developed a comprehensive 3D finite-element model of an integral bridge system that accounted for the nonlinear soil response. Through a parametric study on a sample bridge, they varied the soil compaction levels in the cohesionless soils behind the wall and adjacent to the piles. Their results underscored the significant influence of granular backfill compaction on the overall soil reaction and its subsequent impact on the structural response of the bridge system.

Dicleli and Erhan (2010) conducted an investigation into the impact of modelling assumptions and simplifications on the seismic analysis results of integral bridges (IBs). They developed five structural models of integral bridges, progressively simplifying the complexity from a nonlinear model that incorporated the true behavior of the foundation and backfill soil to models where the effects of backfill and foundation soil were entirely excluded. These models were subjected to nonlinear time history analyses using ground motions representing varying intensities of earthquakes. The findings of their study highlighted the significant influence of nonlinear soil-bridge interaction on the seismic behavior of integral bridges, particularly under medium and large-intensity earthquakes.

Bardakis and Fardis (2011) conducted nonlinear dynamic and elastic analyses to assess seismic deformation demands in concrete bridges with integral decks and piers. They investigated eight bridge configurations featuring prestressed box girder decks with bonded tendons, comprising three or five spans and piers of varying cross-sections and heights. Each bridge was analyzed in two versions: one designed conventionally based on force, and another with reduced over-strength in the piers to minimize inelastic action in the deck. Seven spectrum-compatible ground motions with peak ground accelerations (PGA) of 0.25, 0.35, and 0.45 g on rock were applied longitudinally or transversely with 5% damping. The study found that modal response spectrum analysis provided generally accurate and conservative predictions of inelastic deformation demands at the deck and piers of standard bridges, particularly during longitudinal earthquakes. However, it was noted that such analysis tended to underestimate inelastic deformation demands in bridges with significantly different pier heights, despite efforts to equalize stiffness across the piers. Moreover, the study observed that stronger ground motions generally led to larger elastic predictions of deformations compared to nonlinear dynamic analysis.

Zordan et al. (2011) conducted nonlinear parametric and pushover analyses on a 400 m long integral bridge situated in the Province of Verona, Italy. Employing a 2D simplified finite element model, they investigated the bridge's response under various soil properties behind the back walls and around the piles. Additionally, temperature pushover analysis was performed to evaluate the bridge's failure pattern due to temperature changes. Their study revealed several key findings:

- High bending moments were observed at the structure's ends, particularly where the stiffness concentration at the abutments was significant.
- Axial forces in the girders and piles were notably influenced by both positive and negative temperature variations.
- Different soil conditions significantly impacted the bending moment near abutments and the axial force along the girder.
- Significant temperature variations greatly influenced the internal force distribution at abutments and in the end parts of the structure.
- Slender and flexible piers exhibited more uniform and predictable responses to temperature variations.
- Flexible abutments or pin connections between the girder and abutments were suggested as preferred solutions.
- Negative temperature variations were highlighted as requiring utmost attention.

Shreedhar and Hosur (2011) investigated the soil-pile interaction for integral abutment bridges using a 3D finite element model constructed with STAAD Pro 2006 software. In their study, they made the following observations:

- The combined effect of temperature variation and different soil types may have a significant impact on integral abutment bridges.
- Analysis indicated a linear response within selected temperature change ranges.
- The properties of soil adjacent to the abutment and pile were identified as major factors governing the response of integral abutment bridges to thermal loads.
- Looser soil behind abutments resulted in larger displacement and subsequently larger maximum bending moment for a particular temperature change. Conversely, denser soil led to reduced displacement and bending moment values.
- Pile top displacement decreased with an increase in the relative compaction of the soil behind the abutment.

Fartaria (2012) investigated soil-structure interaction in integral abutment bridges and proposed a stabilization solution involving soil-cement columns executed with the jet-grouting technique, along with a resilient EPS layer. Through numerical analysis using a 2D finite element model in PLAXIS 2D, critical phenomena were identified, and the reduction in lateral earth pressure achieved by the elastic inclusion was quantified. The study revealed that incorporating a compressible inclusion like resilient EPS resulted in a significant reduction in lateral earth pressures. Resilient EPS was identified as the preferred material due to its low stiffness and elastic behavior, making it suitable for use as a joint. While the proposed stabilization solutions may increase construction costs for integral abutment bridges, they are expected to be cost-effective in the long term by reducing future maintenance and repair expenses.

Mohtashami and Shooshtari (2012) conducted seismic assessments of integral reinforced concrete bridges using adaptive multi-modal pushover analysis and soil-pile interaction. Their paper introduced a new adaptive pushover procedure to improve the accuracy of seismic response estimation by accounting for higher modes. The study included a parametric analysis of regular and irregular configurations of integral bridges, comprising nine bridge configurations with varying spans and pier heights. The proposed method updated displacement capacity at each step of the nonlinear analysis and compared it with the displacement demand until reaching the performance point of the structure. Numerical results indicated that the proposed method accurately predicted displacements and internal forces in most cases, showing good agreement with inelastic time-history analysis results. The response of the proposed procedure was deemed satisfactory compared to current pushover procedures, highlighting its potential for seismic assessment of integral bridges.

Bloodworth et al. (2012) proposed a method that integrates laboratory cyclic stress-path testing within a numerical model to evaluate thermal cycling effects. Samples of sand and stiff clay underwent tri-axial testing under stress paths typical behind integral abutments. Stiff clay exhibited relatively little lateral stress buildup with cycles, while sand experienced continuously increasing stresses, surpassing at-rest pressure and reaching full passive pressures. A numerical model was developed to assess the implications of these findings on soil-abutment interaction and estimate lateral stresses on the abutment. The model showed good agreement with published centrifuge and field data, suggesting that current standards' stress profiles may be conservative.

Masrilayanti (2013) investigated the earthquake effects on integral bridges across various soil types through computer simulations. Using Eurocode 8 recommendations for earthquake analysis, a symmetrical medium-length integral bridge was analyzed. Artificial EC8 spectrum-compatible time histories were applied to the structure for a range of soil stiffnesses. Both static and dynamic relative displacements were studied. Synthetic time histories for five soil types were generated using Mathcad, with validation through Seismospect by Seismosoft. Full integration time history analyses in ANSYS were conducted to simulate the bridge's dynamic response. The study highlighted the significant role of relative displacements in the overall structural response of integral bridges, with lower-stiffness soils exhibiting more detrimental effects compared to higher-stiffness soils.

Erhan et al. (2014) conducted a comparative analysis of the seismic performance between integral and conventional bridges, focusing on differences in their abutments. They designed three conventional jointed bridges based on existing integral bridges with varying spans. Structural models were then developed for both integral and conventional bridges, accounting for nonlinear structural and dynamic soil-bridge interaction effects. Nonlinear time history analyses were conducted using a range of ground motions scaled to peak ground accelerations from 0.2 to 0.8 g. The results indicated that integral bridges exhibited superior seismic performance compared to conventional bridges, demonstrating smaller inelastic rotations at piers and piles, reduced deck displacements, decreased pile axial forces, minimized abutment rotations, limited pier column drifts, and reduced bearing displacements.

Far et al. (2015) investigated the combined effects of thermal and seismic loads on integral bridges. They developed a 2D finite element model considering nonlinear behavior for the near-field soil behind the abutments, with the soil around the piles modelled using nonlinear springs based on p-y curves. The study incorporated uniform temperature changes observed during significant earthquakes worldwide, applied concurrently with corresponding earthquake time history ground motions. A comparison of the analysis results with prescribed AASHTO LRFD load combinations revealed that pile forces and abutment stresses were influenced by this new load combination, with the effect being more severe for contraction mode induced by negative uniform temperature changes.

Wood (2015) conducted a comprehensive review of the earthquake performance of bridges featuring integral abutments, along with the available design methodologies for determining stiffness, passive pressure resistance, and damping for different types of integral abutments. His findings revealed that bridges equipped with integral abutments have exhibited robust performance during strong ground-shaking events in both New Zealand and California. This resilience is attributed to the passive resistance and damping provided by the integral abutments, which effectively limit longitudinal response and consequently reduce damage compared to bridges with seat-type abutments. Wood also noted that the inclusion of friction slabs with integral abutments, aimed at minimizing gapping, contributes to increased damping.

Peric et al. (2015) developed a comprehensive finite element model of a three-span integral bridge subjected to combined gravity and thermal loads. The substructure of the bridge comprised two sets of concrete piers, two abutments, and fourteen HP steel piles (seven at each abutment), with their strong axis of bending oriented parallel to the longitudinal direction of the bridge. Various load cases, representing different levels of temperature increase in the presence of diverse backfill soil types, were simulated. The analysis results indicated that the effects of compaction on backfill and the magnitude of thermal loading exhibit contrasting behaviors between the substructure and superstructure elements.

Panikkavettil and Raveendran (2017) conducted a comprehensive study on the seismic performance of integral bridges with different span lengths. They employed static analysis, modal analysis, and response spectrum analysis using ANSYS2015 to assess the effectiveness of bridges with varying spans. Utilizing a simplified finite-element model of the East Logansport Bridge at West, they conducted static, modal, and response spectrum analyses. Additionally, they developed a design chart to facilitate bridge design for various span lengths and its validity was verified through ANSYS.

Kozak et al. (2018) investigated the seismic performance of integral abutment highway bridges in Illinois. Their study involved modelling two integral bridges subjected to design-level earthquakes: one with prestressed concrete girders and the other with steel plate girders as the main superstructure elements. Static pushover analysis and dynamic analysis were conducted for each 3-span integral abutment bridge in both transverse and longitudinal directions. Using 20 ground motions representing a 1000-year return period hazard level for Cairo, Illinois, they observed that the yielding of piles at the abutments was a critical limit state for both steel and concrete span integral abutment bridges in dynamic analyses. Damage to the pier columns and retainers was more severe in the concrete span bridge compared to the steel span bridge. Consistent damage was found in the retainers of both bridges under transverse excitation. Their recommendations included increasing abutment pile size, using smaller retainer anchor bolts for steel integral abutment bridges, and enlarging the size of pier columns.

Mahjoubi and Maleki (2018) introduced a comprehensive non-linear finite element (FE) model for integral abutment bridges, designed to facilitate analysis using commercial software, particularly under seismic loading. Their model accounts for non-linearity in both the structure and soil, including far-field soil response, while remaining practical for real-world applications. They conducted a parametric study using the model to investigate the effects of bridge length, abutment type, and soil type on the seismic behavior of integral abutment bridges. Through non-linear direct integration finite element analyses, they demonstrated the importance of accurately modelling soil and pile behavior for capturing realistic seismic responses in integral abutment bridges.

Choi et al. (2019) focused on the nonlinear behavior and seismic capacity of fully integral bridges, aiming to determine the appropriate stiffness of end-restraining abutments to withstand design earthquake loadings. They conducted a rigorous parametric study using OpenSees software to perform nonlinear static pushover analysis and obtain force-deflection curves for various bridge models. Their findings indicated that the fully integral bridge prototype in their study met the seismic performance criteria set by Caltrans. Through nonlinear static pushover analysis, they observed that the end-restraining effect of the abutment reduced lateral displacement of the fully integral bridge, resulting in less lateral force and displacement in intermediate piers. Proper application of end-restraining abutments effectively controlled sectional member forces in the intermediate piers.

Ibrahim et al. (2019) conducted a study on the theoretical dynamic characteristics of integral bridge abutments with bored piles using finite element modal analysis with ABAQUS software. They selected a single-span integral bridge in Pahang, Malaysia, as their case study. The modal characteristics of this bridge differed from those of a simply supported bridge, with higher modal frequencies observed in the latter. Their finite element modelling results showed that integral bridges with bored piles exhibited lower natural frequencies compared to simply supported bridges with similar types of foundations.

Malekjafarian et al. (2020) proposed a novel pier scour indicator based on the ratio between mode shape amplitudes at two points on an integral bridge structure. This indicator, termed mode shape ratio (MSR), complements the use of changes in natural frequency as a scour indicator. Using numerical modelling, they demonstrated that MSR is more sensitive to scour erosion compared to the natural frequency. They extracted MSR from acceleration signals resulting from ambient and vehicle-induced vibrations in the structure. MSR exhibited higher sensitivity to scour erosion and showed an inverse relationship with temperature fluctuations, unlike natural frequency, which decreased with increasing temperature. This inverse relationship potentially enables the separation of scour effects from temperature influences on the system's dynamics.

Naji et al. (2020) conducted a study on the parameters affecting integral abutment bridges (IABs) considering soil-structure interaction. They found that vertical loads did not significantly affect abutment stresses, while thermal loads and soil pressure had a substantial impact on abutment behavior. Bridge length notably influenced girder axial force, pile lateral force, pile moment, and pile head displacement, although its effect on girder bending moment was relatively weak. The choice of backfill material behind IABs significantly influenced their performance, with the use of compressible material enhancing in-service performance. Furthermore, the thermal expansion coefficient had a notable influence on girder axial force, girder bending moment, and pile head/abutment displacement.

Joshi and Patel (2020) reviewed the analysis and design of integral bridges across various span types using finite element methods. They noted that integral bridges, which integrate the superstructure and abutments without bearings or expansion joints, offer structural efficiencies and can reduce maintenance costs by improving durability. Integral bridges can be single or multi-span, with abutments cast integral with the superstructure to avoid the need for maintenance-intensive expansion joints and bearings. Piers for integral abutment bridges may be constructed integrally with or independently from the abutments. The elimination of expansion joints and bearings simplifies integral bridges, making them easier and less expensive to maintain.

Shilpa et al. (2021) conducted a seismic analysis of an integral bridge to assess its behavior during major earthquakes, focusing on its suitability and safety in seismic regions, particularly in Bangalore. They modelled a 150-meter-long viaduct portion of a flyover, consisting of five continuous spans of reinforced concrete (RC) voided deck slab, each with individual spans ranging from 22.5 meters to 40 meters, with 2.5 meters overhang on either side. The total deck width was 9.9 meters, including a 9-meter wide clear carriageway and 450-mm wide crash barriers at the base level on both sides. The analysis was conducted using SAP 2000 software, considering loads specified in IRC:6-2000 and seismic analysis for Seismic Zone-II. Their findings indicated that the combination of dead load and temperature (DL+ temp.) was critical compared to other load combinations. They observed that shrinkage induced compressive stresses, while creep induced tensile stresses. Additionally, they found that the stiffness in the vertical direction was smaller compared to the horizontal direction. Moreover, deflection in the deck and pier joints was more significant in the horizontal direction than in the vertical direction.

2.2 Literature review on skewed integral bridges

Several researchers have been researched on skewed integral bridges. To carry out this study some literature has been studied and summarized below-

Greimann et al. (1983) conducted a survey of the highway departments of all 50 states to gather information regarding the design and performance of skewed bridges with integral abutments. The objective was to establish tentative recommendations on maximum safe lengths and skew angles for concrete and steel skewed bridges with integral abutments. The survey revealed that 26 states utilize integral-type abutments on skewed bridges. Most states rely on empirical experience rather than theoretical analysis in the design of integral abutments for skewed bridges.

Regarding the orientation of piles with integral abutments on skewed bridges, 15 states reported orienting their piles with the web perpendicular to the centerline of the abutment to primarily introduce bending about the strong

axis, thereby incorporating thermally induced biaxial bending stresses into the piles. However, it was noted that many states overlooked the thermally induced bending stress due to transverse thermal movement.

The survey identified several reasons for the orientation of piles:

- The integral abutment provides restraint, reducing the magnitude of thermal movement.
- Orienting the pile with the strong axis parallel to the centerline of the bearings increases rigidity for earthquake loads.
- The small magnitude of thermal expansion, coupled with backfill material yielding sufficiently, alleviates distress.
- Temperature forces act along the centerline of the roadway, not parallel to the pile web, with active soil pressure acting against the strong axis of the pile. Pre-drilling for driven piles and filling voids with pea gravel or sand helps compensate for temperature effects.

Kaviani et al. (2011) conducted parametric response-sensitivity analyses to discern the critical parameters governing the seismic behavior of skewed bridges. Their study incorporated a simplified modelling technique accounting for bridge-abutment interaction, along with the analysis results obtained from three short bridges situated in California. These bridges exhibited different configurations in terms of the number of spans and columns per bent. By utilizing these bridges as seeds, multiple analytical models were generated, varying geometrical properties such as abutment skew angle, span arrangement, and column height. Furthermore, they investigated the effects of ground motion characteristics by introducing three types of ground motions: soil-site, rock-site, and pulse-like ground motions. Their findings revealed that a smaller gap size between the deck and the back wall resulted in more effective impact forces, leading to increased deck rotation, especially under pulse-like ground motions. Moreover, the column drift ratio was found to be significantly sensitive to parameters such as column height, abutment skew angle, and the number of columns in each bent. Additionally, abutment unseating increased with higher skew angles, particularly for bridges with tall columns.

Akib et al. (2011) delved into the effects of various parameters on the structural behavior of skewed integral bridges, with a focus on scour depths at the piles and subsequent impacts on the substructure. They conducted laboratory tests on a scaled-down hydraulic model to simulate the structural behavior of the scoured integral bridge. Different flow velocities, representing actual river flow velocities, were considered and scaled accordingly. Two different truck locations were adopted to assess their influence on scour depth and structural behavior. The main data acquired included displacements and strains at specific locations on the deck slab and piles. Their investigation revealed that flow velocities affected scouring over time, directly impacting structural behavior such as strains and displacements of the bridge substructure. Strain increased with increasing scour depth for most strain gauges, and flow velocity had a direct effect on structural behavior due to increased flow force. Strains and displacements on the slab and piles varied based on location and flow velocities, with vehicle location also exerting a distinct influence on structural behavior. These findings provide valuable insights for accurately designing skewed integral bridges and developing effective scour protection systems.

Wright et al. (2015) conducted field monitoring of two bridges located in northern Illinois, including a 30-degree skew four-span continuous integral abutment bridge and a 42.5-degree skew single-span integral abutment bridge, both featuring steel superstructures and HP14 piles with pile top relief. Construction commenced in spring 2013, with instrumentation data collection starting in May 2014. Various instruments such as pile, girder, and concrete embedment strain gages, displacement transducers, and tiltmeters were employed. Data was collected for a year, covering a summer-to-winter-to-summer temperature cycle, and compared with 3-D finite element models. The findings after the first year revealed that low pile strain readings indicated adequate pile capacity under typical service conditions. Tiltmeter readings suggested minimal differential rotations between girders and abutments, indicating the mostly rigid behavior of connections. Superstructure movement, as measured by crackmeter displacement at the pier-girder interface, was less than expected from free expansion, consistent with observations from parametric studies. Other response parameters like girder, deck, and approach slab strains were also investigated and compared with finite element models, yielding data consistent with expected trends.

Popoola and Waslu (2015) investigated the long-term performance of skewed integral bridges using Midas Civil software, modelling four types of integral bridges and analyzing results in terms of displacement, deflection, moments, and torsion. Accounting for factors like creep, shrinkage, traffic, and temperature loadings, they varied skew angles and abutment sizes. Their findings revealed that skewed bridges exhibited majority displacement in the short term (within 40 days) with a significant percentage occurring over the long term (up to 25%). Abutment angle significantly influenced displacement, with acute angles exhibiting greater horizontal displacement compared to obtuse angles. Skewed bridges experienced more deflection than square bridges, with deflection

increasing with skew angle. Approximately 5% of deflection occurred over the long term. Compared to square bridges, skewed bridges exhibited substantially higher displacement, with the 8.6° skew bridge showing 73% more displacement than prestressed bridges and 44.5% more than non-prestressed bridges. Higher skew angles resulted in greater deflection. Traffic loading induced hogging moments, with the highest sagging moment observed in the non-prestressed 13° skew bridge deck. As the skew angle increased, hogging moments also increased.

Mallick and Raychowdhury (2015) conducted seismic analysis on highway-skewed bridges considering nonlinear soil-pile interaction. They examined the impact of skew angle on the seismic response of bridge-foundation systems subjected to bi-directional ground motions. Their study revealed that the rotational demand of the bridge deck increased significantly with skewness, indicating a heightened vulnerability of skewed bridges to rotational movement and deck unseating. Additionally, they observed a substantial increase in shear and moment demand on the piers with increasing skew angles, up to 54% and 37% respectively. Moreover, the maximum bending moment on the pile shaft also showed a notable increase of up to 55%, suggesting higher design requirements for the foundation components of skewed bridges compared to normal bridges.

Muhammad et al. (2015) conducted research to evaluate the impact of concrete creep on the long-term performance of skewed Integral Abutment Bridges (IABs). They utilized a time-history transient analysis approach employing the Finite Element method over a 75-year period in the LUSAS software. Their analysis considered variations in bridge total length (60m, 90m, 150m), skew angles (0°, 10°, 20°, 30°, 40°), and backfill soil stiffness (dense sand, loose sand). The study focused on assessing the behavior of the bridge, specifically measuring girder and abutment displacement, moment, and shears. To model the bridge components, a three-dimensional nonlinear thick beam element with CEP-FIP 1990 creep material properties was employed for the girders, while other structural members were modelled using three-dimensional thick beam elements. Their findings revealed that bridge span and skew angle exerted a significant influence on the behavior of skewed integral abutment bridges compared to backfill soil stiffness. Thus, the authors emphasized the importance of considering bridge span and skew angle as primary factors in the design of skewed IABs. Furthermore, they noted that loose sandy backfill soil resulted in higher values of deformations compared to dense sandy soils. The study observed that most deformations occurred within skew angles of zero to 20°, with variations in deformation becoming more prominent after 20° skew angles. These findings underscore the necessity of meticulous attention to bridge span and skew angle considerations in the design of skewed IABs, particularly in addressing long-term performance aspects.

Haymanmyintmaung and Kyawlinnhtat (2017) conducted a comprehensive study on integral bridges, focusing on various span lengths and skew angles. They designed and modelled integral bridges with span lengths ranging from 40m to 70m and skew angles of 15°, 30°, 45°, and 60° using SAP2000 software. Compliance with AASHTO standard specifications was ensured for geometric dimensions and loading conditions. Both static analysis and dynamic nonlinear time history analysis were performed to evaluate the seismic performance of the integral bridges. Parameters such as shears, bending stresses, axial forces, and deflections were assessed using the allowable stress method. To address extreme stresses exceeding allowable limits, six different stress reduction methods were applied. Their findings revealed that in skewed bridges, the stress on cross-frame members increased significantly due to the rotational tendency during seismic events, leading to excessive transverse movement. Additionally, they determined that the MSE+HLAC method was the most effective stress reduction technique for both non-skewed and skewed bridges. Furthermore, the study concluded that integral bridges can withstand maximum skew angles up to 60° and span lengths up to 60m when stress reduction methods are employed under extreme seismic loading conditions.

In a related study, Haymanmyintmaung and Kyawlinnhtat (2017) investigated the performance of skewed integral bridges under dynamic loading conditions. They compared integral and simply supported bridges with a total length of 200m, considering both non-skewed and skewed configurations in SAP2000 software. The analysis included moments, shears, and stresses under static and dynamic loading, adhering to AASHTO standard specifications. Extreme stresses exceeding allowable limits in both superstructure and substructure components of integral bridges were mitigated using six different stress reduction methods. Comparison with simply supported bridge results allowed for the assessment of skew and integral effects. The study aimed to analyze the behavior of integral bridges under dynamic loading conditions, considering parameters such as bridge support type, skew angle, and stress reduction methods. Static analysis, dynamic moving load analysis, and nonlinear time history analysis were conducted to evaluate seismic performance. The findings indicated that under static live load, integral bridge girder shear force was minimized at a skew angle of 60°, while the maximum moment was observed opposite to simply supported bridge girder behavior. Dynamic analyses revealed varying stress

distributions across different bridge components, with MSE wall identified as the most effective stress reduction method for both skewed and non-skewed integral bridges.

Parachos and Amde (2020) conducted a study to investigate the relationship between the depth of predrilled holes and the reduction in bending stresses experienced by piles supporting skewed integral abutment bridges. They developed a three-dimensional nonlinear finite element model incorporating the bridge superstructure, substructure, and surrounding soil. The model utilized shell elements for the deck slab, girders, and piles, solid elements for the abutments, and nonlinear spring elements for the soil. The analysis was performed using the ABAQUS finite element analysis program.

Their findings highlighted several key observations regarding the behavior of skewed integral abutment bridges:

- Increased bridge length and skew angle resulted in higher bending stresses in the piles supporting the integral abutments.
- The use of predrilled holes around the piles of integral abutments and an increased number of spans led to a reduction in pile bending stresses.
- Predrilled holes increased the vertical load-carrying capacity of the piles.

The analysis suggested that employing predrilled holes filled with loose sand around the piles of skewed integral abutment bridges is an effective method to reduce bending stresses in the piles and enhance their vertical load-carrying capacity. The study recommended a predrilled hole depth of 2.75 meters measured from the bottom of the integral abutment.

Zhao et al. (2021) investigated the seismic response of skewed integral abutment bridges under near-fault ground motions, considering soil–structure interaction. They analyzed the nonlinear dynamic response of a skewed integral abutment bridge under both near-fault pulse and far-fault non-pulse ground motions while conducting parametric studies on bridge skew angle and the compactness of abutment backfill.

Their analysis, based on three sets of near-fault pulse ground motion records and corresponding far-field non-pulse artificial records, revealed several key findings:

- Near-fault pulse ground motions were generally more destructive to the nonlinear dynamic response of skewed integral abutment bridges compared to non-pulse motions, although the presence of abutment backfill mitigated the pulse effects to some extent.
- The coupling of longitudinal and transverse displacements, as well as the rotation of the bridge deck, increased with the skew angle, resulting in higher internal forces in the steel H piles.
- The influence of the skew angle was most significant when the abutment backfill was densely compacted.

These studies provide valuable insights into the behavior and seismic response of skewed integral abutment bridges, offering important considerations for their design and construction.

2.3 Literature review on curved integral bridges

Several researchers have researched skewed integral bridges. To carry out this study some literature has been studied and summarized below-

Kalayci et al. (2009) conducted a comprehensive study on the impact of curvature and backfill material on the response of curved integral bridges. They utilized 3D finite element models (FEMs) representing the structural characteristics of bridges in Vermont. The study varied the degree of curvature (ranging from 0° to 50°) of the superstructure and considered different backfill material properties (loose sand and dense sand), resulting in a total of 10 distinct models.

The investigation focused on assessing the thermal response of integral abutment bridges by comparing various parameters, including longitudinal and vertical deformations of the bridge deck, abutment displacements and rotations, weak and strong axis pile moments, and backfill pressures behind abutments under the influence of thermal loading.

Key findings of the study include:

- Temperature increases led to a decrease in vertical displacement.
- Maximum vertical displacement increased with curvature across all cases.
- Backfill material had minimal effect on the vertical deflection of the bridge deck.
- Changes in abutment displacements and rotations due to increased bridge curvature were primarily influenced by self-weight, with thermal loading having less pronounced effects on these parameters.

Kalayci et al. (2012) conducted a parametric study on the thermal response of curved integral abutment bridges, utilizing finite element (FE) modelling to analyze the connections between abutments, piles, and superstructure. They employed a detailed three-dimensional FE model of a curved integral abutment bridge located in Stockbridge, Vermont, USA, as a prototype to assess the behavior of such bridges under thermal loading. The study investigated the effects of bridge curvature and abutment backfill soil type, while additional FE models were developed to explore the impact of lateral restraint provided by U-shaped wing walls integral with abutments and interior piers. Results, including abutment displacements, moments at abutment piles, earth pressures on abutments and wing walls, and bridge superstructure forces, were analyzed and compared with conventional curved bridges containing expansion joints.

Kataria and Jangid (2013) examined the seismic response of horizontally curved concrete box girder bridges isolated by elastomeric rubber bearings. Their study focused on evaluating the effect of curved geometry on the performance of the isolation system under excitation from four different ground motions, each with distinct frequency spectrum characteristics and three directions of motion. The bridge studied consisted of a three-span continuous concrete box girder superstructure supported on piers and abutments. Modelling the bridge as a single spine beam, they utilized Newmark's step-by-step method to solve the coupled equations of motion for the isolated system incrementally. Additionally, they compared the response of curved isolated bridges with straight isolated bridges of similar cross-section and material properties to analyze the impact of curved geometry on the isolation system's response. The findings indicated that the elastomeric rubber bearing system effectively controlled the seismic response of curved bridges, with curved geometry showing no significant difference in the peak response of the isolation system compared to straight bridges.

Phares (2014) conducted field monitoring of horizontally curved girder bridges with integral and semi-integral abutments to evaluate their behavior under various loading conditions. Six in-service bridges were monitored over an 18-month period for both short-term and long-term assessments.

Key observations from the study include:

- **Thermal Effects:** No significant difference was observed in the behavior of horizontally curved bridges compared to straight bridges under thermal effects. Strains in the composite girders were primarily induced by thermally induced restrained expansion and contraction, with axial strain showing the largest ranges. Bridges exhibited more expansion and contraction near expansion piers than fixed piers.
- **Pile Analysis:** The equivalent cantilever method of steel pile analysis did not accurately predict the relationship between weak axis bending strain in the piles and pile head displacement. Internal stress in abutment piles due to bridge expansion and contraction remained generally below 50 percent of yield stress.
- **Soil Pressures:** Soil pressures on abutment back walls were generally below approximate passive soil pressures.
- **Live Loading:** Moment distribution factors were influenced by the amount of curvature, and the V-Load equation provided an approximation of lateral bottom flange bending, especially for minimally skewed bridges.
- **Design Considerations:** A three-dimensional analytical model of the bridge and support conditions should be used to calculate thermal stresses for the final design of curved bridges, as required by AASHTO standards. However, for bridges meeting specific geometric requirements, such as a 10-degree skew and 0.06 radians arc span length to radius ratio, they can be designed as straight bridges if a stress tolerance of 10% is acceptable.
- **Expansion Piers:** Expansion piers reduced thermal stresses in the girders of straight bridges but did not significantly reduce stresses in the girders of curved and skewed bridges, even though overall restraint was reduced.

Deng et al. (2015) conducted a comprehensive study involving field monitoring and numerical analysis to investigate the behavior of curved and skewed bridges with integral abutments. The study involved field monitoring of a newly constructed three-span one-lane bridge under changing ambient conditions, as well as testing the bridge with a dump truck across the bridge walkway. Additionally, a parametric study was carried out to predict the behavior of such bridges under design load conditions.

Key findings from the study include:

- **Significant Changes in Stresses:** The study revealed that changes in curvature and skew led to significant changes in stresses within the bridge structure.
- **Thermal Stress:** Thermal stresses were found to be significant, with magnitudes reaching up to 3 ksi and accounting for up to 15% of the maximum stress in the bridge structure.

Jayeshbhai and Sanghvi (2020) conducted a review focusing on the behavior of curved integral bridges, and their findings include:

- **Thermal Stress Magnitude:** Similar to Deng et al. (2015), they observed that the value of thermal stress and its magnitude relative to the maximum stress can reach up to 3 ksi and 15% of the maximum stress, respectively.
- **Effect of Curvature and Skew:** Changes in the curvature and skew of integral bridges have a considerable effect on stress distribution within the bridge structure.
- **Backfill Compaction and Thermal Changes:** There is an inverse relationship between the effect of backfill compaction and thermal changes on substructure and superstructure elements.
- **Vertical Deflection:** Increasing curvature results in an increase in the maximum vertical deflection of the bridge.
- **Pile Yielding:** The yielding of piles at the abutments is identified as a critical limit state, occurring in both steel and concrete piles.
- **Temperature Effects:** Temperature increases result in a decrease in the vertical displacement of the bridge.

Civjan et al. (2021) conducted field monitoring of four curved steel girder integral abutment bridges located in Vermont, USA. These bridges have spans ranging from 86 ft. to 140 ft., which are typical for many bridge replacement projects. The arc span divided by the girder radius varies from 0.067 to 0.358 radians, and the girder stiffness differs across the spans. Each bridge has unique characteristics, including:

- **Danby Bridge:** This bridge features a curvature of 23.87 degrees, along with super-elevation and a grade change.
- **Bradford Bridge:** With a 30-degree skew and curvature of 2.75 degrees, this bridge presents distinct design elements.
- **Stockbridge Bridge:** This two-span structure has a curvature of 11.25 degrees and has been in service for twelve years.

Site visits were conducted to assess the current condition of all four structures, documenting any observed cracking or distress. The study found that any distress noted was not attributable to the bridge curvature but was common to the detailing used. Overall, based on the authors' site visits and bridge inspection reports, all four bridges were found to be in very good condition and were performing as expected.

2.4 Critical discussion

Review of literature leads to the following findings:

- **Limited research on Skewed and Curved Integral Bridges:** While there are ample research papers available on the seismic effects of straight integral bridges, studies on skewed and curved integral bridges are scanty. Few researchers have specifically focused on these types of bridges, particularly within the context of Indian environmental conditions and IRC codal provisions.
- **Applicability of Seismic Recommendations:** Recommendations from national and international codes, such as IRC-SP-114: 2018, could potentially be applied to study the seismic response of skewed and curved integral bridges. However, it remains unclear whether these recommendations adequately capture the actual structural response of such bridges under seismic excitations.

- **Need for Study on Soil-Structure Interaction:** The effect of soil-structure interactions on the seismic response of skewed, curved, and skewed-curved bridges has not been thoroughly investigated. This interaction is a crucial factor that can significantly influence the overall seismic behavior of these bridges.
- **Lack of Focus on Foundation Types:** The different effects of shallow or deep foundations on the seismic behavior of skewed, curved, and skewed-curved bridges have not been given sufficient attention in existing research. Understanding how foundation type affects bridge response is essential for accurate seismic design and assessment.
- **Fatigue Life Considerations:** Continuous loading-unloading-reloading cycles of bridge structures under repetitive bidirectional ground shaking can lead to fatigue and reduce the bridge's lifespan. However, this aspect has not been adequately addressed in published literature, highlighting a need for further study.
- **Time-Dependent Degradation of Concrete:** The seismic response of bridges with time-dependent degradation of concrete properties has not been thoroughly explored. Understanding how concrete degradation affects bridge performance over time can help determine the residual lifespan of bridges and inform repair and retrofitting strategies.
- **Seismic Response of Bridges with Long Piers:** Integral bridges with long piers present unique challenges in terms of seismic response, yet this area has not received significant attention from researchers. Further investigation into the seismic behavior of bridges with long piers is warranted.

On the whole, addressing these research gaps will contribute to a better understanding of the seismic behavior of skewed, curved, and skewed-curved integral bridges, ultimately improving their design and performance in seismic-prone regions.

2.5 Scope of the present study

Based on the identified gaps and lacunae in existing research, the scope of the present work can be outlined as follows:

1. Structural Modelling and Response Spectrum Analysis:

- Develop a detailed structural model of a straight integral bridge using software like Midas Civil 2024.
- Simulate the seismic behavior of the bridge under various loading conditions, particularly seismic excitation.
- Utilize response spectrum analysis to evaluate the structural response of the bridge based on recommendations from IRC: SP: 114-2018.
- Compare the response spectrum outputs of the structural model with those obtained through IRC: SP: 114-2018 recommendations to assess the adequacy of existing code provisions.

2. Time History Analysis:

- Conduct actual time history analysis to compute seismic response parameters for integral bridges.
- Utilize historical earthquake data, such as the earthquake at Bhatwari, India on October 19, 1991, recorded at station Bhat by IITR, for time history analysis.
- Apply time history analysis to assess the seismic response of curved and skewed integral bridges, particularly focusing on high seismic risk zones.

3. Investigation of Practical Parameters:

- Explore variations in practical parameters such as skew angle, radius of curvature, superstructure design, and foundation arrangements.
- Systematically vary these parameters to understand their influence on the seismic response of integral bridges.
- Analyze the data to derive conclusions of engineering significance, which will serve as valuable inputs for the seismic design of integral bridges.

4. Addressing Research Gaps:

- Fill the gap in research by focusing on skewed and curved integral bridges in Indian conditions, considering different substructure and foundation arrangements.

- Evaluate the adequacy of national and international seismic design codes in capturing the variations of structural response for skewed and curved integral bridges.
- Contribute to enhancing the seismic resilience and safety of integral bridge infrastructure, especially in regions prone to high seismic activity.

By addressing these aspects, the proposed scope of work aims to bridge the existing gaps in research and contribute to a better understanding of the seismic behavior and design considerations for skewed and curved integral bridges, particularly in the context of Indian conditions and seismic risk zones.

MODELLING AND ANALYSIS

The research methodology involves conducting a case study and complementing it with a series of simulation analyses utilizing a 3D finite element model. The primary objective is to develop a procedural framework for extracting geometric and graphical variations of seismic parameters across different load transfer arrangements. These variations serve as crucial inputs for investigating the seismic behavior of a bridge.

This study focuses on analyzing the behavior of integral bridges under bi-axial earthquake ground motion conditions. The theoretical evaluation of seismic performance primarily relies on structural simulations, emphasizing the concept of structural likeness. The simulation of the bridge, soil, and earthquakes is conducted using computer software programs, particularly Midas Civil. The earthquake and soil conditions are simulated according to the guidelines outlined in IRC: SP:114-2018. The overarching goal of this research is to gain a comprehensive understanding and insight into the structural response of integral bridges to seismic events, encompassing both longitudinal and transverse ground-shaking scenarios.

3.1 Flowchart of methodology

In this research, finite element methods are employed to study the seismic behavior of an integral bridge, employing simplicity and idealization. The process begins with the collection of earthquake data, which is then applied to the boundaries of the structure. Different time histories are incorporated into the same model to capture varied seismic scenarios, enabling the analysis of the structure's responses. Fig. 9 illustrates these sequential steps in the flowchart. Data collection involved the observation of integral bridges deemed suitable for the study. Given the high seismic risk in the Northeast region of India, earthquake data from this area were utilized. Subsequent sub-Sections provide detailed information about the bridge, with certain modifications made to align with the limited scope of the research.

3.2 Finite element modelling

In this research, the finite element method is utilized to explore the seismic behavior of integral bridges. The finite element method stands out as a popular tool for solving intricate structural engineering challenges, as it can accommodate various complexities within the solution process. This method involves replacing the actual continuum with an equivalent idealized structure composed of discrete elements, known as finite elements, connected at multiple nodes. Consequently, the finite element method boasts broad applicability and is often the preferred choice for analyzing challenging deck problems. Employing FE modelling enables a more rigorous analysis approach for evaluating existing bridges and designing new ones, often yielding significantly more precise and cost-effective results compared to some codified methods. While historical structural design codes, such as those from the British Standards Institution, permitted deviation from a strictly codified approach, newer standards like the Euro codes tend to advocate for FE analysis, recognizing its importance in achieving robust structural assessments and designs.

The finite element method offers several advantages, including:

- Modelling irregularly shaped bodies comprised of various materials seamlessly.
- Managing a wide range of load conditions, irrespective of their number and type of boundary conditions.
- Handling nonlinear behavior, particularly large deformations and materials exhibiting nonlinear characteristics.

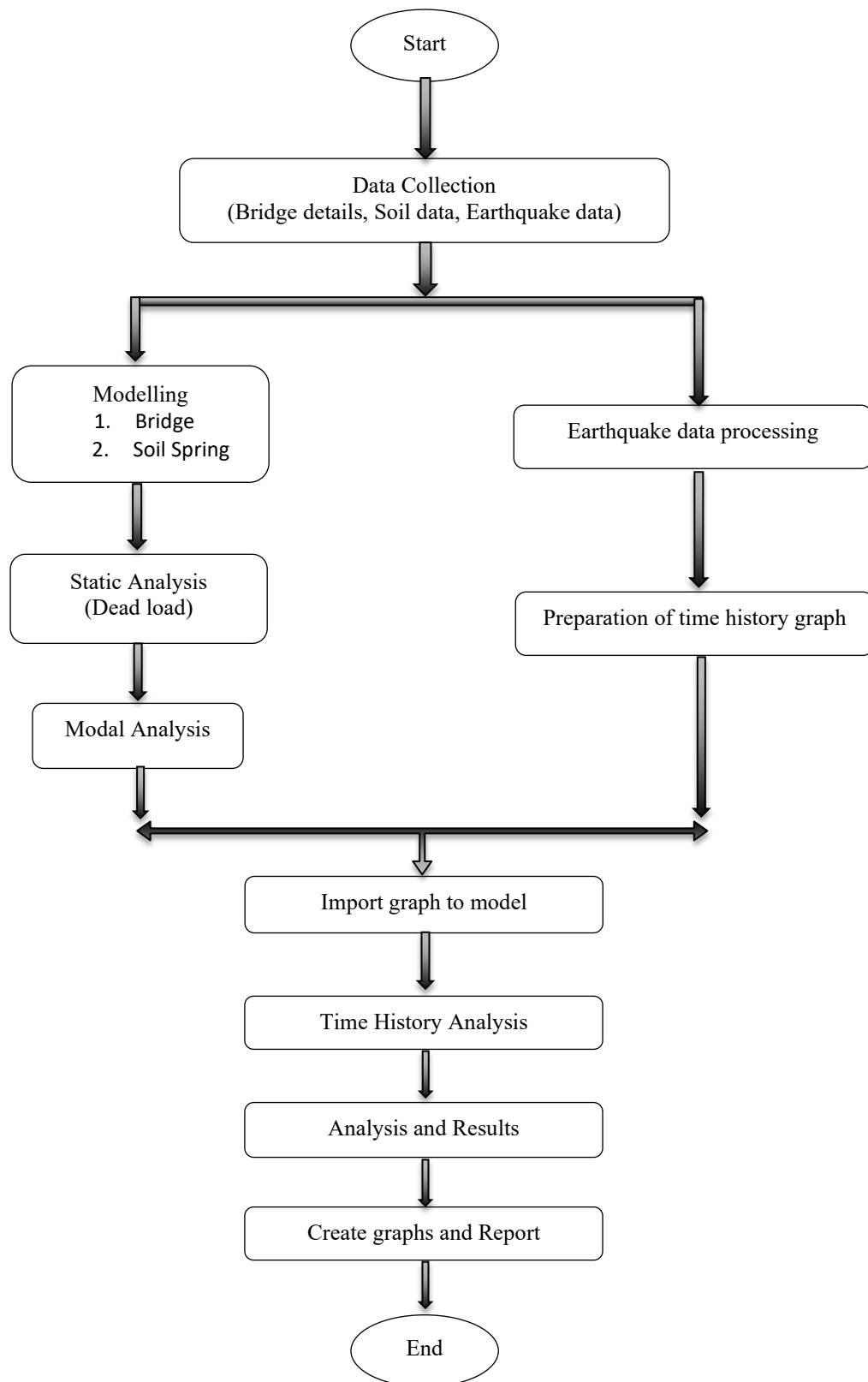


Fig. 9. Flow chart of the study

3.3 Modelling the structure

For the case study, a two-span RCC integral box bridge serves as the foundation for a parametric study aimed at assessing the impact of various variables typically encountered in integral bridges. The bridge features a 2x25 m

span integral slab configuration. Detailed dimensional specifications of the structure are illustrated in the accompanying Fig. 10 and 11.

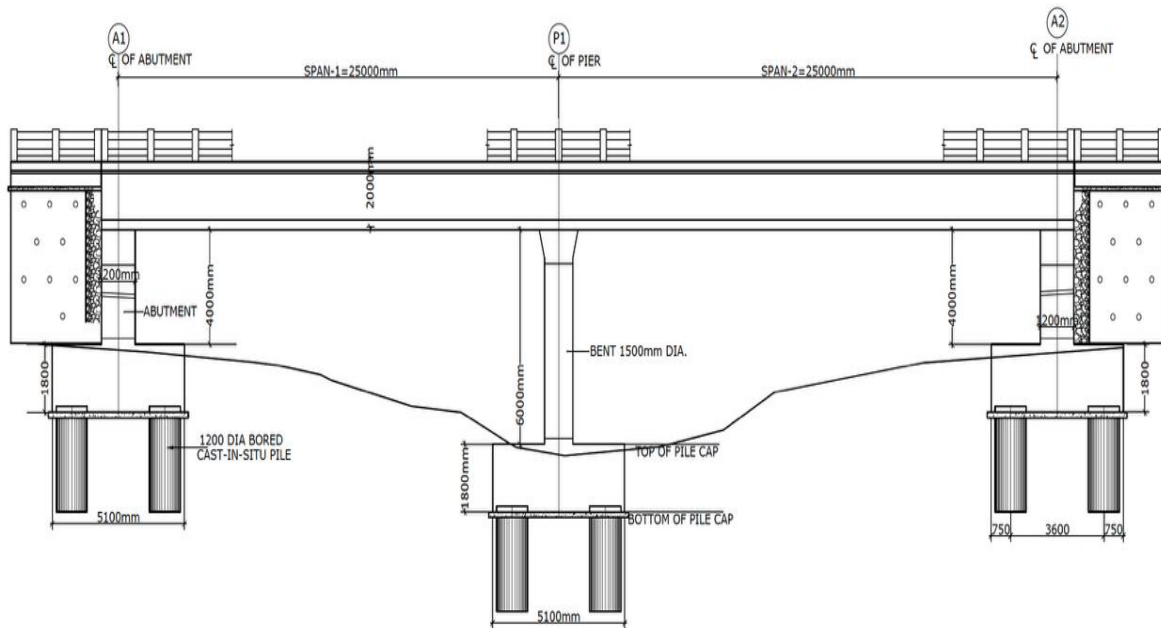


Fig. 10. Elevation of the bridge

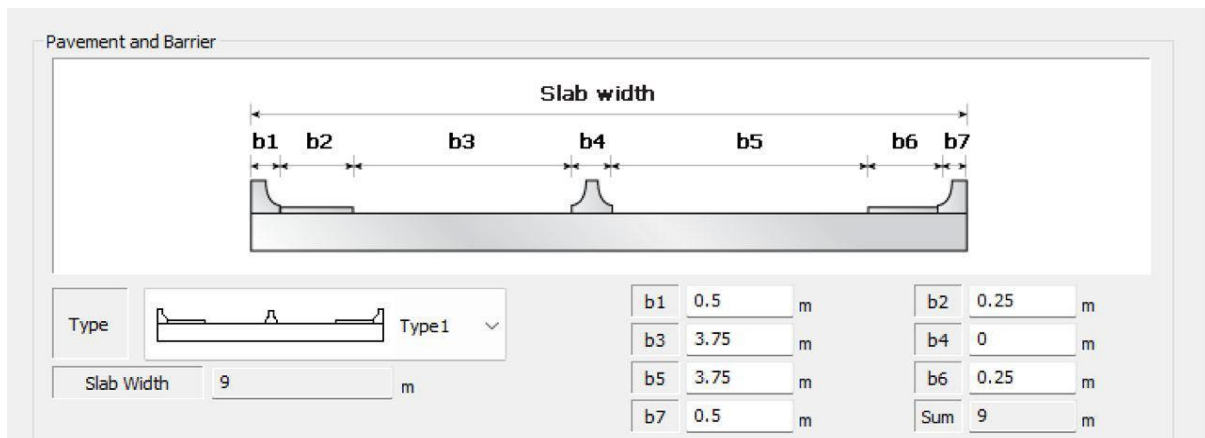


Fig. 11. Section of the superstructure

The bridge comprises two 25-meter spans supported by reinforced concrete bent columns and abutments. These structural elements rest upon a pile cap with a thickness of 1.8 m. The dimensions of the bent columns are 6 m in height and 1.5 m in diameter, while the abutments measure 4 m in height and have a thickness of 1.2 m. Each bent and abutment is supported by six concrete piles, each with a diameter of 1.2 m. The length of the piles beneath the abutments is 20 m, while those beneath the bent measure 21 m. The density of the concrete material is 2500 kg/m³. The superstructure of the bridge consists of a thickness of 2 m. The carriageway width is 7.5 m, resulting in a total bridge width of 9 m.

A comprehensive 3D study of the bridge was chosen for several reasons. Firstly, it offers a straightforward method to capture the longitudinal response within the plane. While the bridge's width and capacity typically provide sufficient strength for most cross-deck loading scenarios, potential torsion becomes a concern. However, the piers' locations are expected to offer greater torsional stiffness and capacity, ensuring adequate performance in most situations. Torsional displacements may be more significant in the deck spans, but the selected deck section is deemed capable of withstanding such forces with sufficient deformation and forced capacity.

3.4 Element type and properties in Midas Civil

For the analysis, the material specified is M30, following IRC: 112-2020 standards. As per the code, the modulus of elasticity (E) for this material is 31 GPa, while the compressive strength (f_{ck}) is 30 N/mm².

The structural components, including abutments, bent columns, and superstructure, are modelled using beam elements and a grillage model. Additionally, the piles are represented using beam elements to ensure an accurate simulation of their behavior. The pile caps are modelled using plate elements to capture their structural response effectively. This approach ensures a comprehensive and detailed analysis of the bridge's seismic performance.

Fig. 12 and 13 present the 3D view of a straight integral model in Midas Civil, while Fig. 14 and 15 depict the 3D view of a skewed model. Additionally, Fig. 16 and 17 showcase the 3D view of a curved model.

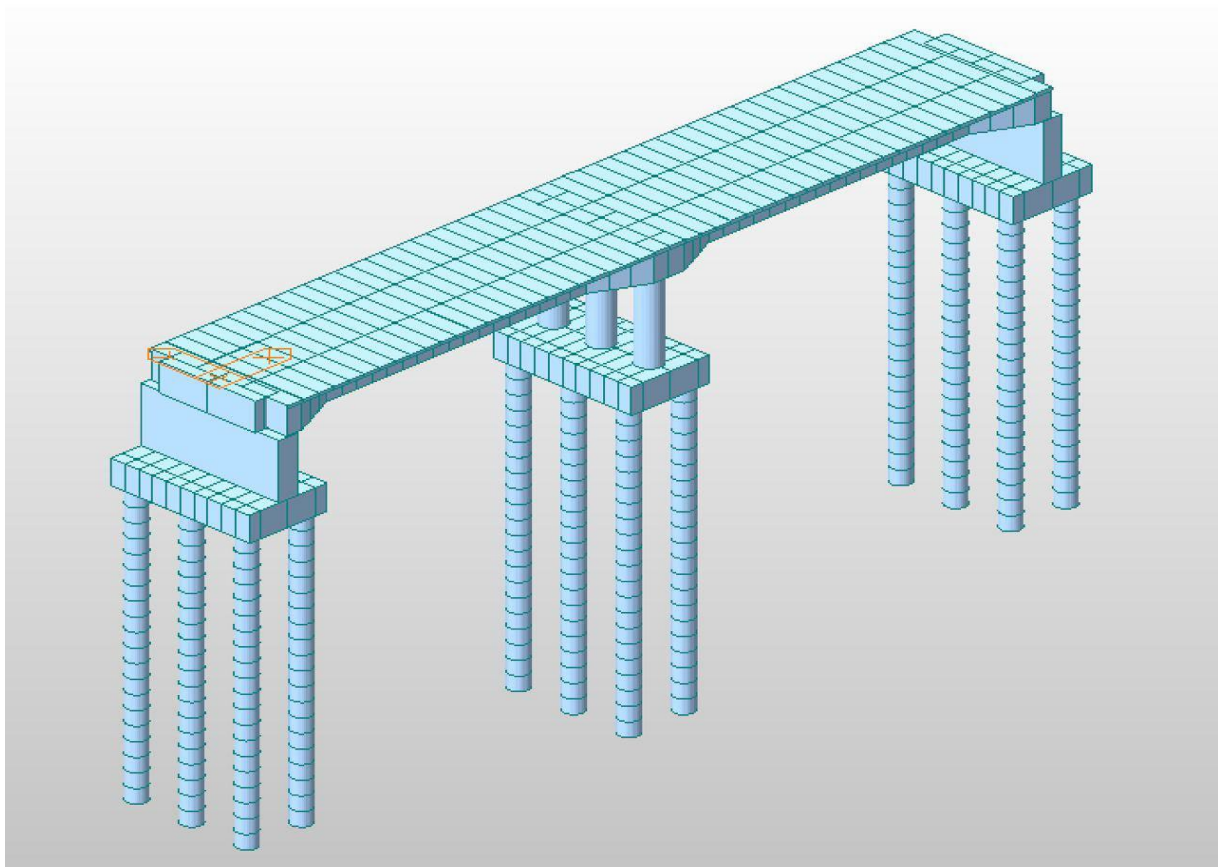


Fig. 12. 3D view of a straight integral bridge

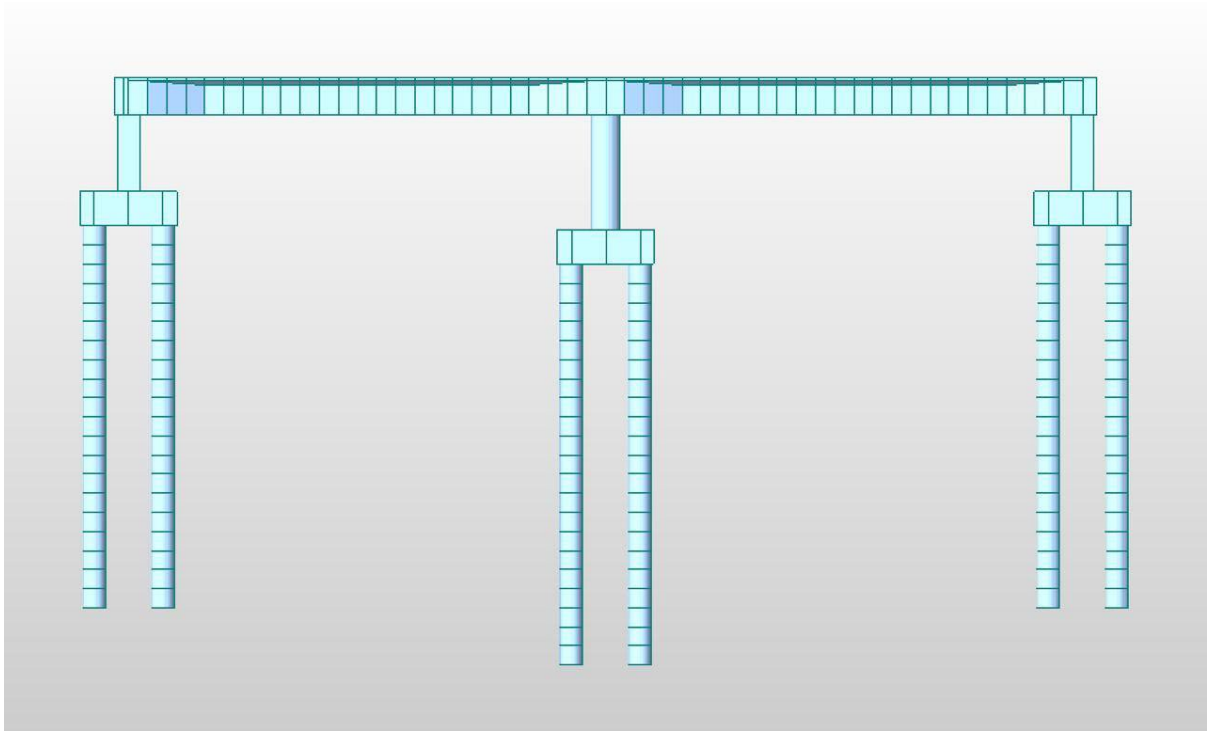


Fig. 13. Elevation of straight integral bridge

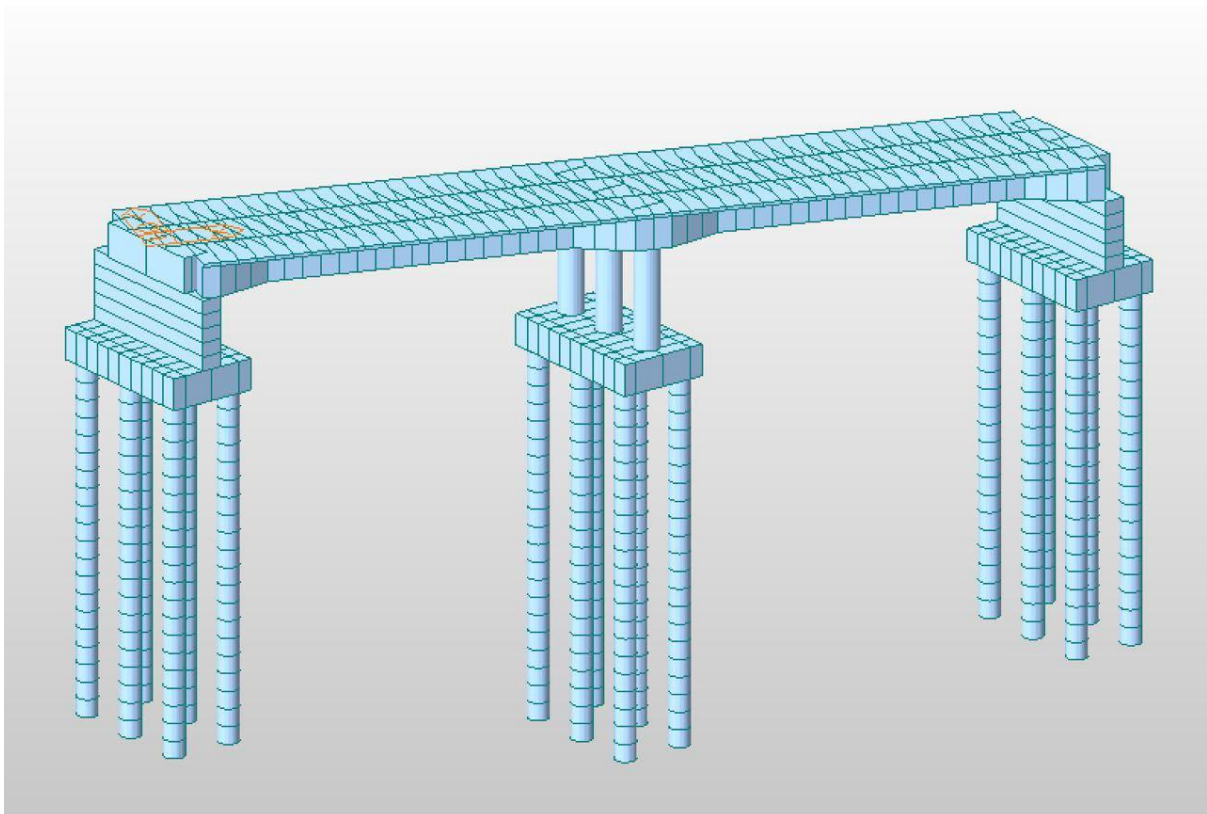


Fig. 14. 3D view of skewed integral bridge

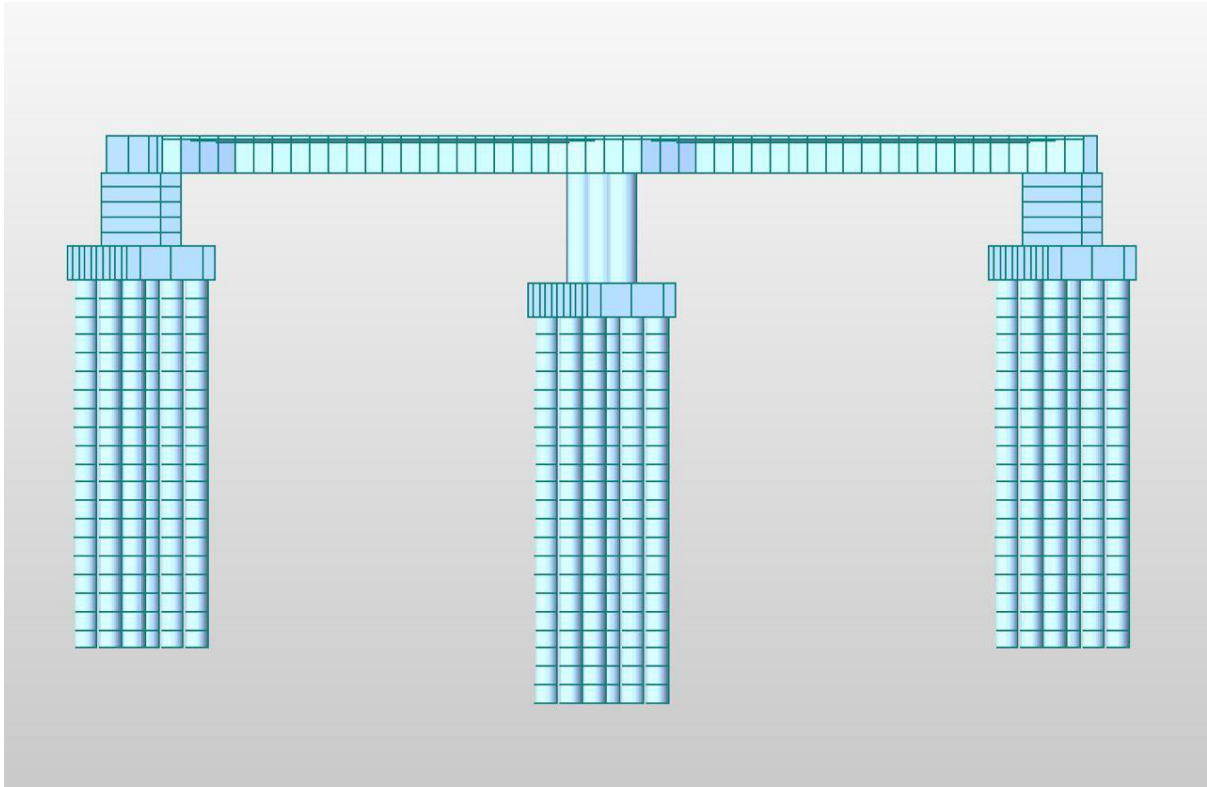


Fig. 15. Elevation of skewed integral bridge

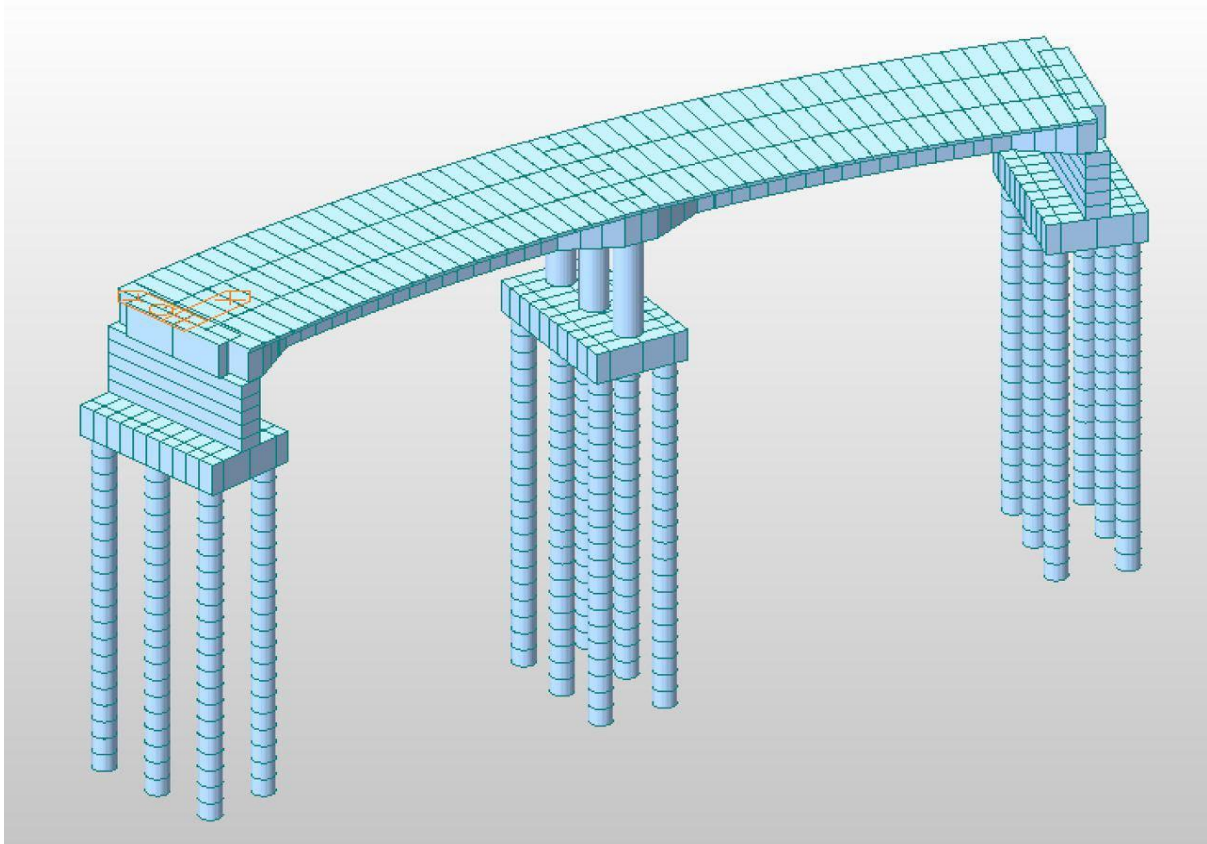


Fig. 16. 3D view of curved integral bridge

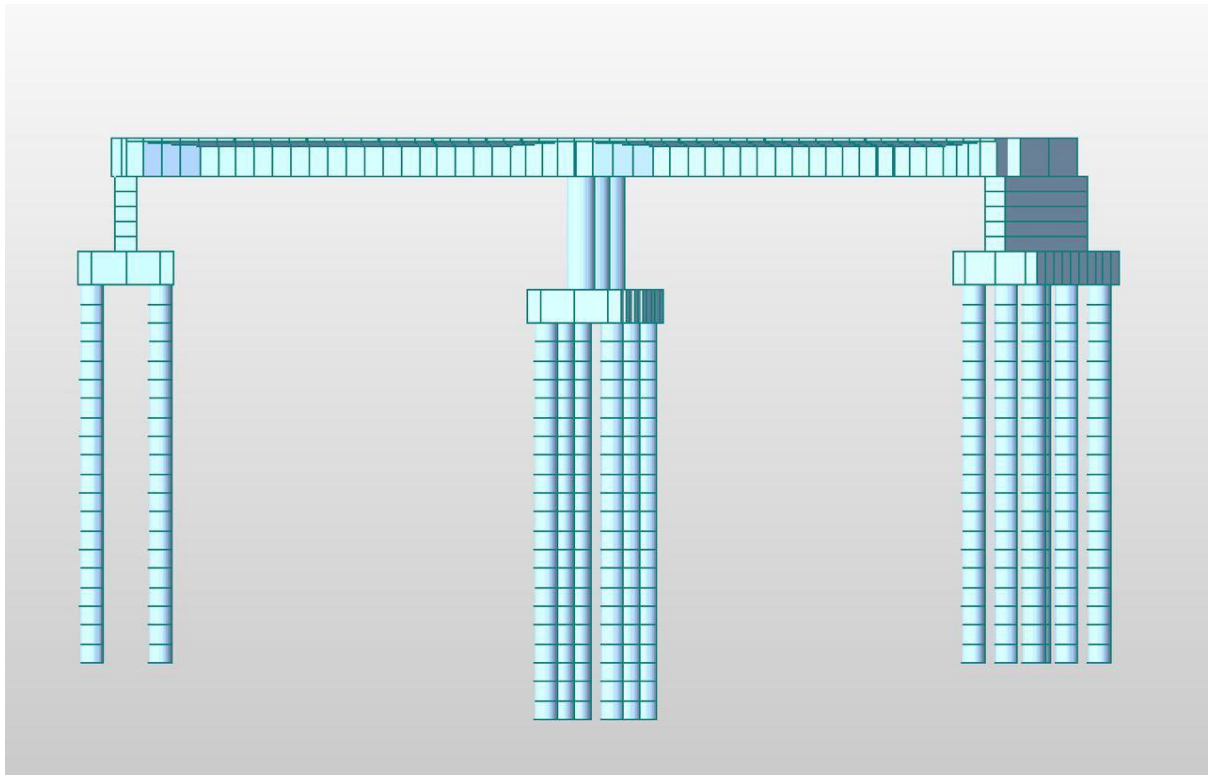


Fig. 17. Elevation of curved integral bridge

3.5 Soil properties and springs

In this thesis two types of foundations (Pile and open) are compared. So, two types of soil are used. For an open foundation hard soil below the foundation is considered. Here, The bearing capacity of soil used is 60 T/sqm for 25mm settlement.

So the spring stiffness (subgrade modulus) is $= 60 \cdot 10 / .0025 = 24000 \text{ kN/m}^3$.

Now the properties of backfill soil are used $\phi = 30^\circ$, void ratio $= 0.6$, specific gravity $= 2.65$, cycle factor $= 2$, thermal expansion $= 30^\circ \text{ C}$.

For Abutment pile the soil properties used are

Layer		Layer thickness (m)	Bulk Density, gms/cc	Dry Density, gms/cc	Specific gravity	Cohesion kN/sqm	Friction angle $^\circ$	K0	Subgrade Modulus (kN/m ³) (K)
From (m)	To (m)								
0	11	11	1.83	1.42	2.7	63	0	1	4800
11	20	9	1.8	1.47	2.71	0.000	32	0.47	3220

For Bent pile the soil properties used is

Layer		Layer thickness (m)	Bulk Density, gms/cc	Dry Density, gms/cc	Specific gravity	Cohesion kN/sqm	Friction angle $^\circ$	K0	Subgrade Modulus (kN/m ³) (K)
From (m)	To (m)								
0	9	9	1.83	1.42	2.7	63	0	1	4800
9	20	11	1.8	1.47	2.71	0.000	32	0.47	3220

The primary concern for integral bridges lies in the fluctuating temperatures, which induce deck deformations, causing either contraction or expansion. These cyclical deformations exert a notable influence on the backfill adjacent to the abutment, leading to a repetitive cycle of soil compaction and sliding. Consequently, this cyclic behavior alters the modulus of subgrade reaction and pressure distribution within the backfill, particularly with depth. Over time, this cycle tends towards stabilization, resulting in a constant modulus of subgrade reaction for the backfill.

To address this phenomenon, Barry Lehane proposed a formulation aimed at calculating this behavior using soil springs to model the interaction between the soil and the abutment/piles. In software like Midas Civil, an Integral Bridge function is readily available, facilitating the automated calculation of these soil springs based on Barry Lehane's method. This functionality streamlines the assignment of corresponding Compression-only Lateral Springs and Linear Elastic Springs within the abutment and piles. By providing the necessary parameters, this function aids in accurately representing the complex interaction between the structure and the surrounding soil, enhancing the overall analysis and design process.

The relationship between the lateral soil resistance and the lateral displacement Y at a specific depth X is represented as shown on the left (Fig. 18). The values of P_k , P_m , P_u , Y_k , Y_m and Y_u are defined at a specific depth (i.e., where pile springs are). The method of calculating P_u varies with Soil Types. The values of P_k , P_m , Y_k , Y_m and Y_u are calculated using P_u as explained below. The calculation method is divided into two major cases - Sand and Clay. Different J values are used for soft clay and stiff clay, respectively. Fig. 19 shows the model with pile spring.

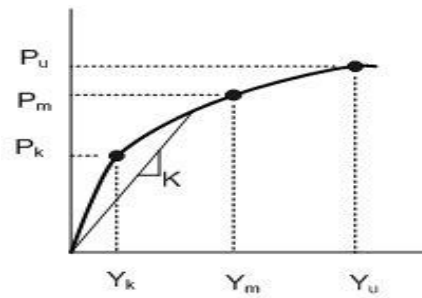


Fig. 18. Pile spring

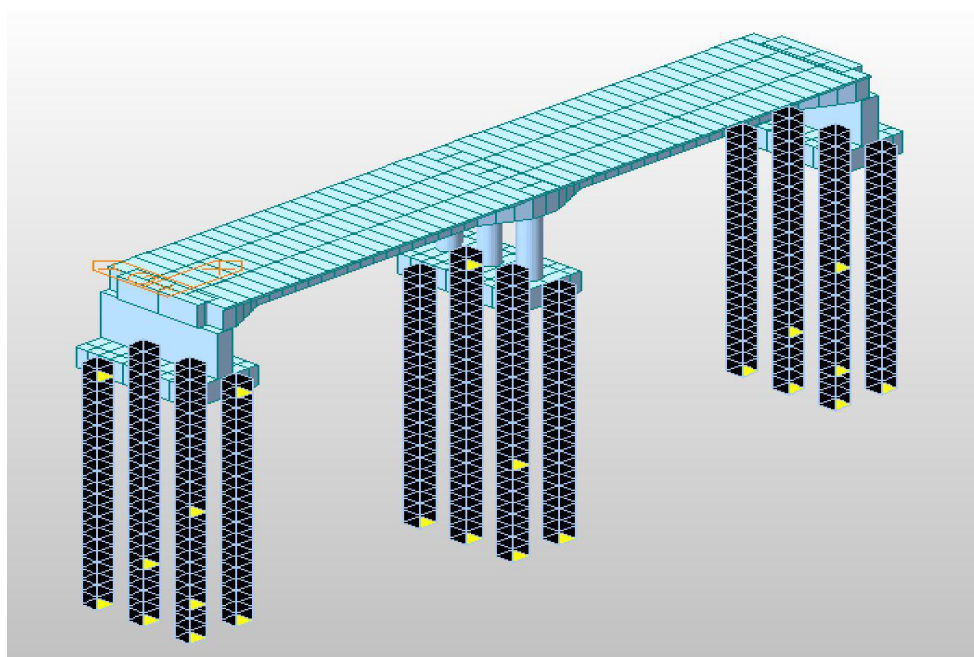


Fig. 19. Pile spring in Midas Civil

3.6 Dynamic analysis

Dynamic analysis is indispensable in the design of earthquake-resistant structures and in assessing the vulnerability of existing ones to seismic waves. The seismic analysis of bridges is conducted employing a range of methods tailored to the complexity of the structure and the characteristics of the input ground motion. These methods are selected based on their applicability to ensure accurate evaluation and robust seismic performance assessment.

- Elastic seismic acceleration method (seismic coefficient method)
- Elastic response spectrum method
- Time history method

According to IRC:SP: 114 – 2018 guidelines, integral bridges are recommended to undergo analysis via either the elastic response spectrum method or the time history method. In this study, all models have been rigorously analyzed using the time history method. To facilitate dynamic analysis, a comprehensive understanding of design response, eigenvalue analysis, and mode superposition method is essential. These analytical techniques are instrumental in calculating dynamic characteristics like natural periods and mode shapes of the structure, ensuring a thorough assessment of seismic performance.

3.7 Eigenvalue analysis

Structures possess inherent vibration characteristics determined by their shape, material properties, and boundary conditions. These natural vibration characteristics manifest in a free vibration state, devoid of external forces. The analytical method employed to determine these characteristics is commonly referred to as mode analysis, eigenvalue analysis, or free vibration analysis.

Through eigenvalue analysis, insights into the structure's natural frequency and corresponding eigen-mode are obtained. The natural frequency signifies the rate at which the structure oscillates per unit time, while the eigenmode represents a distinct shape that the structure can adopt under given constraints, allowing for free deformation.

The natural vibration characteristics of a structure are derived from undamped free vibration, a state unaffected by external forces. In this undamped free vibration scenario, a dynamic equilibrium equation can be formulated with zero damping matrix and external force components.

To determine the natural frequency and eigenmode, the displacement vector $u(t)$ is typically assumed to be the product of the displacement shape function and the time function. In multi-degree-of-freedom (MDOF) systems, this calculation parallels that of single-degree-of-freedom (SDOF) systems, with stiffness and mass represented in matrix form.

The mode superposition method leverages eigenvectors to solve equations of motion. In this method, all matrix terms become diagonal matrices, transforming each degree of freedom into an uncoupled ordinary differential equation.

For eigenvalue analysis, the Ritz Vector method is used.

3.8 Time history analysis

The time history analysis method is employed to ascertain the actual behavior of a structure, encompassing displacement, member forces, and other pertinent parameters, by considering the dynamic characteristics of the structure and the external forces applied. This method proves beneficial when the distinction between modes is indistinct or when nonlinear analysis is necessitated.

For this study, earthquake data from the seismic event that occurred at Bhatwari, India on October 19, 1991, recorded at 21:23 IST, is utilized. The data was recorded by the Indian Institute of Technology Roorkee (IITR) at station Bhat, with a hypocentral distance of 21.7 km. Peak acceleration in both longitudinal and transverse directions is recorded as 2.48 m/s/s.

Fig. 20 and 21 illustrate the time versus acceleration input for the time history analysis.

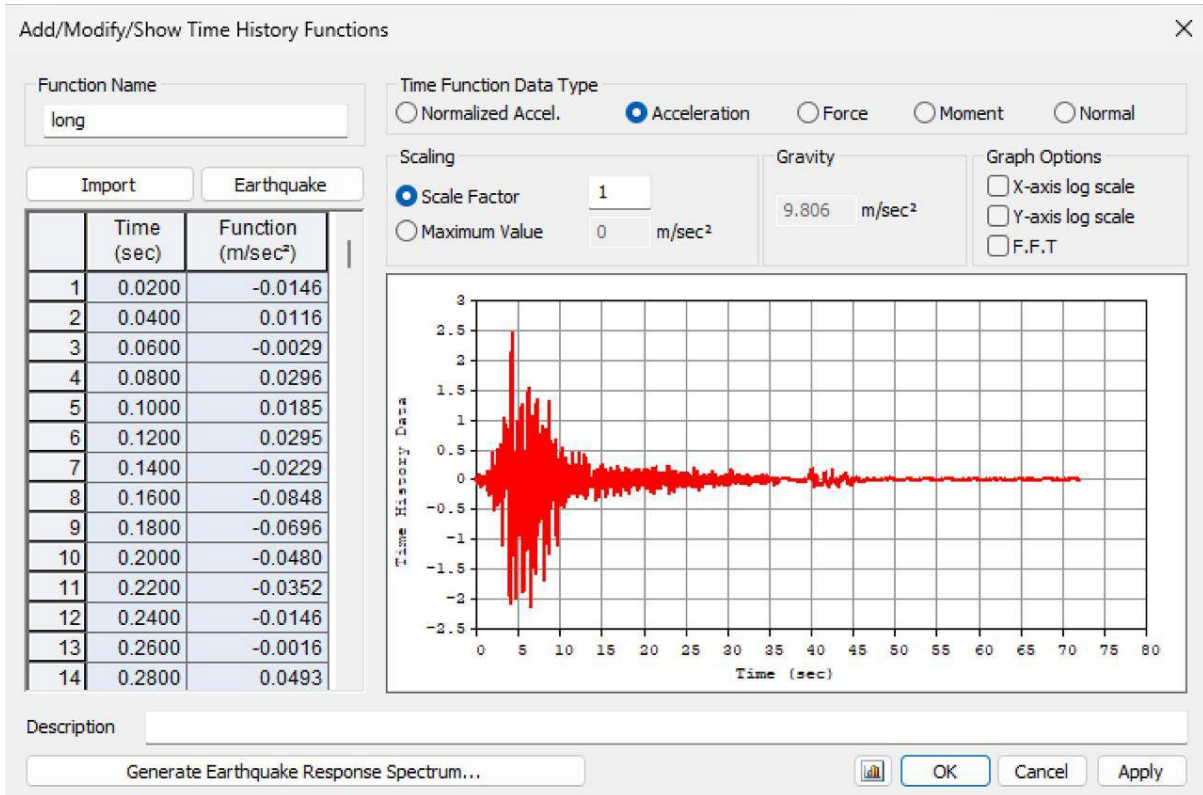


Fig. 20. Time history graph longitudinal direction

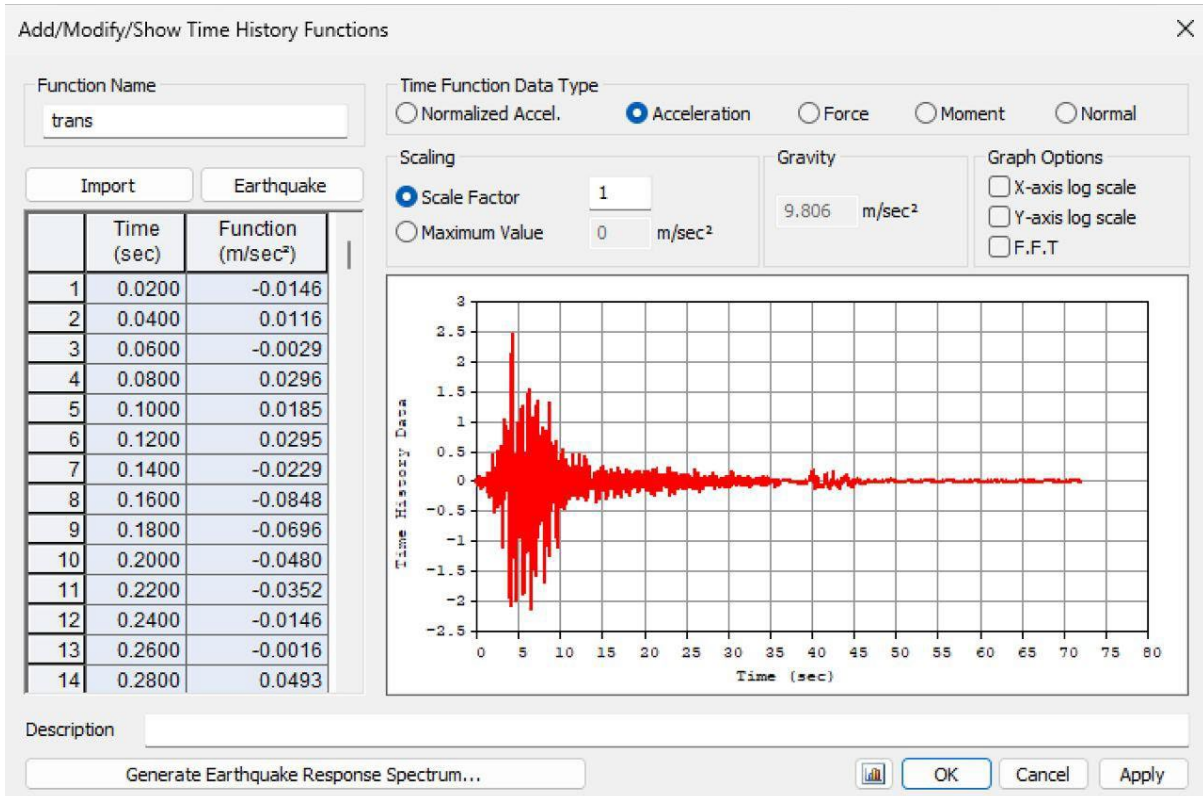


Fig. 21. Time history graph transverse direction

RESULTS AND DISCUSSION

The seismic responses of RCC integral bridges are thoroughly examined and discussed for the following scenarios, utilizing the bridge models detailed in the preceding Section:

- Exploration of first mode-time period variations concerning changes in skew angle and radius of curvature.
- Analysis of base shear value fluctuations in relation to alterations in skew angle and radius of curvature.
- Assessment of moment variations (about longitudinal, transverse axis, and torsional) at the top and bottom of abutments and piers, considering changes in skew angle and radius of curvature.

4.1 Benchmark validation

4.1.1 Model validation

Based on the provided information, the benchmark bridge selected for the study is derived from Appendix-A2 Example 1, as outlined in Clause 5.2.2 of the Indian Highways Amendment No.2/IRC:SP:114/October 2019. This bridge exemplifies the Elastic Seismic Response Spectrum Method (ERSM). It features a two-span continuous straight PSC (Pre-Stressed Concrete) box-girder design, with each span spanning 30 meters in length. Detailed cross-section specifications of the bridge are depicted in Fig. 22. The study compares the results of this benchmarking model with other relevant data, as presented in Table 1. The result of the benchmark problem proves the validity of the present approach.

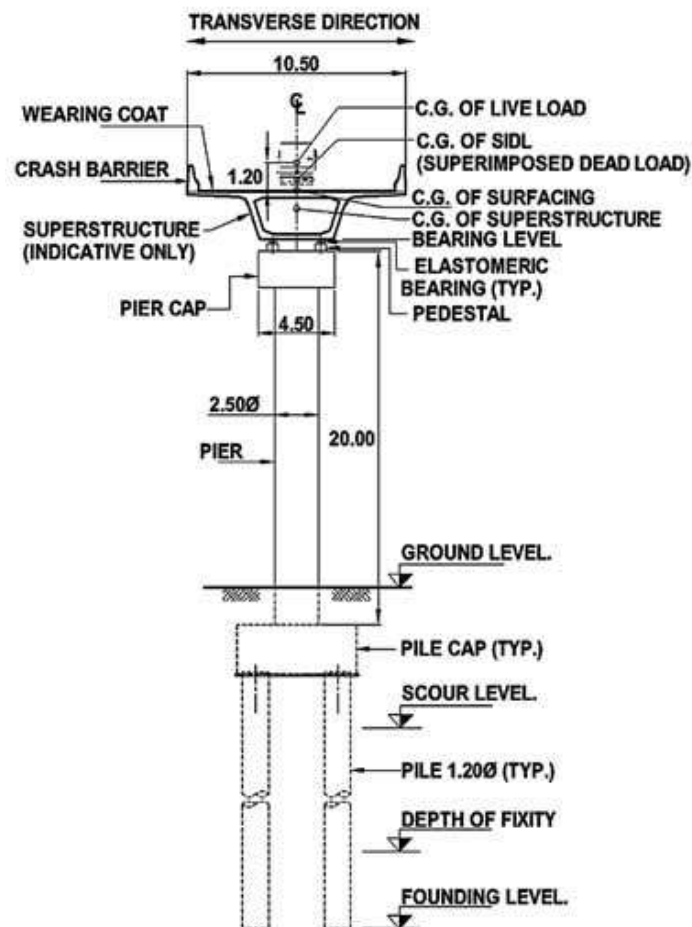


Fig. 22. Cross section of benchmarking bridge

Mode 1	Present study	Previous study	Deviation (%)
Frequency (Cycles/Sec.)	0.475442	0.48	0.95
Time period (Sec.)	2.103305	2.10	0.16
Participation factor (%)	84.87	85.01	0.16

Table 1: Benchmarking results comparison

4.2 Numerical study

Numerical experiments are conducted on several bridge models to investigate the seismic response of various significant design parameters. The study focuses on a pair of RCC integral bridges, each spanning 25 meters. Different skew angles ranging from 10 to 70 degrees and various radii of curvature including 200m, 150m, 100m, and 75m are considered.

These bridge models are subjected to analysis using the time history method (THM), employing earthquake data from Bhatwari, India, classified as Zone IV. Through this comprehensive analysis, the impact of different design parameters on the seismic response of integral bridges is thoroughly examined.

Structural models have been developed to accommodate parametric variations, allowing for a comprehensive study of the response of these bridges. A table for a list of the bridges is presented below (table-2):

The models are distinguished based on the following parameters:

- ST: Type of superstructure (ST-1 denotes integral bridge superstructure)
- AT: Type of substructure/abutment (AT-1 indicates wall-type abutment)
- PT: Type of substructure/pier (PT-1 signifies pier)
- FT: Type of foundation (FT-1 represents open foundation, FT-2 indicates pile foundation)
- TH: Time history analysis method

Through these parameterized variations, the structural response of the bridges is systematically examined, providing valuable insights into their seismic behavior.

Sl no	Model ID no	Span length (L) (m)	Radius (R) (m)	Skew angle (α) (in $^{\circ}$)	S T	A T	P T	F T	T H	Remarks	Remarks
1	M-L25R0S0ST1AT1PT1FT2TH	25	0	0	1	1	1	2	3	L=25m and R=infinity Skew Angle Varied	a. ST - 1 for Integral superstructure b. PT - 1 for Rectangular Shape c. FT-2 for pile foundation d. TH for Time History Analysis
2	M-L25R0S10ST1AT1PT1FT2TH	25	0	10	1	1	1	2	3		
3	M-L25R0S20ST1AT1PT1FT2TH	25	0	20	1	1	1	2	3		
4	M-L25R0S30ST1AT1PT1FT2TH	25	0	30	1	1	1	2	3		
5	M-L25R0S40ST1AT1PT1FT2TH	25	0	40	1	1	1	2	3		
6	M-L25R0S50ST1AT1PT1FT2TH	25	0	50	1	1	1	2	3		
7	M-L25R0S60ST1AT1PT1FT2TH	25	0	60	1	1	1	2	3		
8	M-L25R0S70ST1AT1PT1FT2TH	25	0	70	1	1	1	2	3		
9	M-L25R75S0ST1AT1PT1FT2TH	25	75	0	1	1	1	2	3		
10	M-L25R100S0ST1AT1PT1FT2TH	25	100	0	1	1	1	2	3	L=25m and S = 0 $^{\circ}$ Radius of Curvature Varied	
11	M-L25R150S0ST1AT1PT1FT2TH	25	150	0	1	1	1	2	3		
12	M-L25R200S0ST1AT1PT1FT2TH	25	200	0	1	1	1	2	3		
13	M-L25R0S0ST1AT1PT1FT1TH	25	0	0	1	1	1	1	3	L=25m and R=infinity Skew Angle Varied	a. ST - 1 for Integral superstructure b. PT - 1 for Rectangular
14	M-L25R0S10ST1AT1PT1FT1TH	25	0	10	1	1	1	1	3		
15	M-L25R0S20ST1AT1PT1FT1TH	25	0	20	1	1	1	1	3		
16	M-L25R0S30ST1AT1PT1FT1TH	25	0	30	1	1	1	1	3		

17	M-L25R0S40ST1AT1PT1FT1TH	25	0	40	1	1	1	1	3	L=25m and S = 0° Radius of Curvature Varied	Shape c. FT - 1 for Open / Shallow e. TH for Time History Analysis
18	M-L25R0S50ST1AT1PT1FT1TH	25	0	50	1	1	1	1	3		
19	M-L25R0S60ST1AT1PT1FT1TH	25	0	60	1	1	1	1	3		
20	M-L25R0S70ST1AT1PT1FT1TH	25	0	70	1	1	1	1	3		
21	M-L25R75S0ST1AT1PT1FT1TH	25	75	0	1	1	1	1	3		
22	M-L25R100S0ST1AT1PT1FT1TH	25	100	0	1	1	1	1	3		
23	M-L25R150S0ST1AT1PT1FT1TH	25	150	0	1	1	1	1	3		
24	M-L25R200S0ST1AT1PT1FT1TH	25	200	0	1	1	1	1	3		
25	M-L25R0S0ST1AT1PT1FT2TH	25	0	0	1	1	1	2	3	L=25m and R=infinity Skew Angle Varied	a. ST - 1 for Integral superstructure b. PT - 1 for Rectangular Shape c. FT-2 for pile foundation d. TH for Time History Analysis
26	M-L25R0S10ST1AT1PT1FT2TH	25	0	10	1	1	1	2	3		
27	M-L25R0S20ST1AT1PT1FT2TH	25	0	20	1	1	1	2	3		
28	M-L25R0S30ST1AT1PT1FT2TH	25	0	30	1	1	1	2	3		
29	M-L25R0S40ST1AT1PT1FT2TH	25	0	40	1	1	1	2	3		
30	M-L25R0S50ST1AT1PT1FT2TH	25	0	50	1	1	1	2	3		
31	M-L25R0S60ST1AT1PT1FT2TH	25	0	60	1	1	1	2	3		
32	M-L25R0S70ST1AT1PT1FT2TH	25	0	70	1	1	1	2	3		
33	M-L25R75S0ST1AT1PT1FT2TH	25	75	0	1	1	1	2	3	L=25m and S = 0° Radius of Curvature Varied	
34	M-L25R100S0ST1AT1PT1FT2TH	25	100	0	1	1	1	2	3		
35	M-L25R150S0ST1AT1PT1FT2TH	25	150	0	1	1	1	2	3		
36	M-L25R200S0ST1AT1PT1FT2TH	25	200	0	1	1	1	2	3		
37	M-L25R0S0ST1AT1PT1FT1TH	25	0	0	1	1	1	1	3		
38	M-L25R0S10ST1AT1PT1FT1TH	25	0	10	1	1	1	1	3		
39	M-L25R0S20ST1AT1PT1FT1TH	25	0	20	1	1	1	1	3		
40	M-L25R0S30ST1AT1PT1FT1TH	25	0	30	1	1	1	1	3		
41	M-L25R0S40ST1AT1PT1FT1TH	25	0	40	1	1	1	1	3	L=25m and R=infinity Skew Angle Varied	a. ST - 1 for Integral superstructure b. PT - 1 for Rectangular Shape c. FT - 1 for Open / Shallow e. TH for Time History Analysis
42	M-L25R0S50ST1AT1PT1FT1TH	25	0	50	1	1	1	1	3		
43	M-L25R0S60ST1AT1PT1FT1TH	25	0	60	1	1	1	1	3		
44	M-L25R0S70ST1AT1PT1FT1TH	25	0	70	1	1	1	1	3		
45	M-L25R75S0ST1AT1PT1FT1TH	25	75	0	1	1	1	1	3		
46	M-L25R100S0ST1AT1PT1FT1TH	25	100	0	1	1	1	1	3		
47	M-L25R150S0ST1AT1PT1FT1TH	25	150	0	1	1	1	1	3		
48	M-L25R200S0ST1AT1PT1FT1TH	25	200	0	1	1	1	1	3		
										L=25m and S = 0° Radius of Curvature Varied	

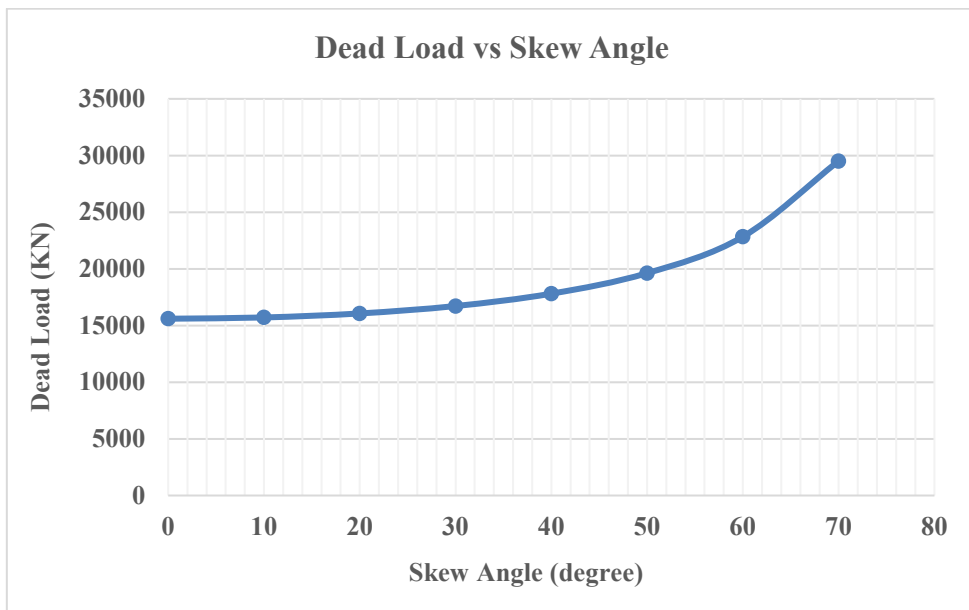
Table 2. List of analysis models

4.2.1 Variation of dead load

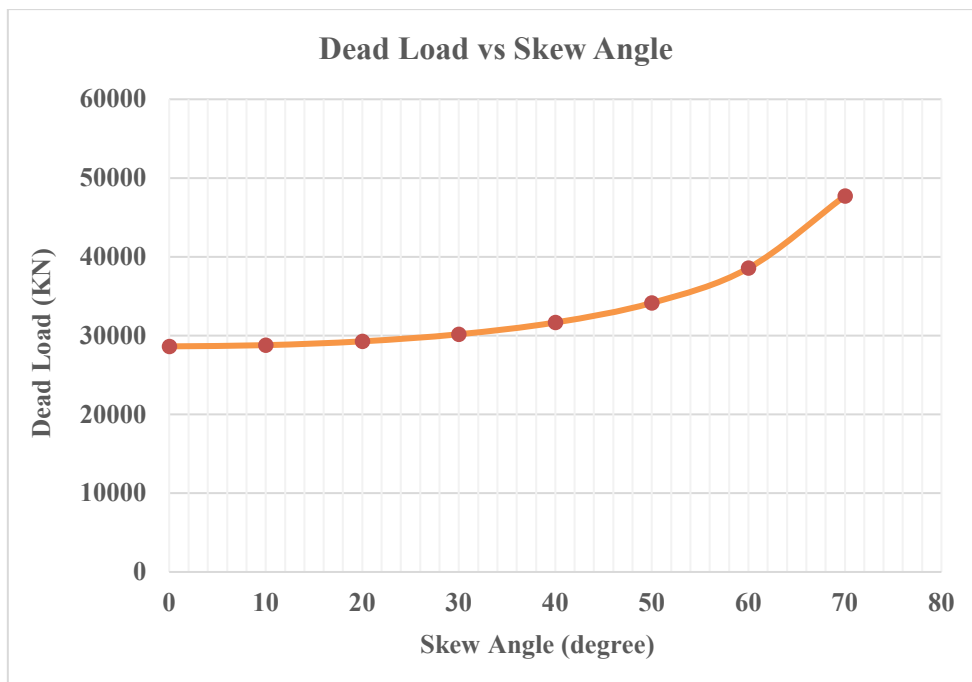
The dead load of the structure is subject to variation corresponding to the skew angle. As the length of the substructure and the pile cap or open foundation increases with the skew angle, the dead load also increases accordingly. Interestingly, for both models with or without abutment springs, the dead load remains constant. Additionally, the dead load remains consistent for curved models.

To comprehend the nature of these variations induced by earthquake forces, the variation of dead load with respect to the skew angle and the angle of plan curvature of the integral bridge is plotted graphically. The degree of curvature is derived by taking the reciprocal of the radius (R in meters). Consequently, all graphs pertaining to curved bridges are plotted against the curvature (1/R).

4.2.1.1 Variation of dead load with skew

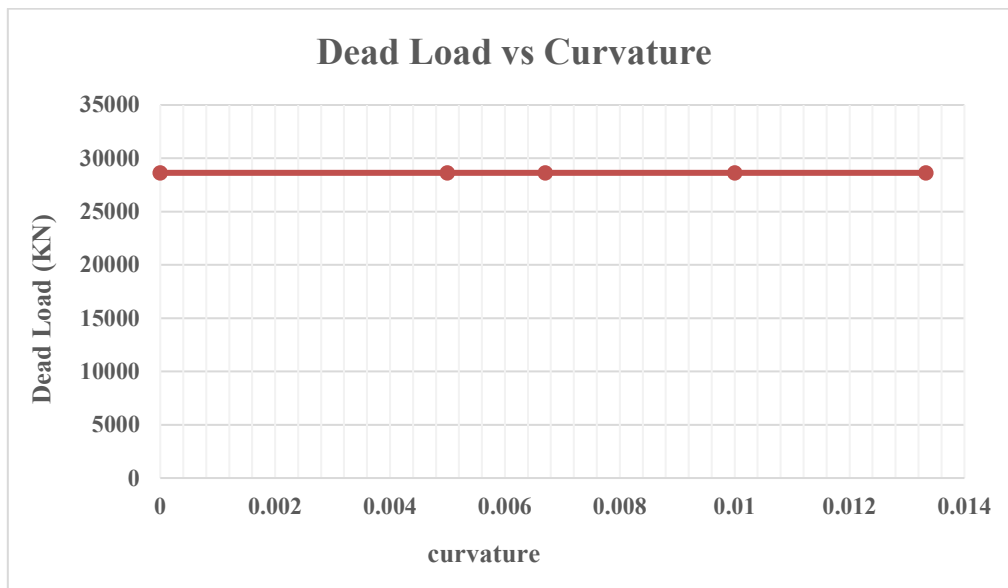


Graph 1. Variation of dead load with respect to skew angle for bridge with open foundation

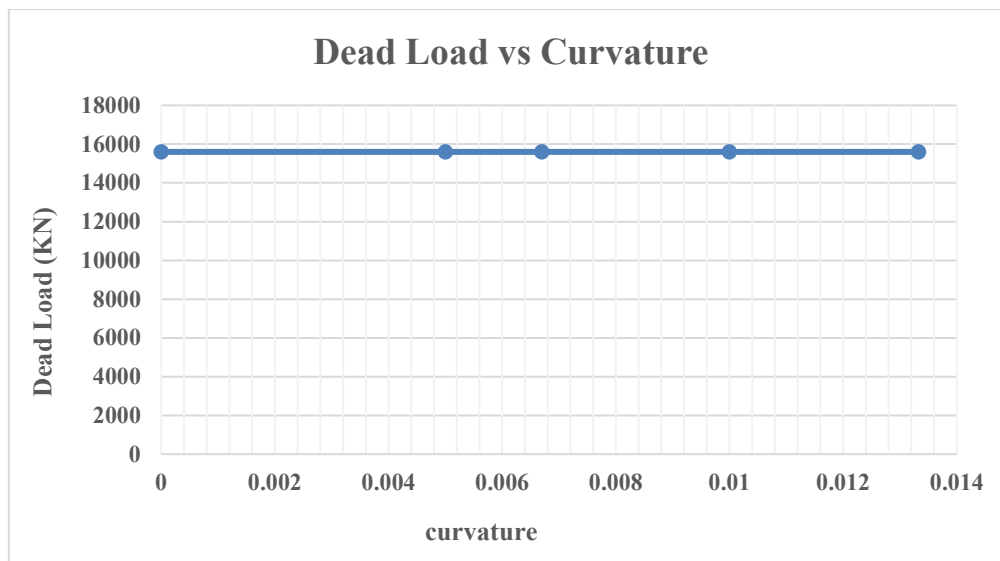


Graph 2. Variation of dead load with respect to skew angle for bridge with pile foundation

4.2.1.2 Variation of dead load with curvature



Graph 3. Variation of dead load with respect to curvature for bridge with pile foundation



Graph 4. Variation of dead load with respect to curvature for bridge with open foundation

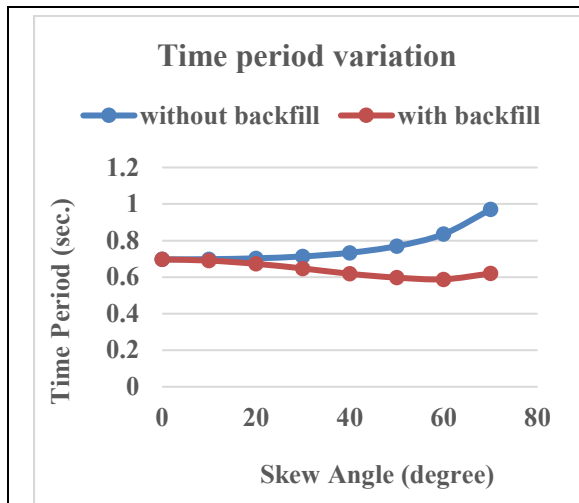
Thus, from the aforementioned graphs, it is evident that the dead load increases proportionally with the skew angle while remaining relatively consistent across different curvature values.

4.2.2 Variation of time period

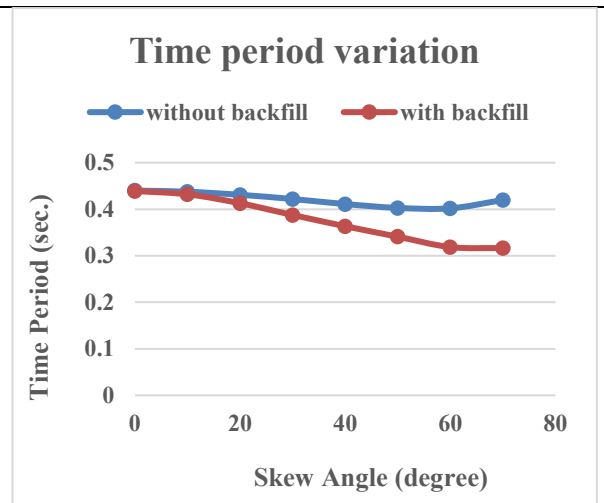
Graphical representations are plotted to illustrate the variation of time period values corresponding to the first mode of longitudinal and transverse modes of vibration with changes in the skew angle and the angle of plan curvature of the Integral Bridge. These visualizations aim to elucidate the nature of such variations induced by earthquake forces.

The degree of curvature is derived by taking the reciprocal of the radius (R in meters). Consequently, all graphs pertaining to curved bridges are plotted against the curvature (1/R). This analytical approach enables a comprehensive understanding of the impact of varying design parameters on the time period values associated with the bridge's modes of vibration.

4.2.2.1 Variation with skew angle

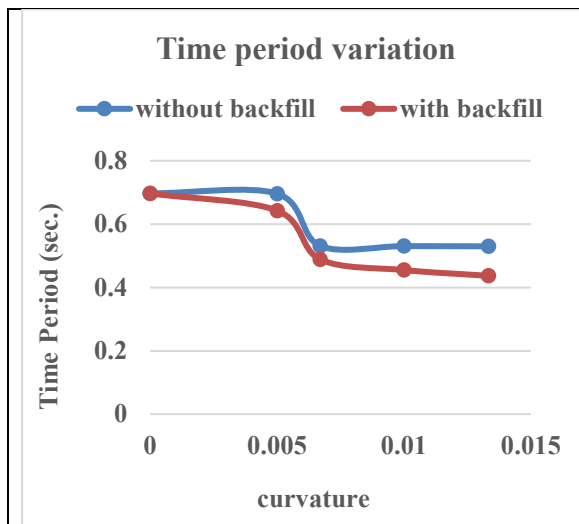


Graph 1. Comparison on variation of time period w.r.t. skew for bridge with pile foundation and with and without earth behind abutment.

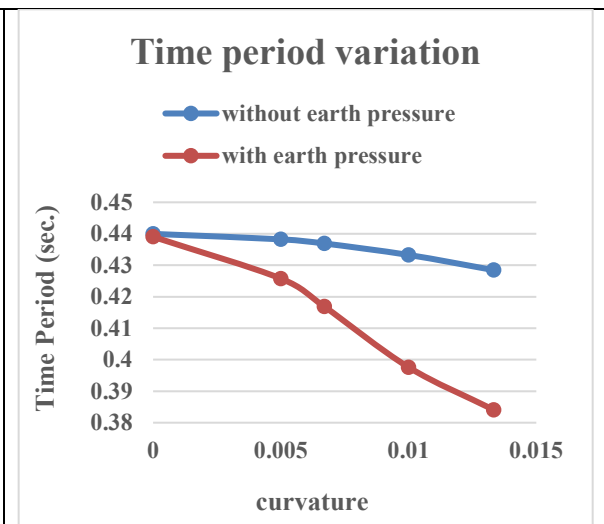


Graph 2. Comparison on variation of time period w.r.t. skew for bridge with open foundation and with and without earth behind abutment.

4.2.2.2 Variation with curvature



Graph 7. Comparison on variation of time period w.r.t. curvature for bridge with pile foundation and with and without earth behind abutment.



Graph 8. Comparison on variation of time period w.r.t. curvature for bridge with open foundation and with and without earth behind abutment.

Based on the observations drawn from the above graphs, the following conclusions can be made:

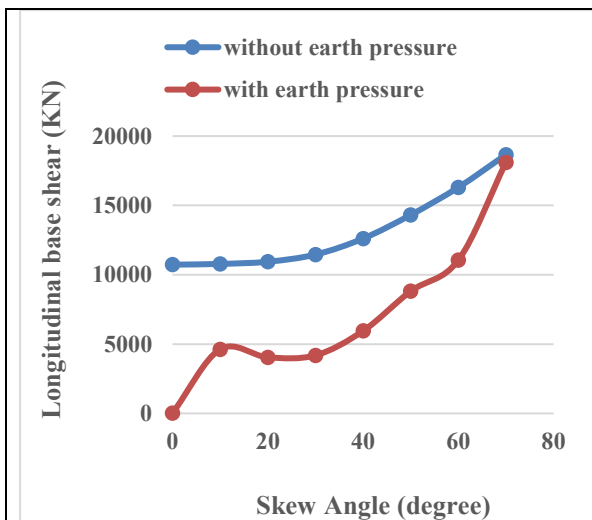
- The time period corresponding to the first mode for pile foundation without backfill increases with an increase in skew angle. However, for configurations with backfill, the time period initially decreases before exhibiting an increase.
- Conversely, the time period associated with the first mode for open foundation configurations with backfill decreases as the skew angle increases, while for configurations without backfill, the time period decreases at a slower rate.
- For integral bridges with open foundation and backfill, the time period experiences a rapid decrease with an increase in curvature, signifying a reduction in the radius of the curve. Conversely, for configurations without backfill, the time period decreases at a slower rate.
- Notably, the time period for bridges with pile foundations is consistently higher compared to those with open foundations.

4.2.3 Variation of base reaction

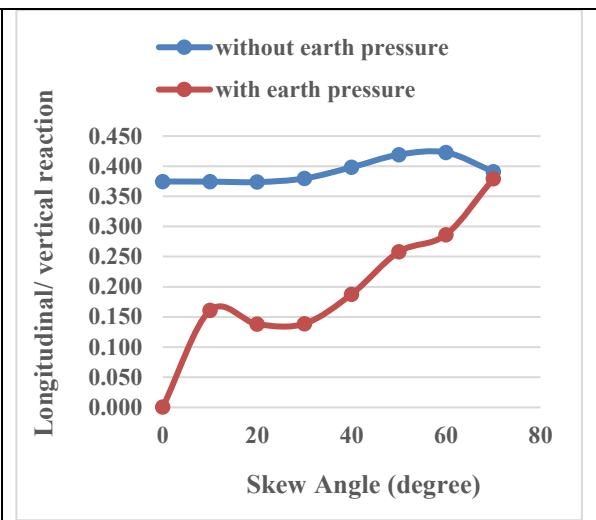
The base shear, representing the total lateral force exerted on the structure's base due to seismic activity, holds paramount importance in the seismic design of bridges. A comprehensive analysis of the variation in base shear for all model variants has been conducted, and the aggregated results are presented below.

The variation in base shear is depicted through two different graphical representations. Firstly, the total base shear is plotted against skew or curvature. Secondly, the ratio of base shear to total dead load (DL) is plotted against skew or curvature. The latter graph accounts for the varying dead load with skew, thereby providing a more accurate depiction of the actual variation in base shear. Both graphical representations offer valuable insights into the behavior of the structure under seismic loading conditions, considering the influence of skew or curvature variations and their interaction with the dead load.

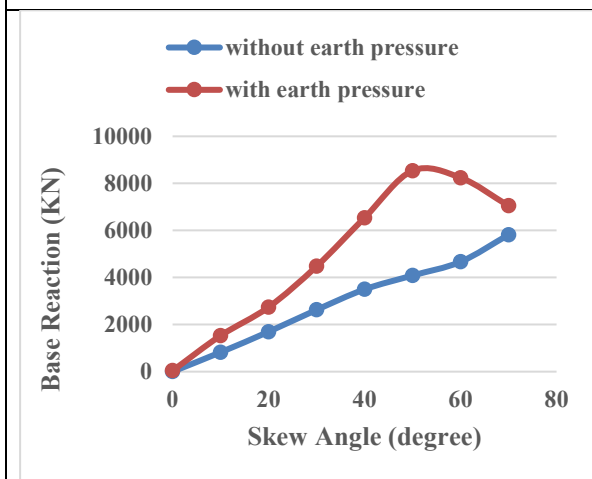
4.2.3.1 Variation with skew angle in longitudinal seismic case



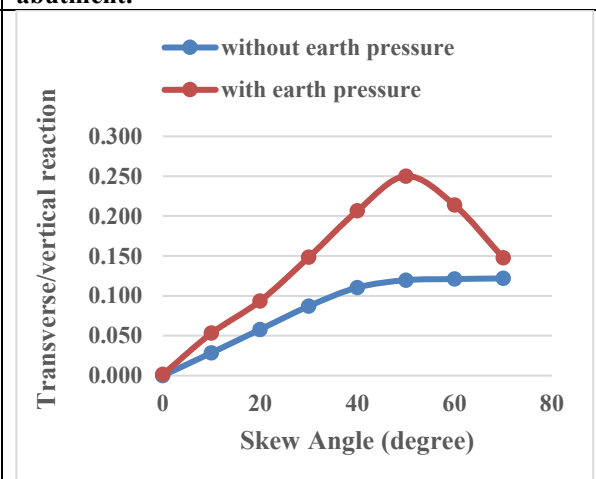
Graph 9. Comparison on longitudinal base shear w.r.t. skew with pile foundation and with or without earth behind abutment.



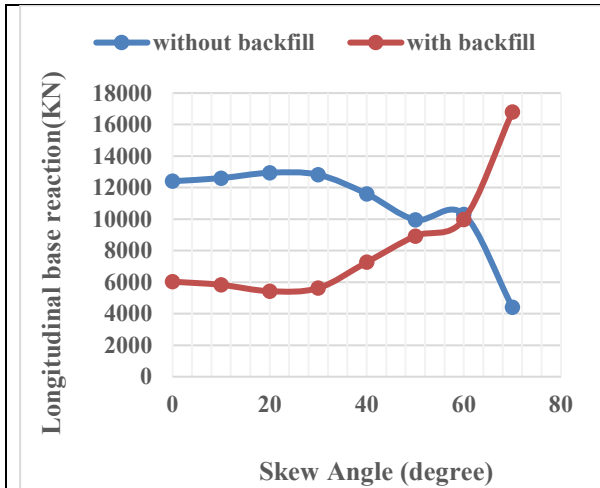
Graph 10. Comparison on longitudinal base shear/Vertical reaction w.r.t. skew with pile foundation and with or without earth behind abutment.



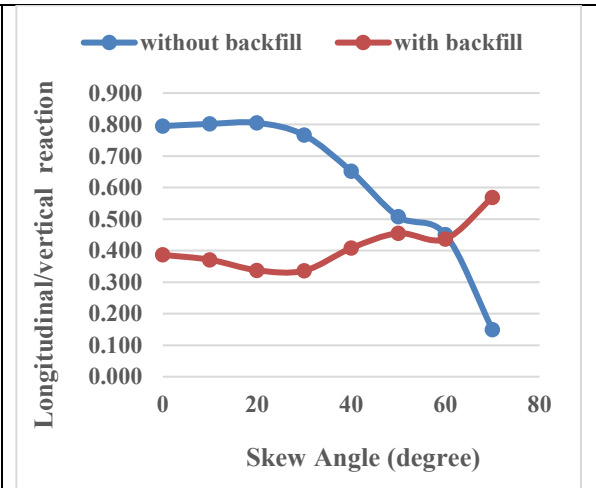
Graph 11. Comparison on transverse base shear w.r.t. skew with pile foundation and with or without earth behind abutment.



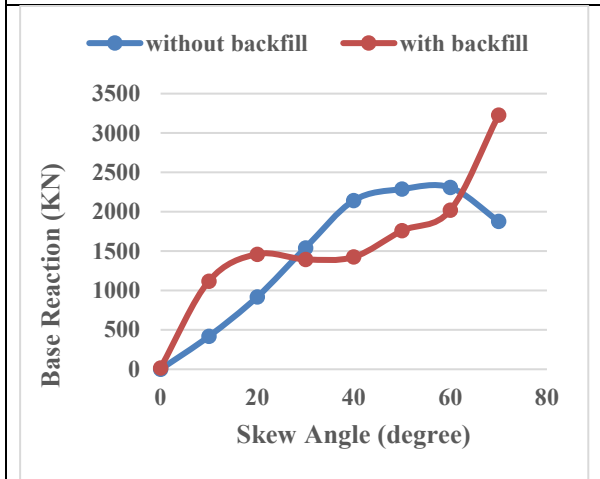
Graph 12. Comparison on transverse base shear/vertical reaction w.r.t. skew with pile foundation and with or without earth behind abutment.



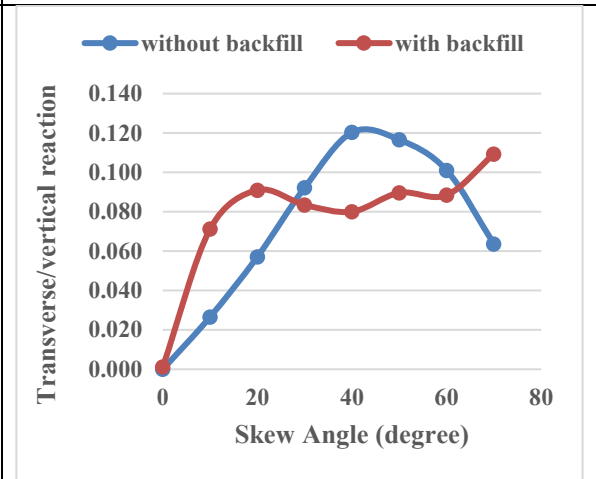
Graph 13. Comparison on longitudinal base shear w.r.t. skew with open foundation and with or without earth behind abutment.



Graph 14. Comparison on longitudinal/vertical base shear w.r.t. skew with open foundation and with or without earth behind abutment.

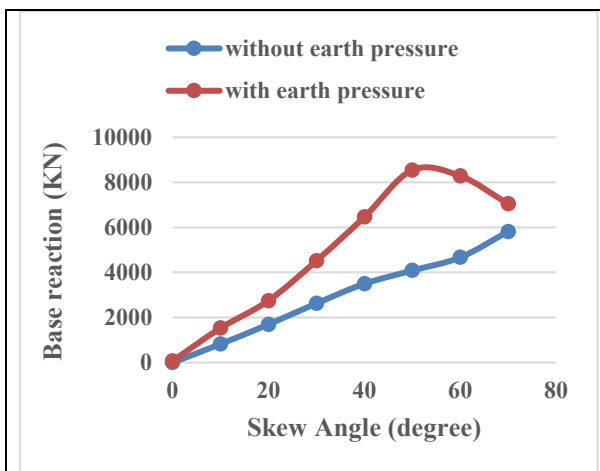


Graph 15. Comparison on transverse base shear w.r.t. skew with open foundation and with or without earth behind abutment.

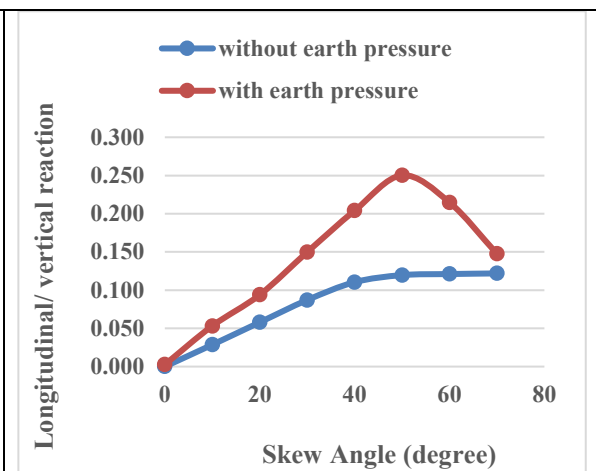


Graph 16. Comparison on transverse/vertical base shear w.r.t. skew with open foundation and with or without earth behind abutment.

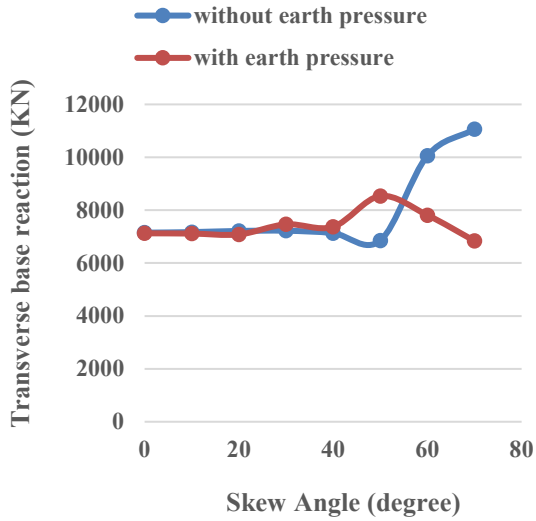
4.2.3.2 Variation with skew angle in transverse seismic case



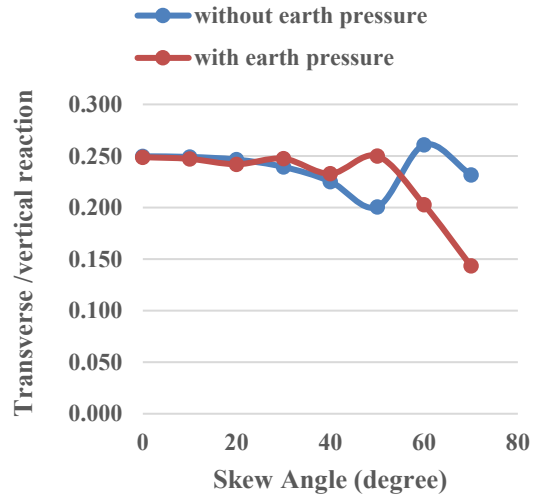
Graph 17. Variation on longitudinal base shear w.r.t. skew with pile foundation and with or without earth behind abutment.



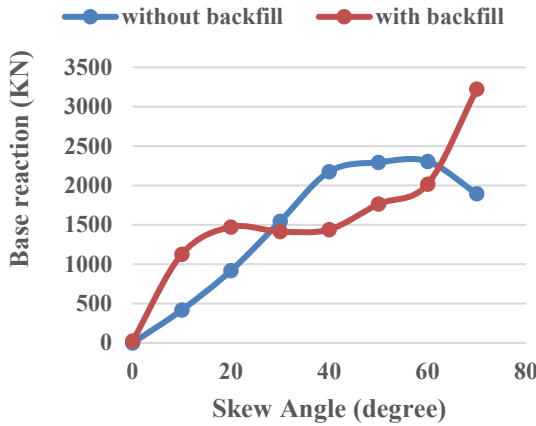
Graph 18. Variation on longitudinal base shear/vertical base shear w.r.t. skew with pile foundation and with or without earth behind abutment.



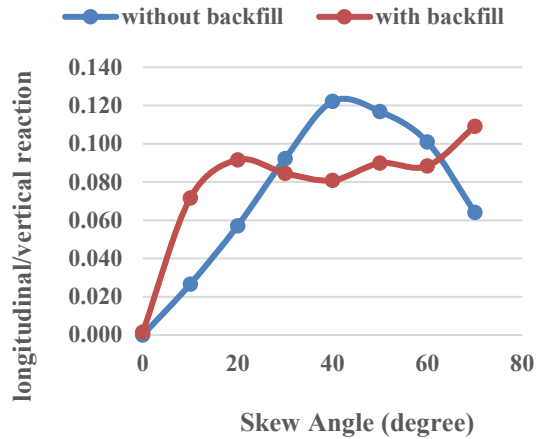
Graph 19. Variation on transverse base shear w.r.t. skew with pile foundation and with or without earth behind abutment.



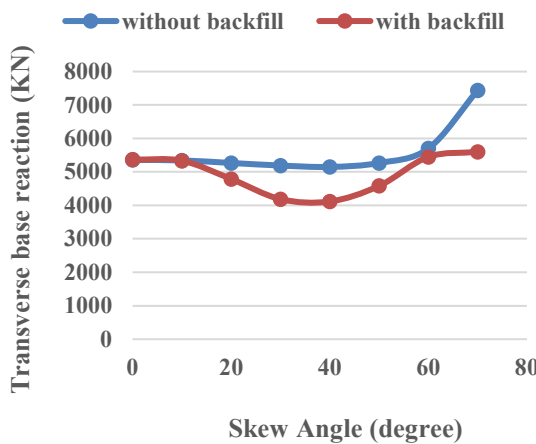
Graph 20. Variation on transverse base shear/vertical base shear w.r.t. skew with pile foundation and with or without earth behind abutment.



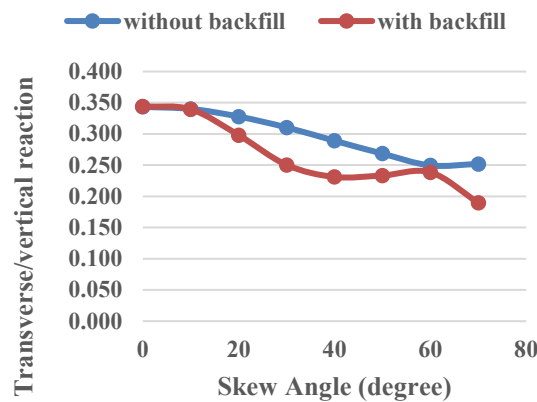
Graph 21. Variation on longitudinal base shear w.r.t. skew with open foundation and with or without earth behind abutment.



Graph 22. Variation on longitudinal base shear/vertical base shear w.r.t. skew with open foundation and with or without earth behind abutment.

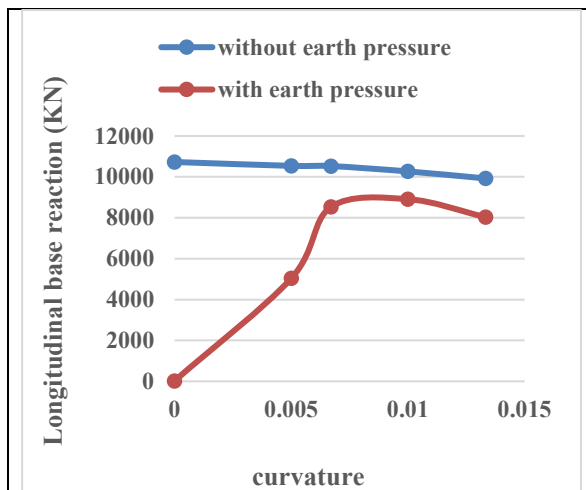


Graph 23. Variation on transverse base shear w.r.t. skew with open foundation and with or without earth behind abutment.

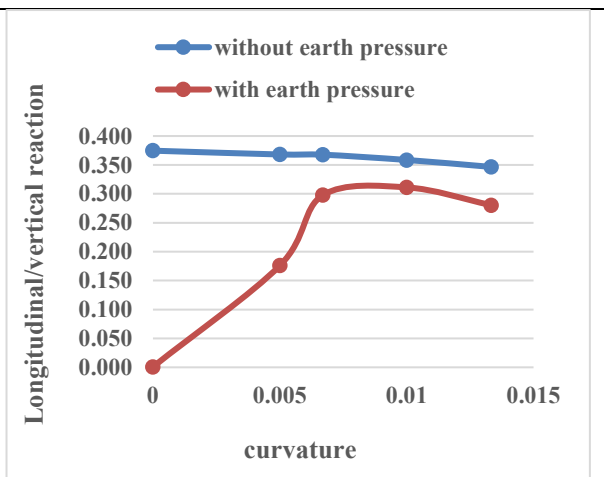


Graph 24. Variation on transverse base shear/vertical base shear w.r.t. skew with open foundation and with or without earth behind abutment.

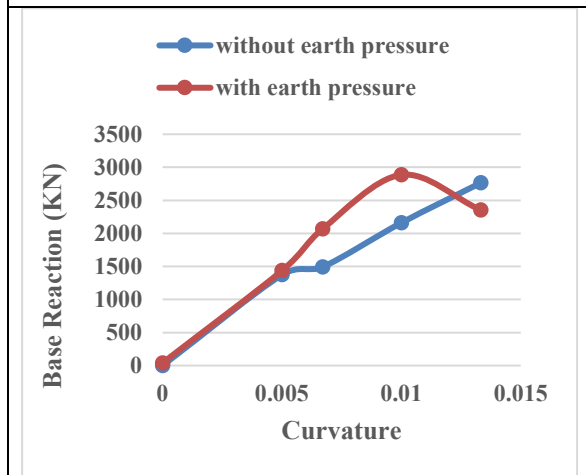
4.2.3.3 Variation with curvature in longitudinal seismic case



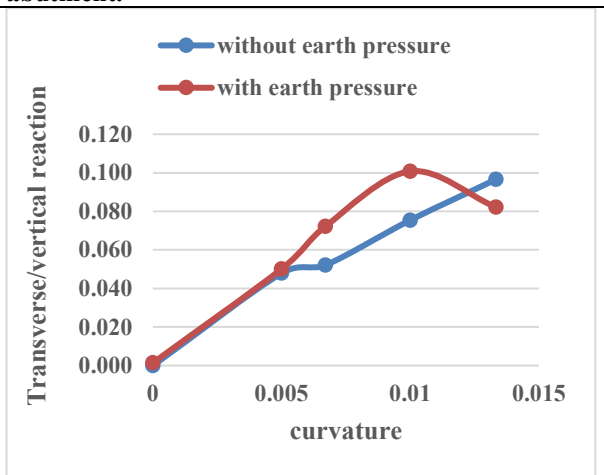
Graph 25. Variation on longitudinal base shear w.r.t. curvature with pile foundation and with or without earth behind abutment.



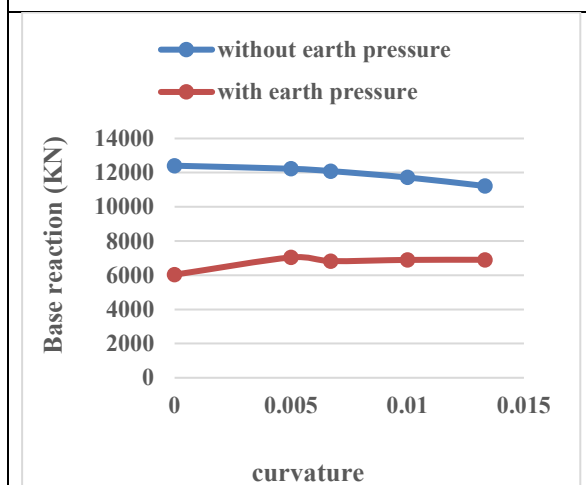
Graph 26. Variation on longitudinal base shear/vertical base shear w.r.t. curvature with pile foundation and with or without earth behind abutment.



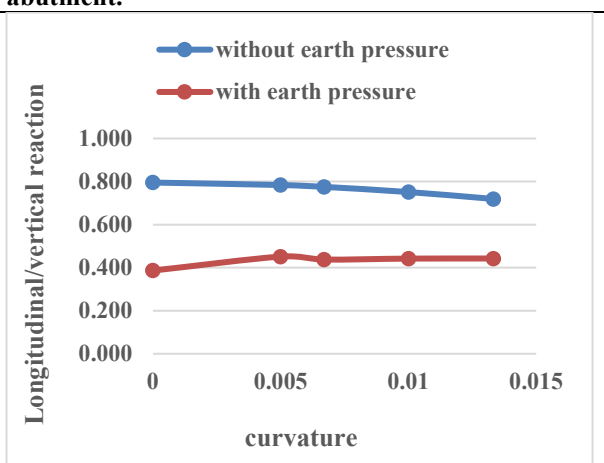
Graph 27. Variation on transverse base shear w.r.t. curvature with pile foundation and with or without earth behind abutment.



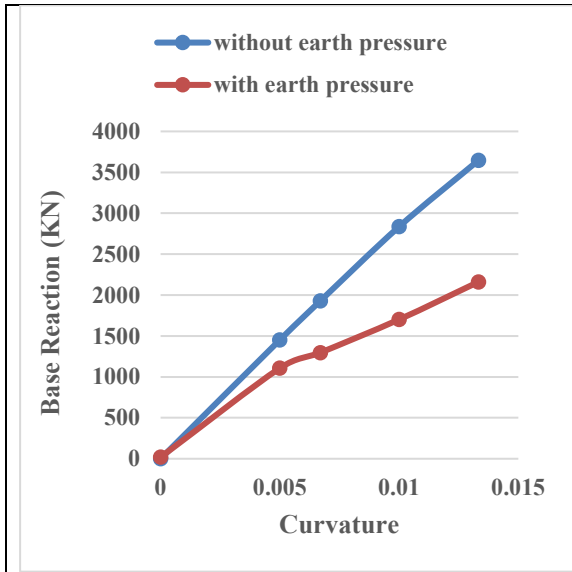
Graph 28. Variation on transverse base shear/vertical base shear w.r.t. curvature with pile foundation and with or without earth behind abutment.



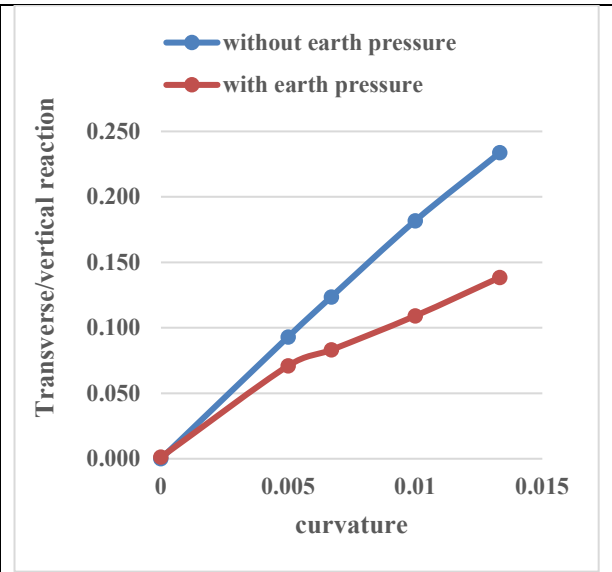
Graph 29. Variation on longitudinal base shear w.r.t. curvature with open foundation and with or without earth behind abutment.



Graph 30. Variation on longitudinal base shear/vertical base shear w.r.t. curvature with open foundation and with or without earth behind abutment.

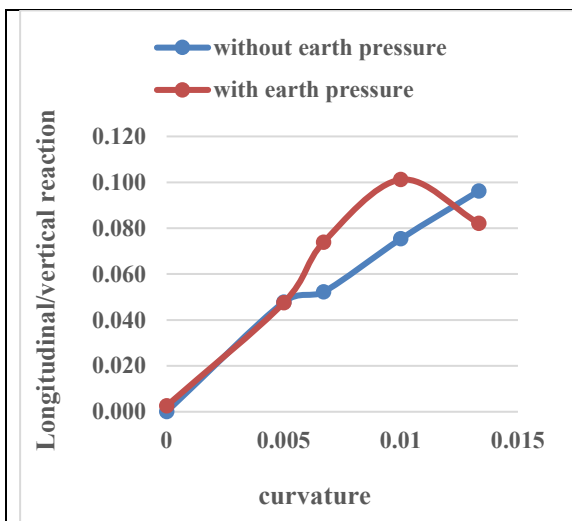


Graph 31. Variation on transverse base shear w.r.t. curvature with open foundation and with or without earth behind abutment.

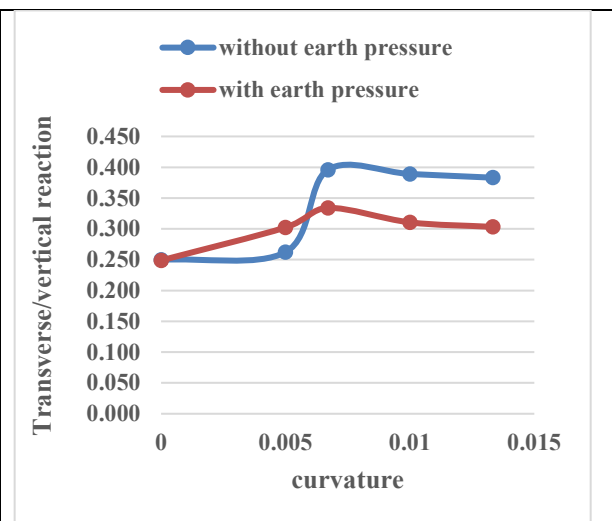


Graph 32. Variation on transverse base shear/vertical base shear w.r.t. curvature with open foundation and with or without earth behind abutment.

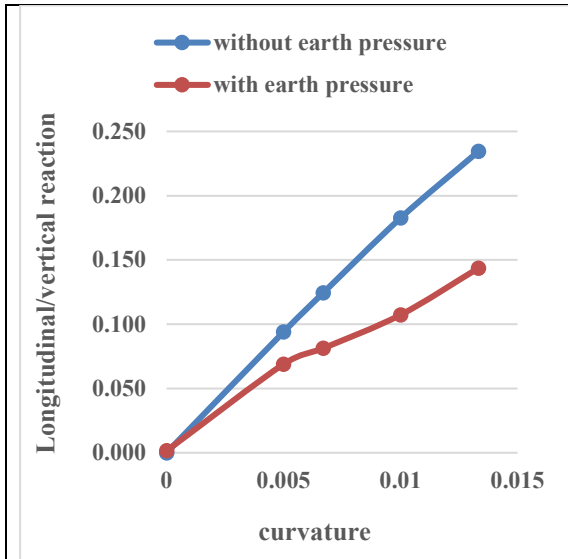
4.2.3.4 Variation with curvature in transverse seismic case



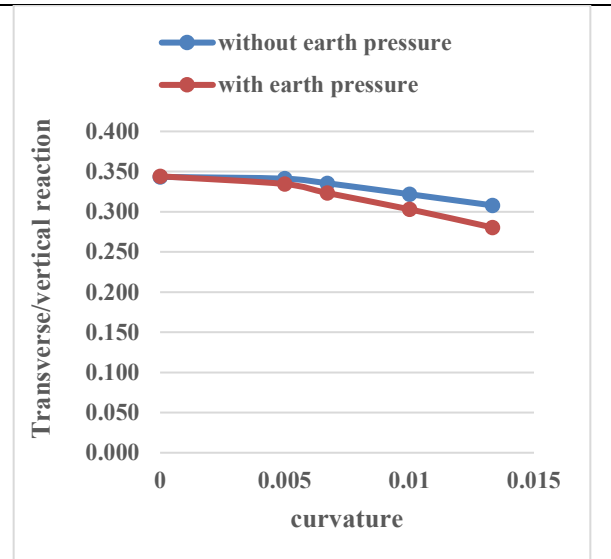
Graph 33. Variation on longitudinal base shear/vertical base shear w.r.t. curvature with pile foundation and with or without earth behind abutment.



Graph 34. Variation on transverse base shear/vertical base shear w.r.t. curvature with pile foundation and with or without earth behind abutment.



Graph 35. Variation on longitudinal base shear/vertical w.r.t. curvature with open foundation and with or without earth behind abutment.



Graph 36. Variation on transverse base shear/vertical base shear w.r.t. curvature with open foundation and with or without earth behind abutment.

Based on the analysis of the aforementioned graphs, the following observations can be made:
For the longitudinal seismic case:

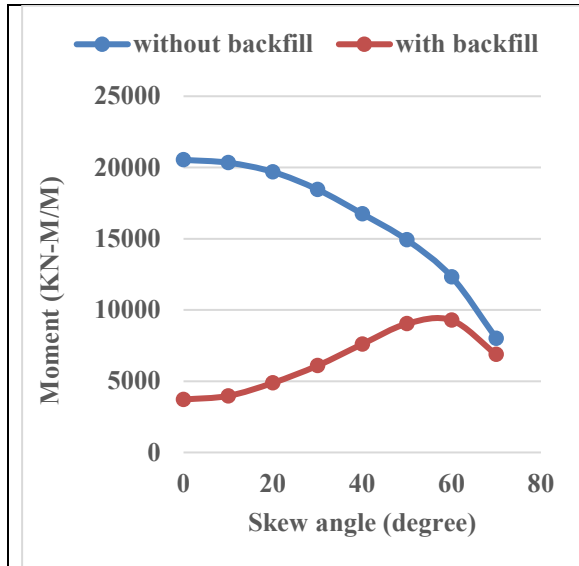
- The longitudinal base shear/vertical reaction increases with the skew angle for pile foundation configurations. Conversely, for bridges with open foundations and backfill abutments, the ratio initially decreases before increasing with the skew angle. However, the rate of decrease is more pronounced for bridges with backfill compared to those without.
- Transverse base shear/vertical reaction initially increases and then decreases with the skew angle. The rate of increase is higher for bridges with backfill compared to those without.
- The longitudinal base shear/vertical reaction is higher for bridges with pile foundations and backfill abutments, while it is greater for bridges with open foundations and without backfill abutments. Similarly, the transverse base shear/vertical reaction is higher for bridges with pile foundations and backfill abutments.
- The longitudinal base shear/vertical reaction is greater for bridges without backfill compared to those with backfill.
- Longitudinal base shear/vertical reaction slightly increases with an increase in curvature for bridges with backfill, while it remains nearly constant for bridges without backfill.
- Bridges with open foundations exhibit higher longitudinal reactions compared to those with pile foundations.
- Transverse base shear is zero for bridges with all curvatures and no skew.

For transverse seismic case:

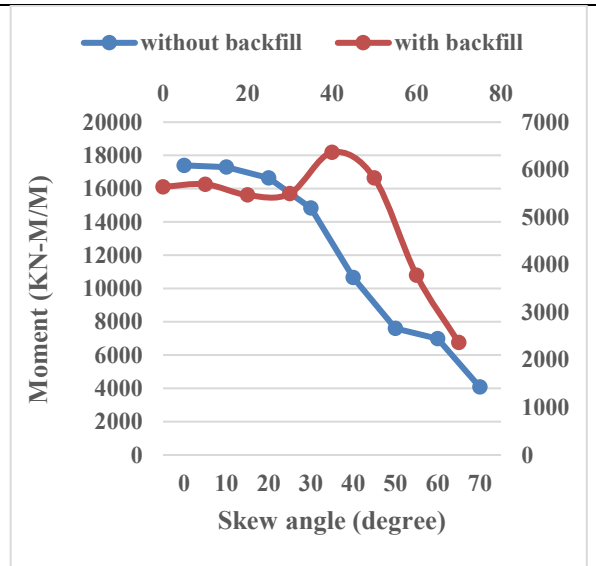
- The longitudinal base shear/vertical reaction is higher for bridges with backfill compared to those without. Initially, it increases with the skew angle before decreasing. Moreover, it is higher for bridges with pile foundations compared to those with open foundations.
- The transverse base shear/vertical reaction decreases for bridges with backfill and increases for those without, with pile foundation. Furthermore, it is higher for bridges with open foundations compared to those with pile foundations.
- The longitudinal base shear is zero for bridges of all curvatures without skew.
- For pile foundations with backfill, the transverse/vertical reaction increases with curvature, while it decreases for open foundation configurations.

4.2.4 Variation of the moment at abutment in longitudinal seismic condition

4.2.4.1 Variation of the longitudinal moment at the top of abutment wall with skew angle in longitudinal seismic

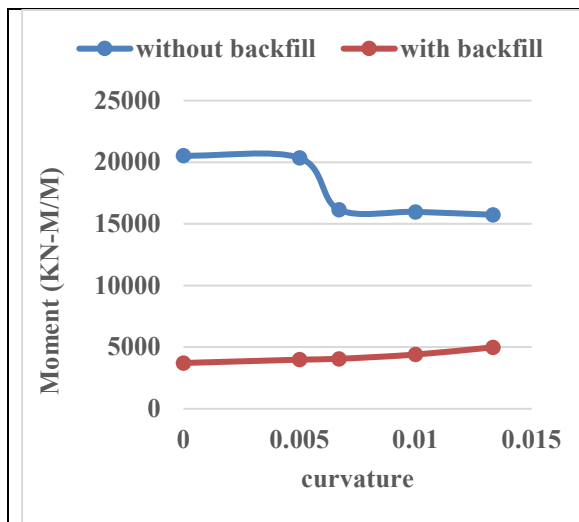


Graph 37. Variation of longitudinal moment at top of abutment w.r.t. skew with pile foundation with or without earth behind abutment.

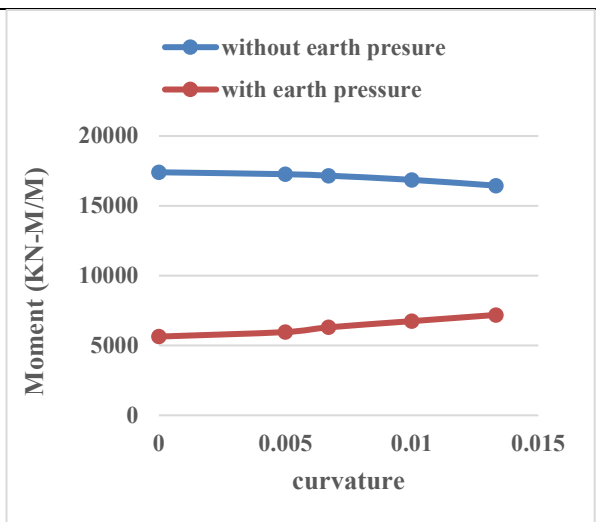


Graph 38. Variation of longitudinal moment at top of abutment w.r.t. skew with open foundation with or without earth behind abutment.

4.2.4.2 Variation of longitudinal moment at top of abutment with curvature in longitudinal seismic

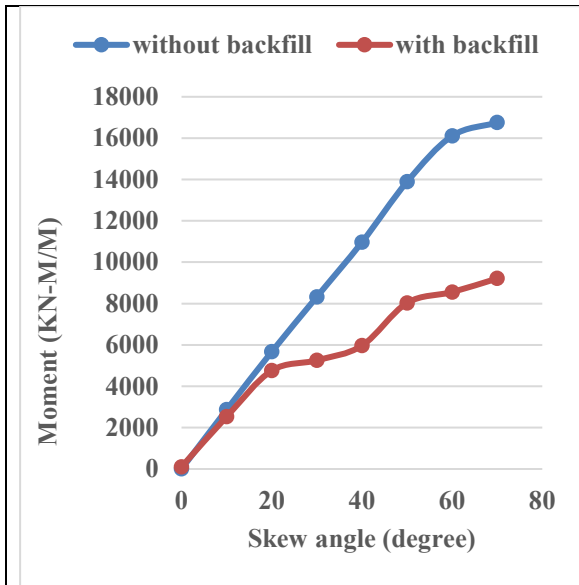


Graph 39. Variation of longitudinal moment at top of abutment w.r.t. curvature with pile foundation with or without earth behind abutment.

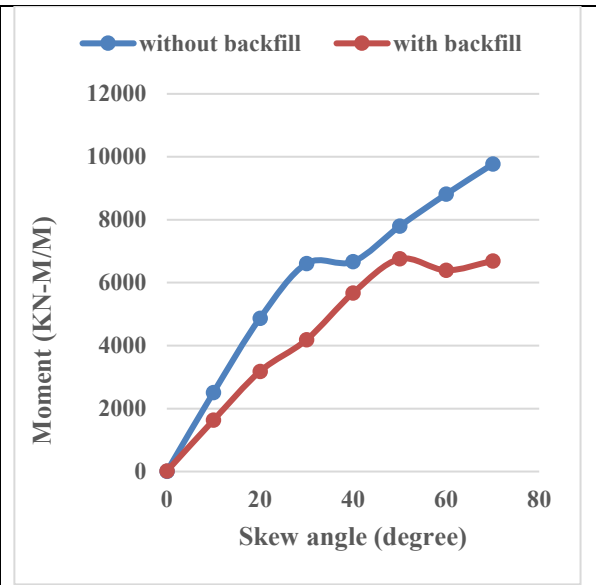


Graph 40. Variation of longitudinal moment at top of abutment w.r.t. curvature with open foundation with or without earth behind abutment.

4.2.4.3 Variation of transverse moment at top of abutment with skew angle in longitudinal seismic

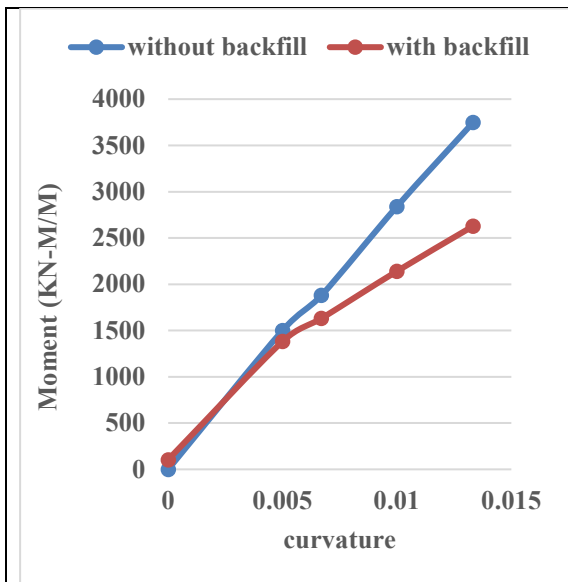


Graph 41. Variation of transverse moment at top of abutment w.r.t. skew with pile foundation with or without earth behind abutment.

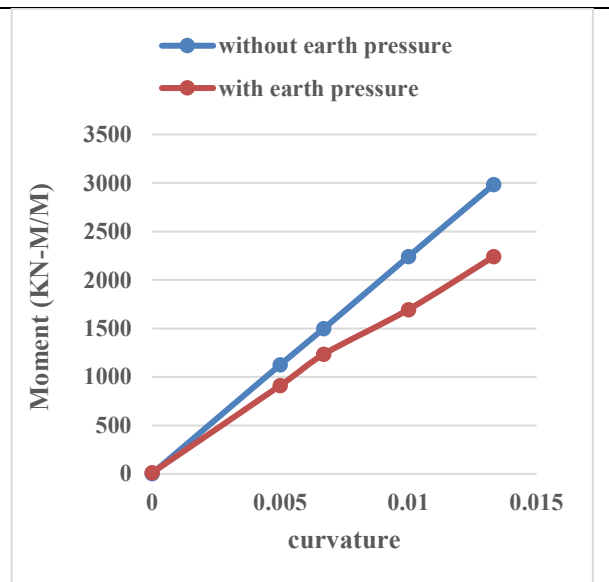


Graph 42. Variation of transverse moment at top of abutment w.r.t. skew with open foundation with or without earth behind abutment.

4.2.4.4 Variation of transverse moment at top of abutment with curvature in longitudinal seismic

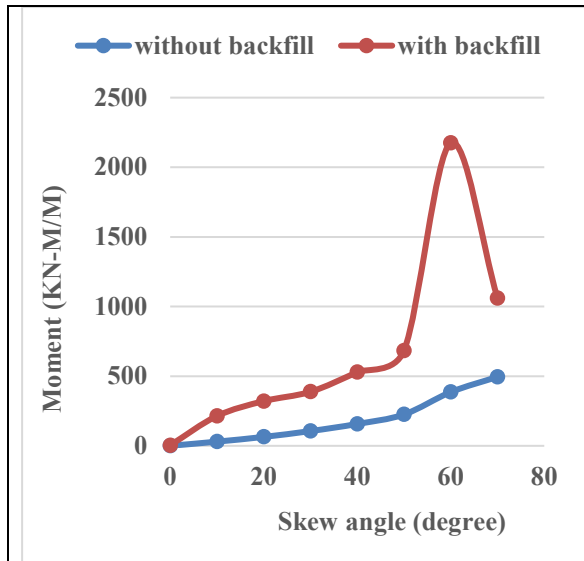


Graph 43. Variation of transverse moment at top of abutment w.r.t. curvature with pile foundation with or without earth behind abutment.

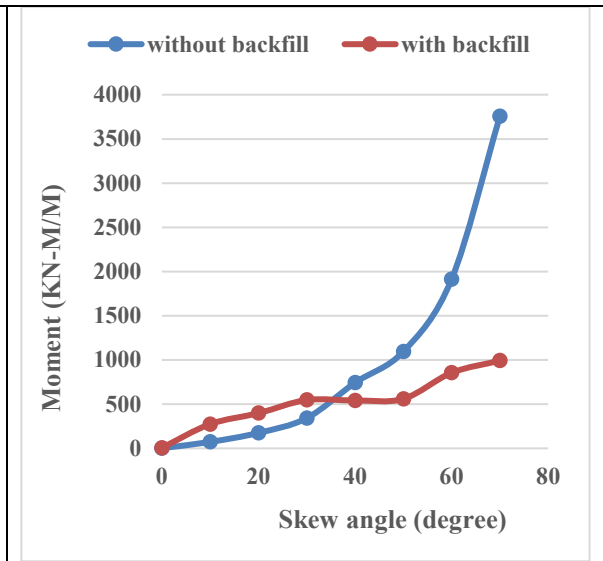


Graph 44. Variation of transverse moment at top of abutment w.r.t. curvature with open foundation with or without earth behind abutment.

4.2.4.5 Variation of torsional moment at top of abutment with skew angle in longitudinal seismic

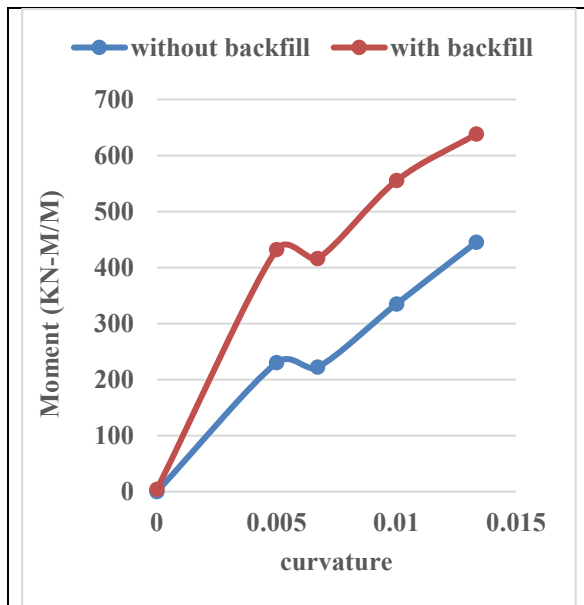


Graph 45. Variation of torsion at top of abutment w.r.t. skew with pile foundation with or without earth behind abutment.

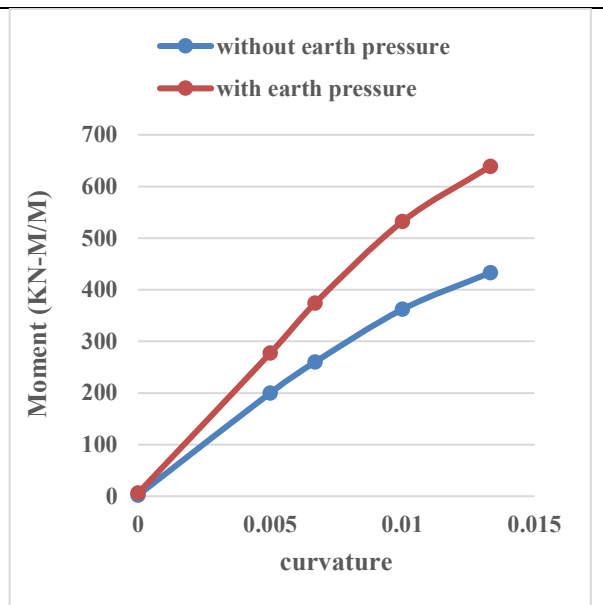


Graph 46. Variation of torsion at top of abutment w.r.t. skew with open foundation with or without earth behind abutment.

4.2.4.6 Variation of torsional moment at top of abutment with curvature in longitudinal seismic

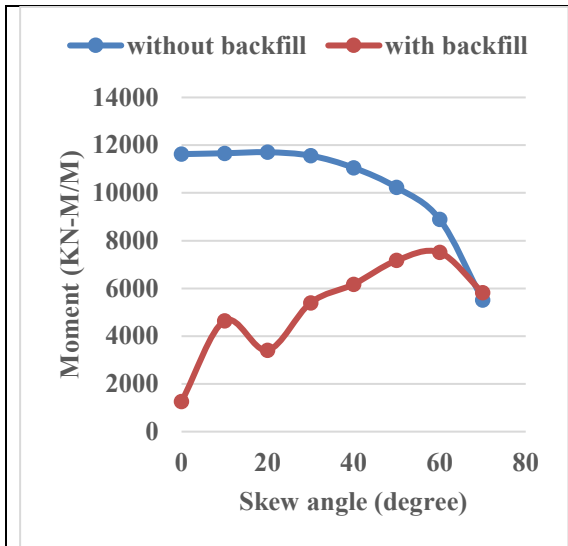


Graph 47. Variation of torsion at top of abutment w.r.t. curvature with pile foundation with or without earth behind abutment.

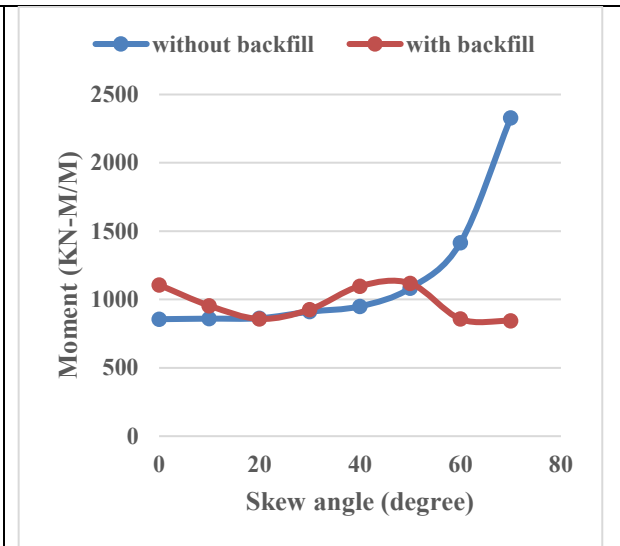


Graph 48. Variation of torsion at top of abutment w.r.t. curvature with open foundation with or without earth behind abutment.

4.2.4.7 Variation of longitudinal moment at bottom of abutment with skew angle in longitudinal seismic

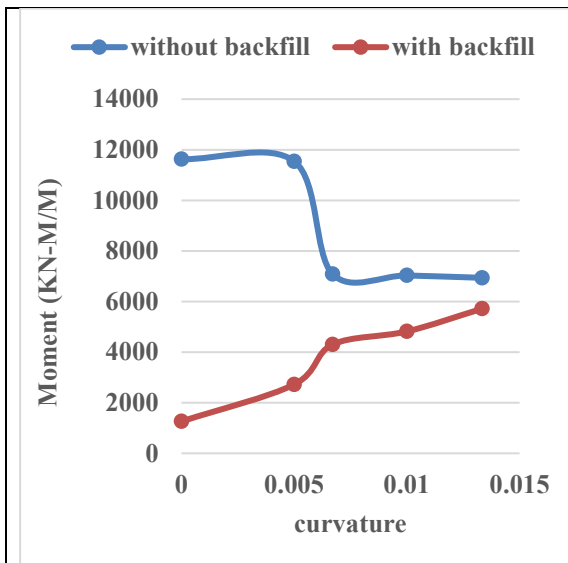


Graph 49. Variation of longitudinal moment at bottom of abutment w.r.t. skew with pile foundation with or without earth behind abutment.

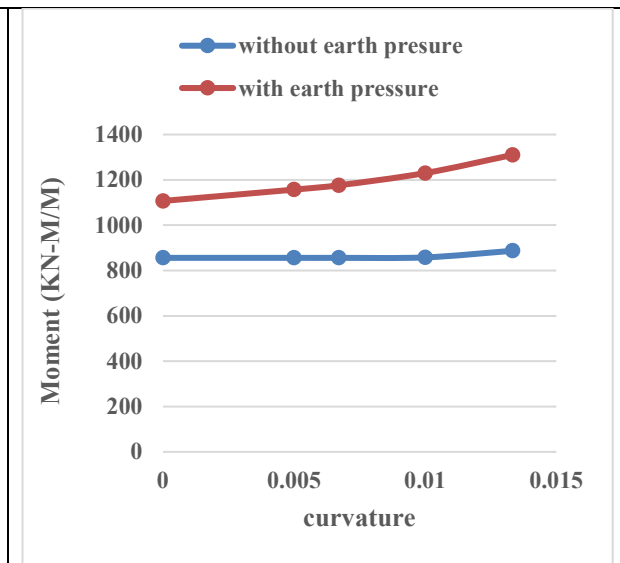


Graph 50. Variation of longitudinal moment at bottom of abutment w.r.t. skew with open foundation with or without earth behind abutment.

4.2.4.8 Variation of longitudinal moment at bottom of abutment with curvature in longitudinal seismic

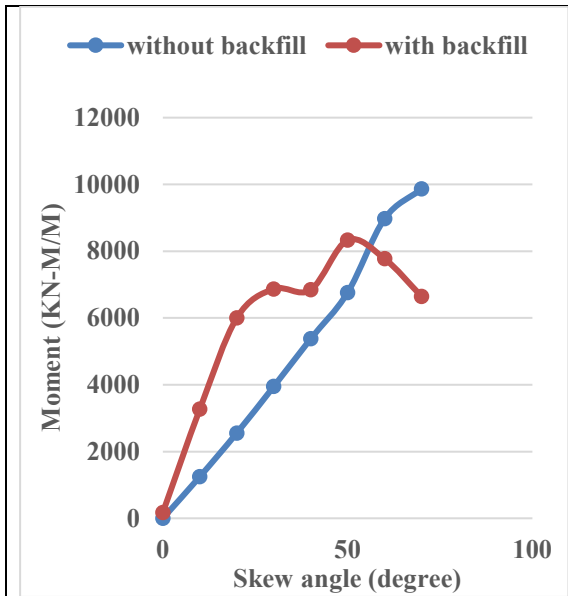


Graph 51. Variation of longitudinal moment at bottom of abutment w.r.t. curvature with pile foundation with or without earth behind abutment.

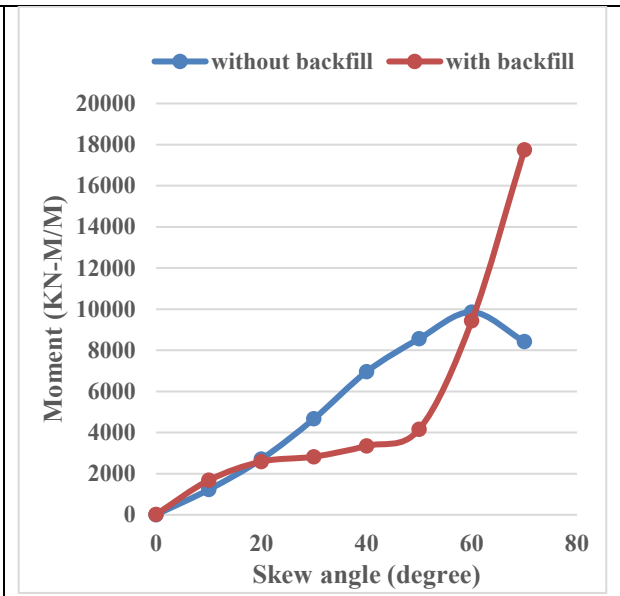


Graph 52. Variation of longitudinal moment at bottom of abutment w.r.t. curvature with open foundation with or without earth behind abutment.

4.2.4.9 Variation of transverse moment at bottom of abutment with skew angle in longitudinal seismic

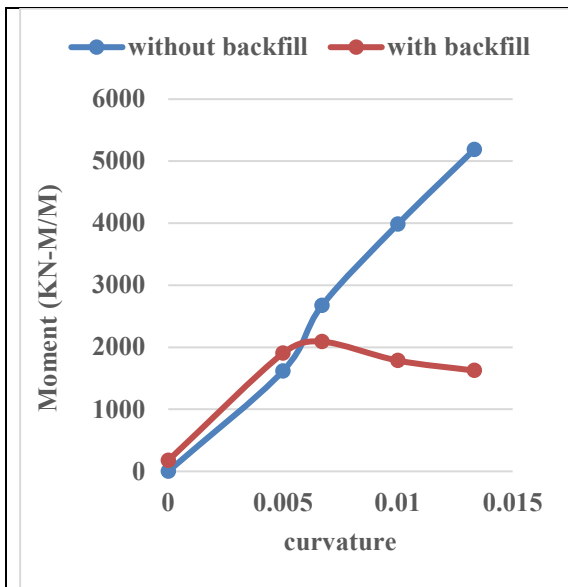


Graph 53. Variation of transverse moment at bottom of abutment w.r.t. skew with pile foundation with or without earth behind abutment.

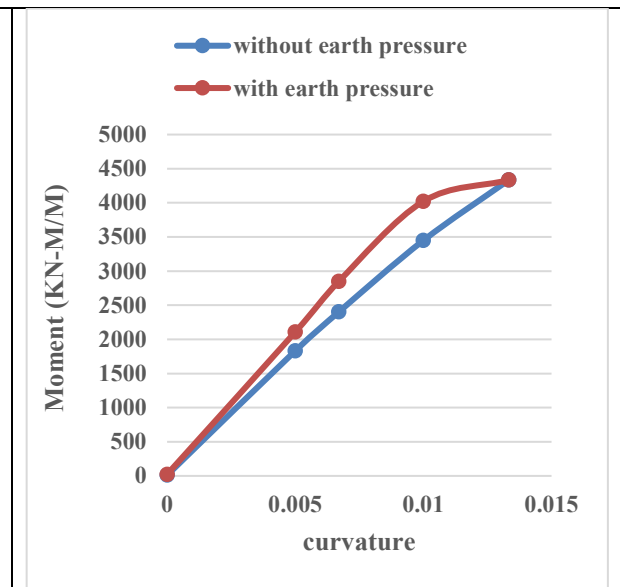


Graph 54. Variation of transverse moment at bottom of abutment w.r.t. skew with open foundation with or without earth behind abutment.

4.2.4.10 Variation of transverse moment at bottom of abutment with curvature in longitudinal seismic

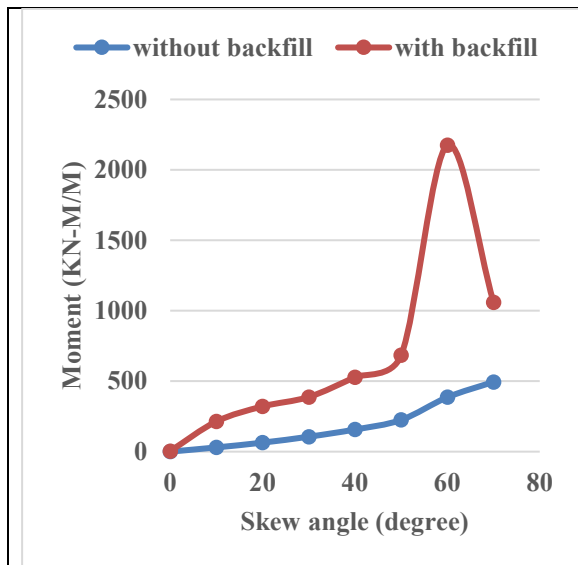


Graph 55. Variation of transverse moment at bottom of abutment w.r.t. curvature with pile foundation with or without earth behind abutment.

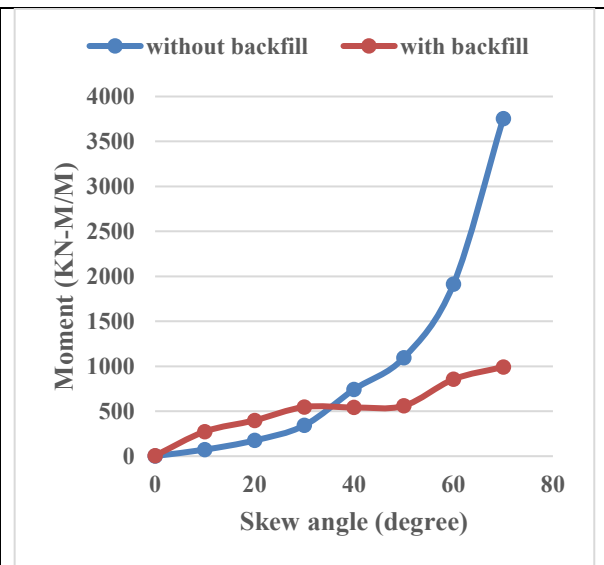


Graph 56. Variation of transverse moment at bottom of abutment w.r.t. curvature with open foundation with or without earth behind abutment.

4.2.4.11 Variation of torsional moment at bottom of abutment with skew angle in longitudinal seismic

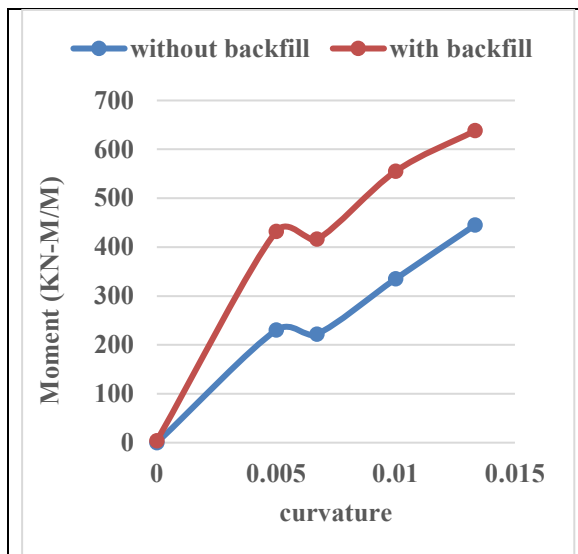


Graph 57. Variation of torsion at bottom of abutment w.r.t. skew with pile foundation with or without earth behind abutment.

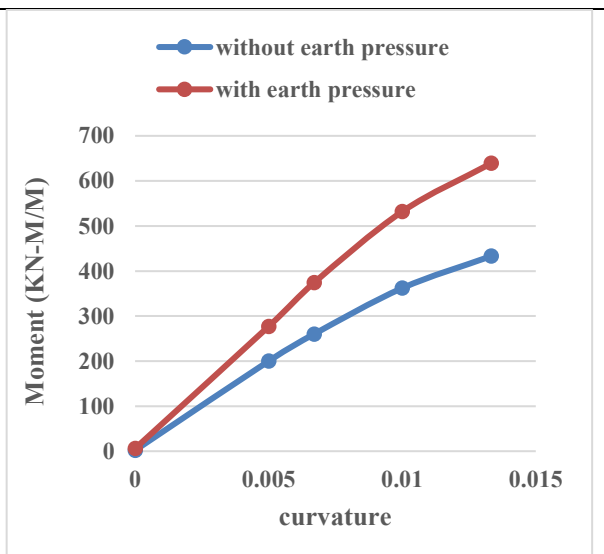


Graph 58. Variation of torsion at bottom of abutment w.r.t. skew with open foundation with or without earth behind abutment.

4.2.4.12 Variation of torsional moment at bottom of abutment with curvature in longitudinal seismic



Graph 59. Variation of torsion at bottom of abutment w.r.t. curvature with pile foundation with or without earth behind abutment.



Graph 60. Variation of torsion at bottom of abutment w.r.t. curvature with open foundation with or without earth behind abutment.

Based on the analysis of the provided data and graphs, the following observations can be made regarding the longitudinal seismic case:

- The longitudinal moment at the top of the abutment decreases with an increase in skew angle for both open and pile foundation configurations. The moment is higher for bridges without backfill compared to those with backfill, and it is greater for pile foundation structures than for open foundation ones.
- The longitudinal moment at the top of the abutment increases with an increase in curvature for both open and pile foundation configurations. Similar to the skew angle, the moment is higher for bridges without

backfill and for open foundation structures.

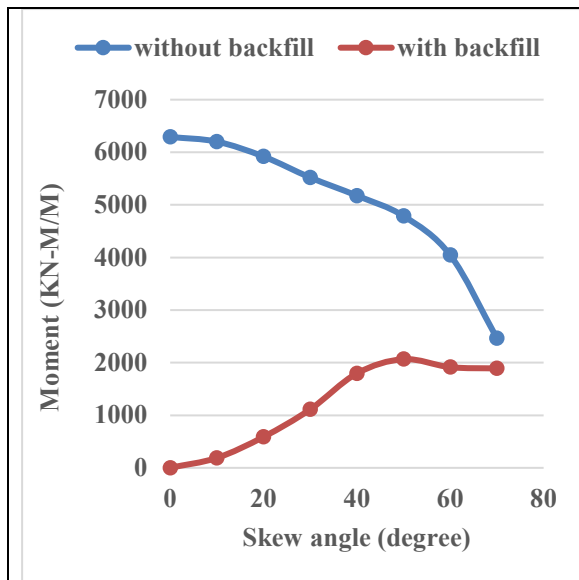
- The transverse moment at the top of the abutment increases with an increase in skew angle for both open and pile foundation configurations, with a higher rate of increase observed for bridges without backfill. Moreover, the moment is higher for pile foundation structures.
- The transverse moment at the top of the abutment increases with an increase in curvature for both open and pile foundation configurations, with a higher moment observed for bridges without backfill.
- Torsion at the top of the abutment initially increases and then decreases with an increase in skew angle for pile foundation configurations, while it consistently increases for open foundation configurations.
- Torsion at the top of the abutment increases with an increase in curvature for both open and pile foundation configurations, with a higher rate of increase observed for bridges with backfill.

Regarding the observations for the bottom of the abutment:

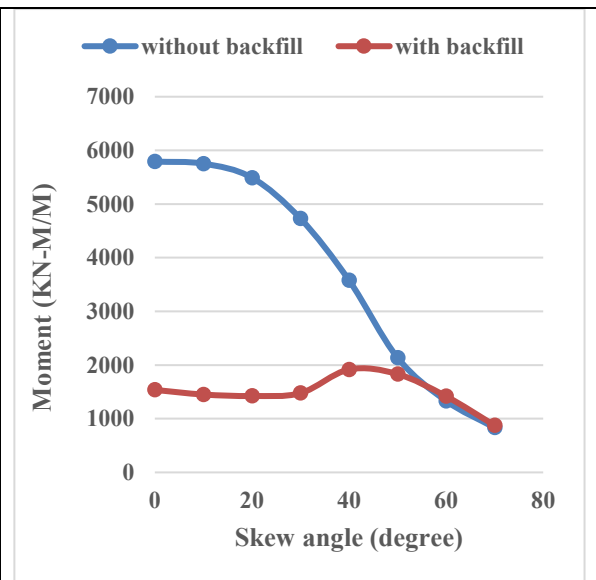
- The longitudinal moment decreases with an increase in skew angle for both open and pile foundation configurations, with a higher rate of decrease observed for bridges without backfill.
- The longitudinal moment increases with an increase in curvature for pile foundation structures, while it remains almost constant for open foundation configurations.
- The transverse moment increases with an increase in skew angle for bridges without backfill, whereas for bridges with pile foundation and backfill, it initially increases and then decreases with the skew angle.
- The transverse moment increases with an increase in curvature.
- Torsion at the bottom of the abutment initially increases and then decreases with an increase in skew angle for bridges with pile foundation and backfill, while it consistently increases rapidly for bridges with open foundation and without backfill.
- Torsion at the bottom of the abutment increases with the increase in curvature, with higher torsional effects observed for bridges with pile foundations compared to those with open foundations, especially for curved bridges.

4.2.5 Variation of the moment at bent columns in longitudinal seismic condition

4.2.5.1 Variation of longitudinal moment at top of bent columns with skew angle in longitudinal seismic

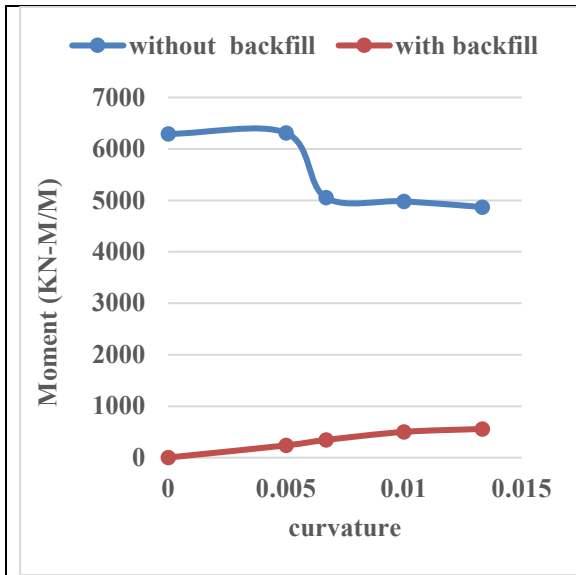


Graph 61. Variation of longitudinal moment at top of bent w.r.t. skew with pile foundation with or without earth behind abutment.

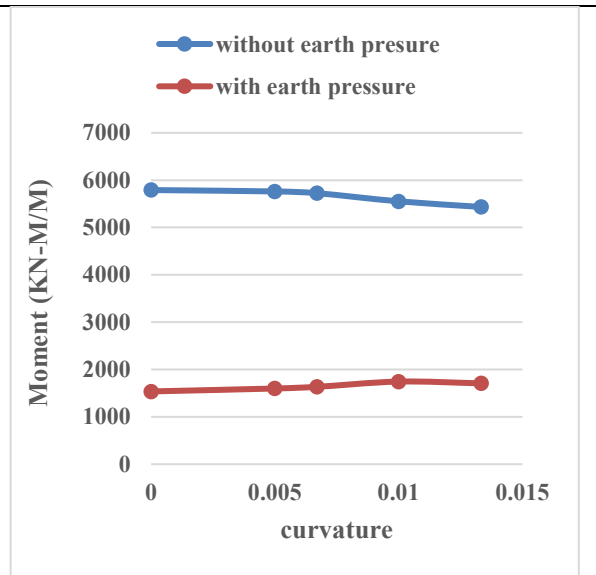


Graph 62. Variation of longitudinal moment at top of bent w.r.t. skew with open foundation with or without earth behind abutment.

4.2.5.2 Variation of longitudinal moment at top of bent columns with curvature in longitudinal seismic

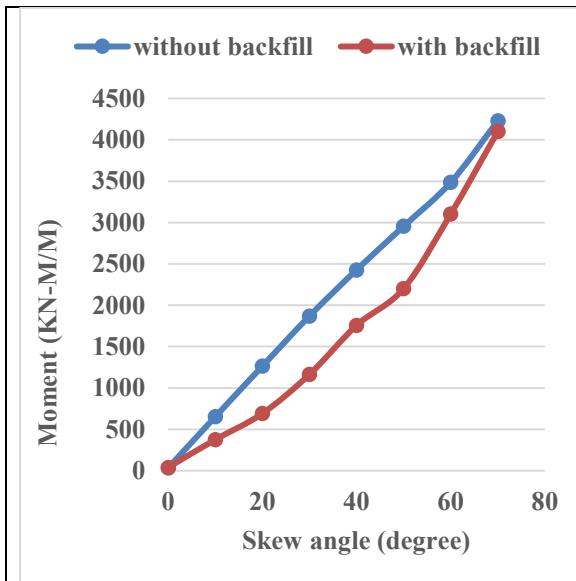


Graph 63. Variation of longitudinal moment at top of bent w.r.t. curvature with pile foundation with or without earth behind abutment.

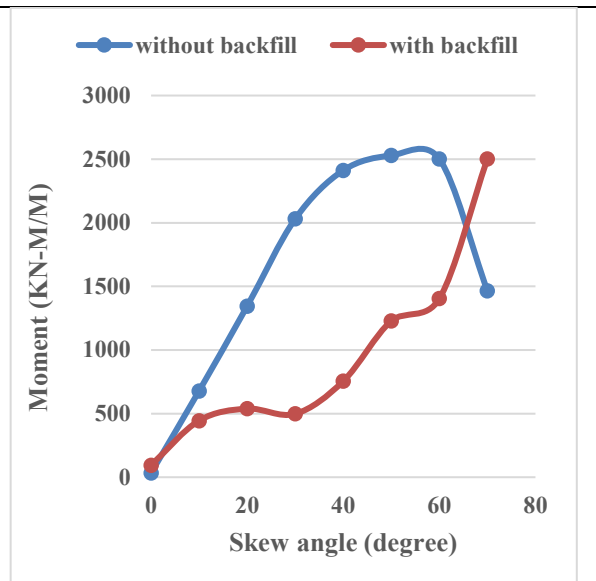


Graph 64. Variation of longitudinal moment at top of bent w.r.t. curvature with open foundation with or without earth behind abutment.

4.2.5.3 Variation of transverse moment at top of bent columns with skew angle in longitudinal seismic

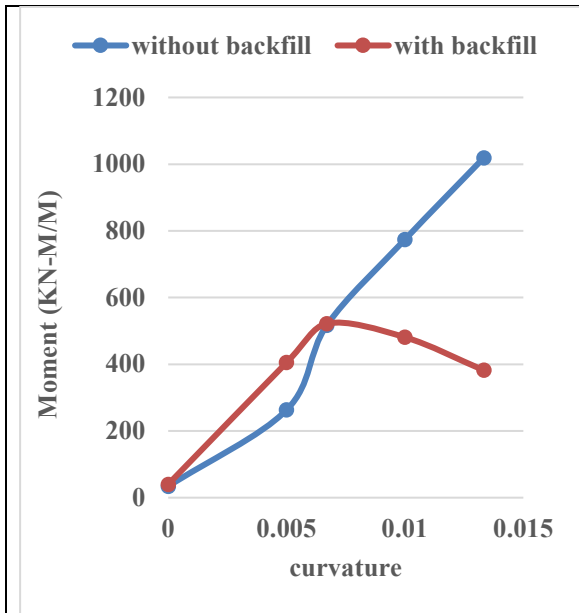


Graph 65. Variation of transverse moment at top of bent w.r.t. skew with pile foundation with or without earth behind abutment.

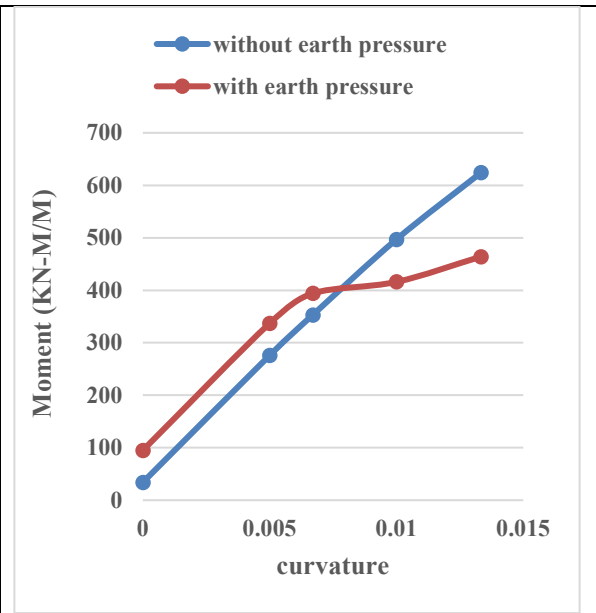


Graph 66. Variation of transverse moment at top of bent w.r.t. skew with open foundation with or without earth behind abutment.

4.2.5.4 Variation of transverse moment at top of bent columns with curvature in longitudinal seismic

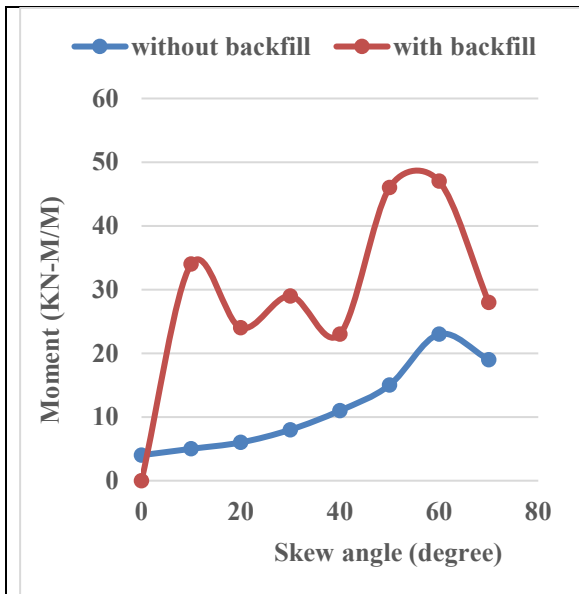


Graph 67. Variation of transverse moment at top of bent w.r.t. curvature with pile foundation with or without earth behind abutment.

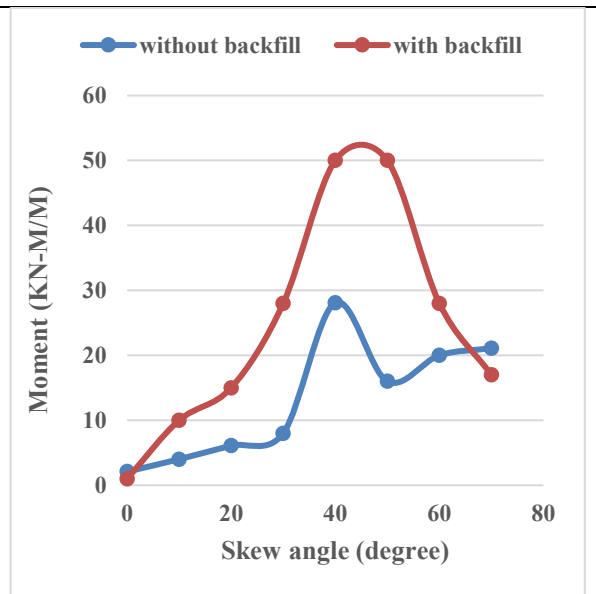


Graph 68. Variation of transverse moment at top of bent w.r.t. curvature with open foundation with or without earth behind abutment.

4.2.5.5 Variation of torsional moment at top of bent columns with skew angle in longitudinal seismic

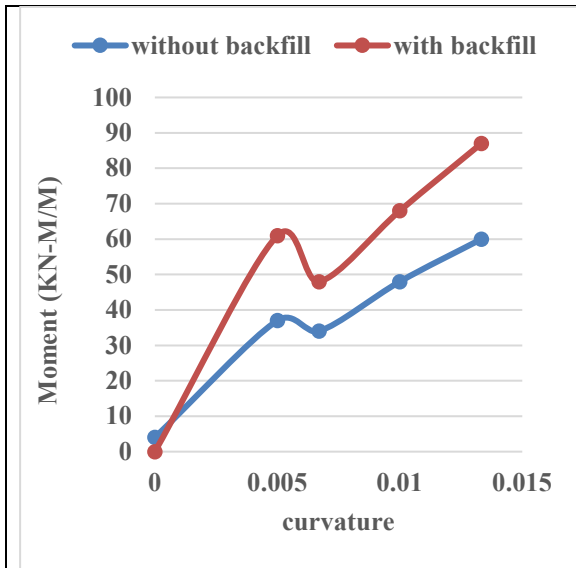


Graph 69. Variation of torsion at top of bent w.r.t. skew with pile foundation with or without earth behind abutment.

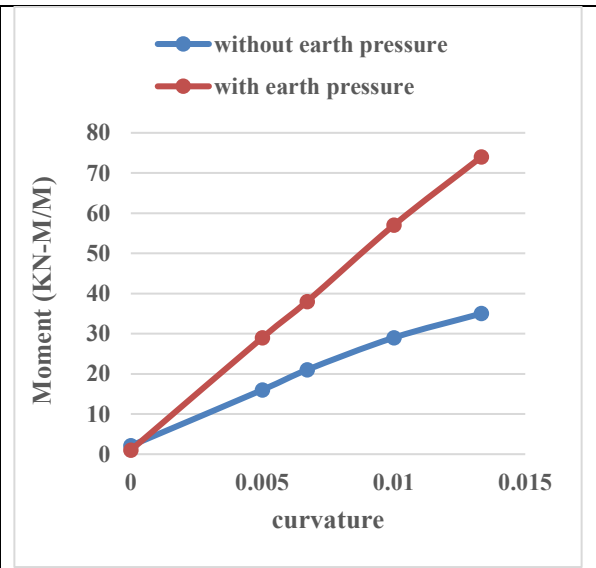


Graph 70. Variation of torsion at top of bent w.r.t. skew with open foundation with or without earth behind abutment.

4.2.5.6 Variation of torsional moment at top of bent columns with curvature in longitudinal seismic

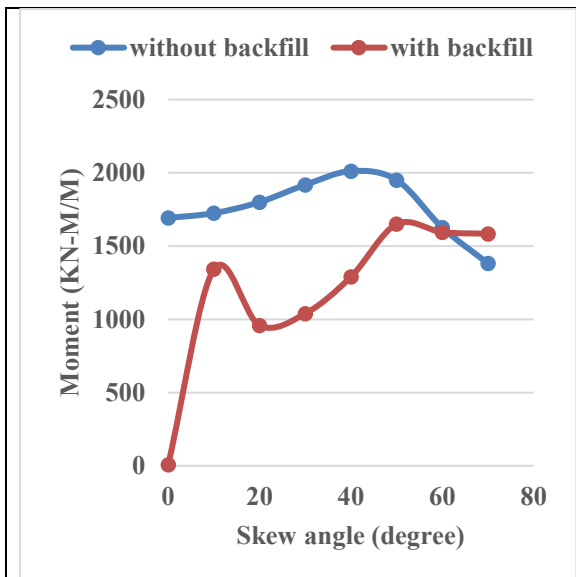


Graph 71. Variation of torsion at top of bent w.r.t. curvature with pile foundation with or without earth behind abutment.

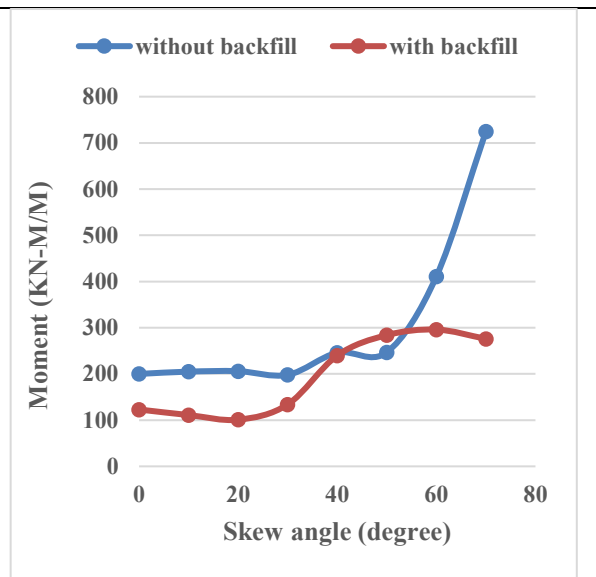


Graph 72. Variation of torsion at top of bent w.r.t. curvature with open foundation with or without earth behind abutment.

4.2.5.7 Variation of longitudinal moment at bottom of bent columns with skew angle in longitudinal seismic

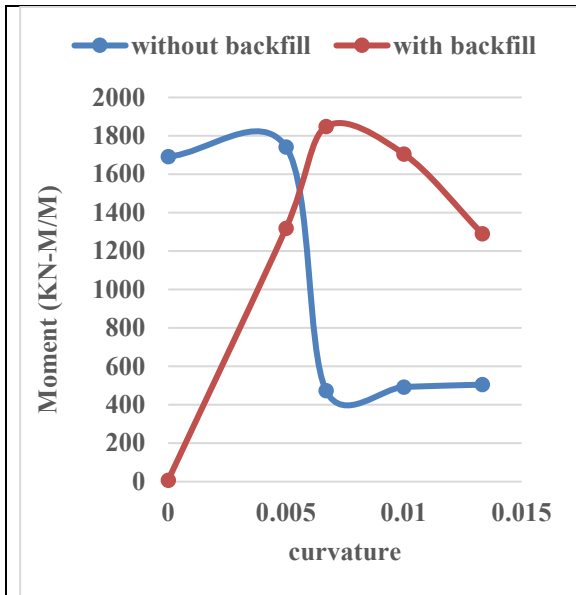


Graph 73. Variation of longitudinal moment at bottom of bent w.r.t. skew with pile foundation with or without earth behind abutment.

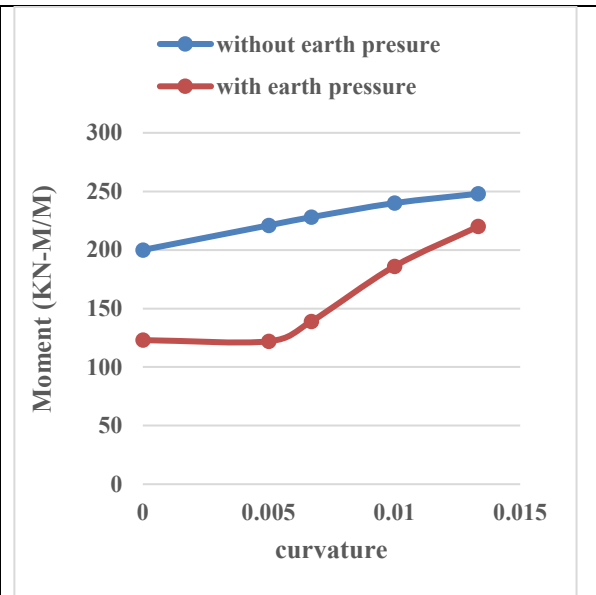


Graph 74. Variation of longitudinal moment at bottom of bent w.r.t. skew with open foundation with or without earth behind abutment.

4.2.5.8 Variation of longitudinal moment at bottom of bent columns with curvature in longitudinal seismic

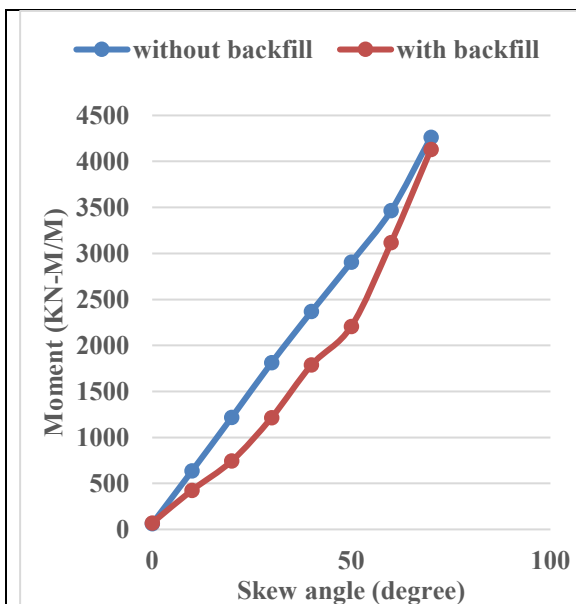


Graph 75. Variation of longitudinal moment at bottom of bent w.r.t. curvature with pile foundation with or without earth behind abutment.

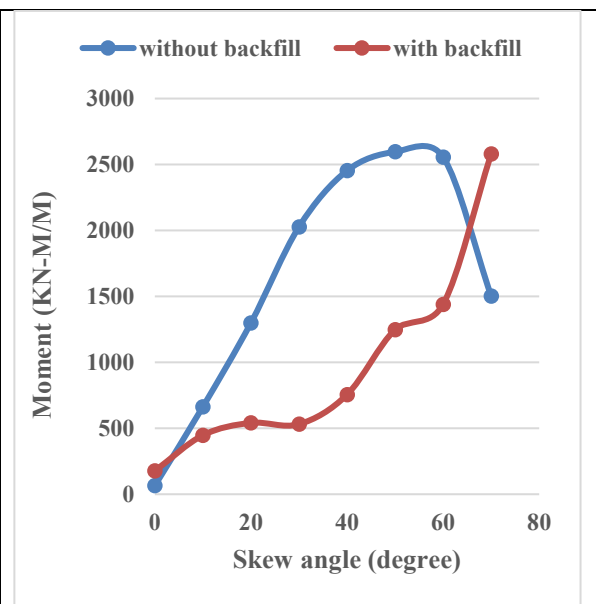


Graph 76. Variation of longitudinal moment at bottom of bent w.r.t. curvature with open foundation with or without earth behind abutment.

4.2.5.9 Variation of transverse moment at bottom of bent columns with skew angle in longitudinal seismic

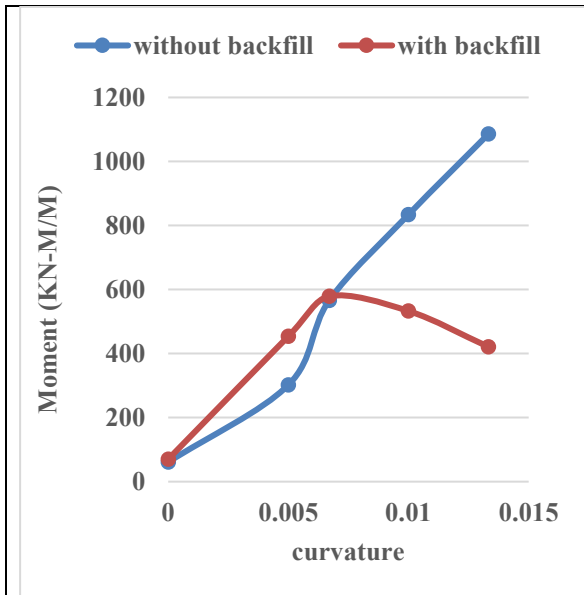


Graph 77. Variation of transverse moment at bottom of bent w.r.t. skew with pile foundation with or without earth behind abutment.

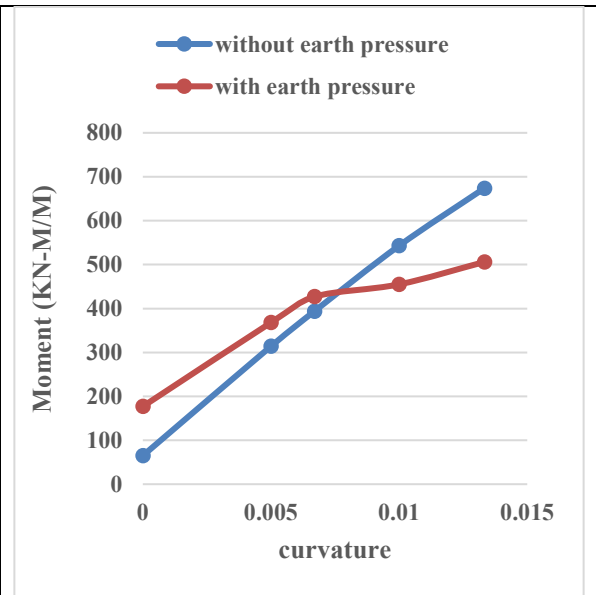


Graph 78. Variation of transverse moment at bottom of bent w.r.t. skew with open foundation with or without earth behind abutment.

4.2.5.10 Variation of transverse moment at bottom of bent columns with curvature in longitudinal seismic

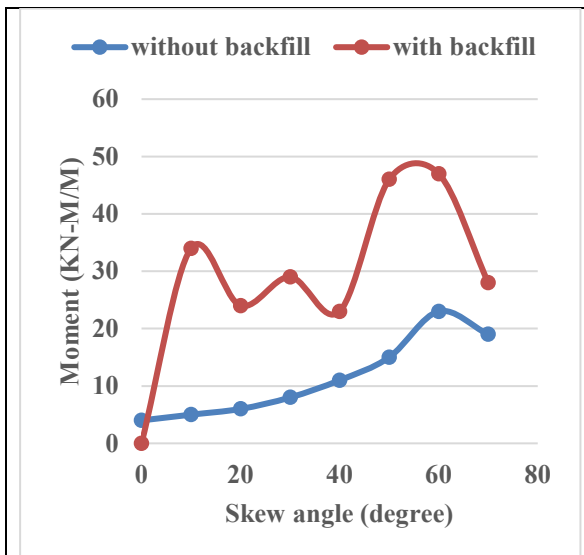


Graph 79. Variation of transverse moment at bottom of bent w.r.t. curvature with pile foundation with or without earth behind abutment.

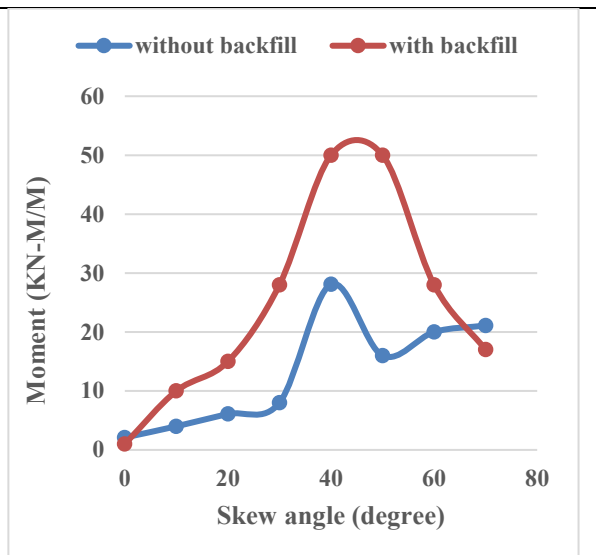


Graph 80. Variation of transverse moment at bottom of bent w.r.t. curvature with open foundation with or without earth behind abutment.

4.2.5.11 Variation of torsional moment at bottom of bent columns with skew angle in longitudinal seismic

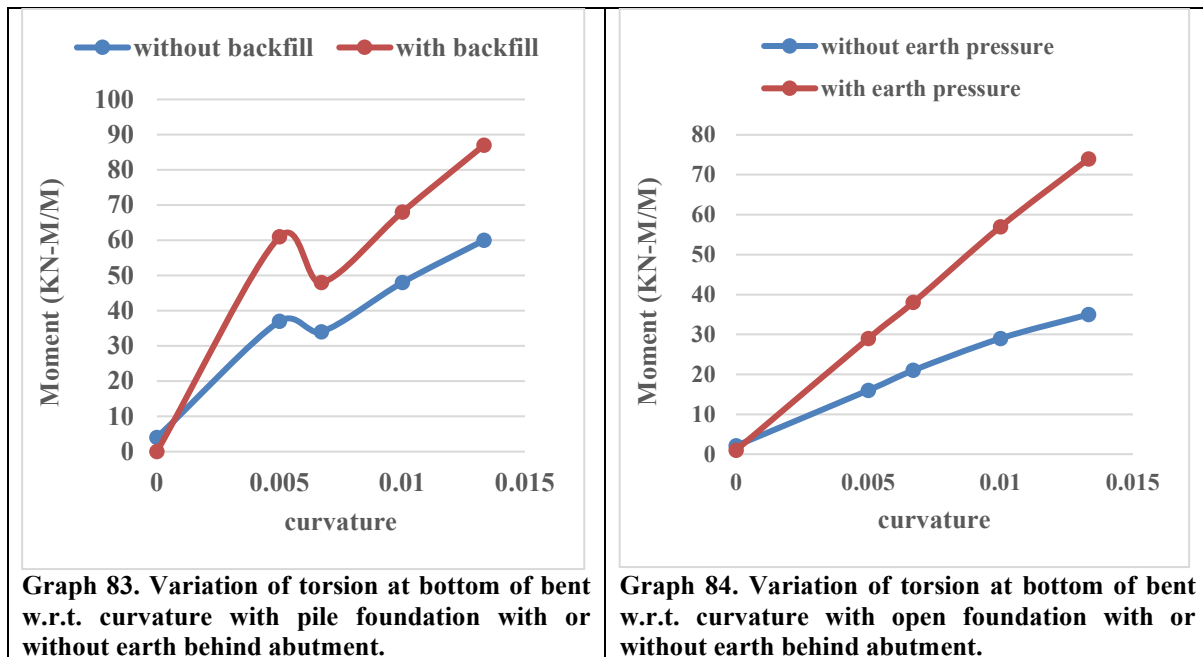


Graph 81. Variation of torsion at bottom of bent w.r.t. skew with pile foundation with or without earth behind abutment.



Graph 82. Variation of torsion at bottom of bent w.r.t. skew with open foundation with or without earth behind abutment.

4.2.5.12 Variation of torsional moment at bottom of bent columns with curvature in longitudinal seismic



Based on the analysis of the provided data and graphs, the following observations can be made regarding the longitudinal seismic case:

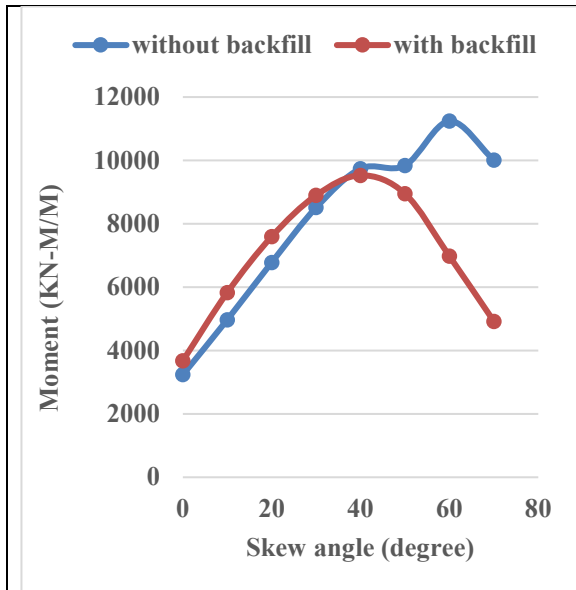
- The longitudinal moment at the top of the bent columns decreases with an increase in skew angle for both open and pile foundation configurations, except for pile foundation with backfill. The moment is higher for bridges without backfill compared to those with backfill.
- The longitudinal moment at the top of the bent columns remains almost the same with changing curvature for bridges without backfill. However, it is consistently higher for bridges without backfill compared to those with backfill.
- The transverse moment at the top of the bent columns initially increases and then decreases with an increase in skew angle, but only for open foundation configurations without backfill. Otherwise, it consistently increases with the skew angle. The rate of increase is similar for both with and without backfill configurations.
- The transverse moment at the top of the bent columns increases with changing curvature, with higher moments observed for bridges without backfill compared to those with backfill.
- Torsion at the top of the bent columns initially increases and then decreases with an increase in skew angle for both open and pile foundation configurations.
- Torsion at the top of the bent columns increases with an increase in curvature for both open and pile foundations, with higher values observed for bridges with and without backfill and for bridges with pile foundations compared to those with open foundations.

Regarding the observations for the bottom of the bent columns:

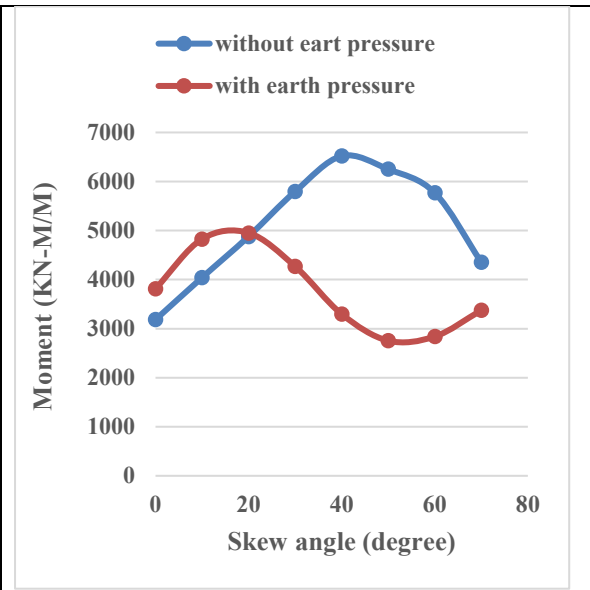
- The longitudinal moment increases with an increase in skew angle for both open and pile foundations. The moment is higher for bridges with pile foundations compared to those with open foundations.
- The longitudinal moment increases with an increase in curvature for both open foundation and for pile foundation with backfill initially, then decreases.
- The transverse moment increases with an increase in skew angle.
- The transverse moment increases with an increase in curvature.
- Torsion at the bottom of the bent columns increases with an increase in skew angle for bridges without backfill.
- Torsion at the bottom of the bent columns increases with an increase in curvature.

4.2.6 Variation of the moment at abutment in transverse seismic condition

4.2.6.1 Variation of longitudinal moment at top of abutment with skew angle in transverse seismic

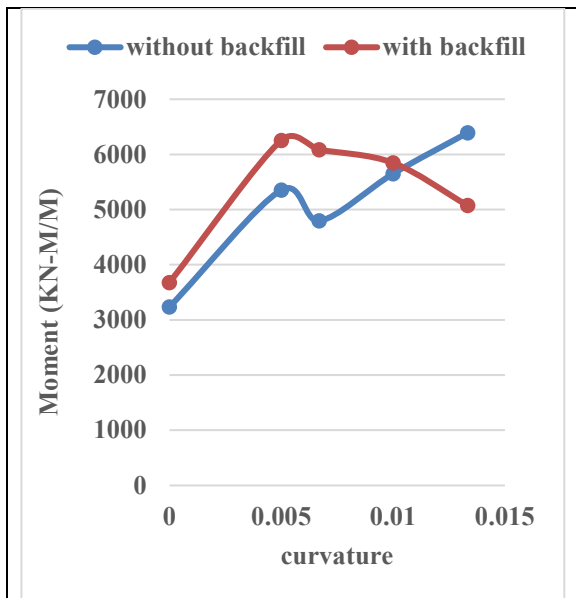


Graph 85. Variation of longitudinal moment at top of abutment w.r.t. skew with pile foundation with or without earth behind abutment.

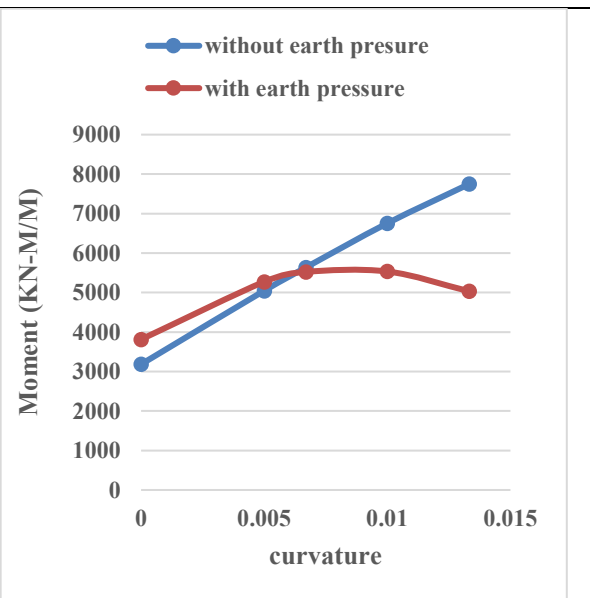


Graph 86. Variation of longitudinal moment at top of abutment w.r.t. skew with open foundation with or without earth behind abutment.

4.2.6.2 Variation of longitudinal moment at top of abutment with curvature in transverse seismic

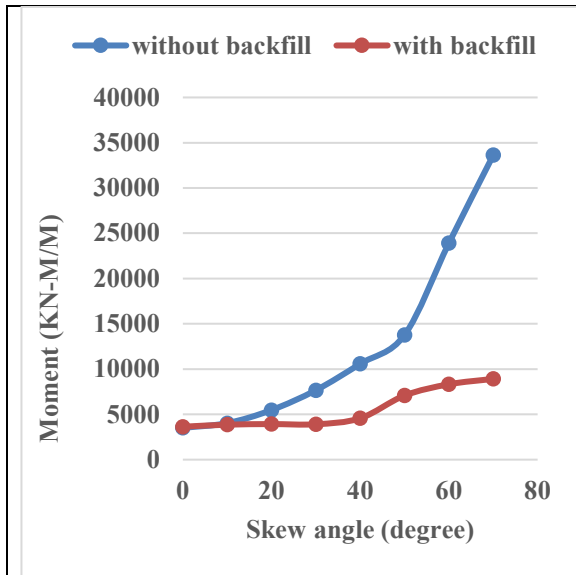


Graph 87. Variation of longitudinal moment at top of abutment w.r.t. curvature with pile foundation with or without earth behind abutment.

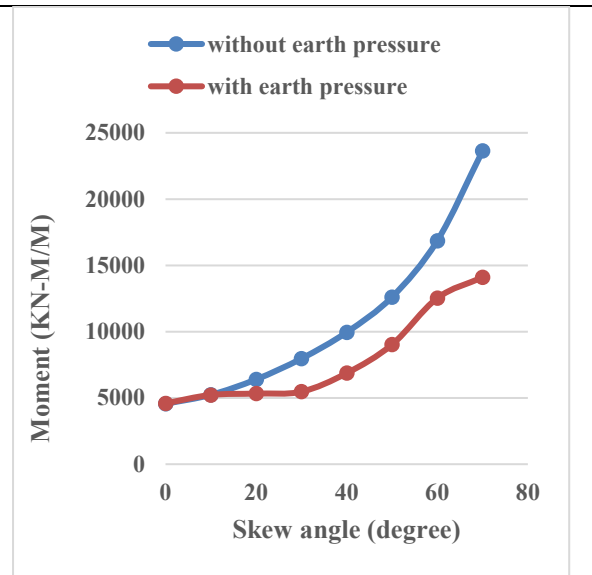


Graph 88. Variation of longitudinal moment at top of abutment w.r.t. curvature with open foundation with or without earth behind abutment.

4.2.6.3 Variation of transverse moment at top of abutment with skew angle in transverse seismic

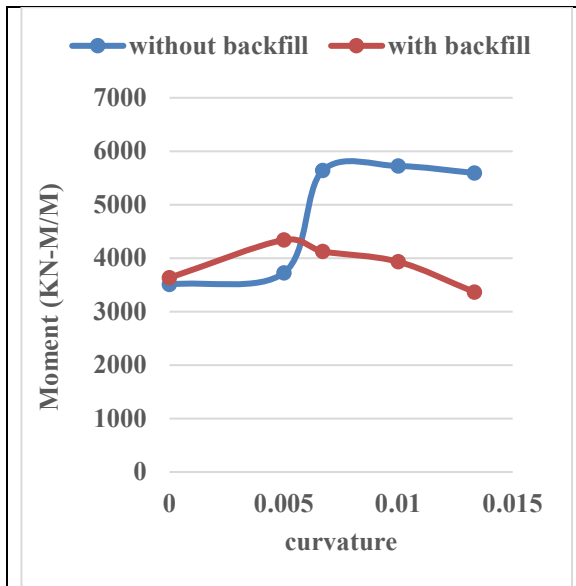


Graph 89. Variation of transverse moment at top of abutment w.r.t. skew with pile foundation with or without earth behind abutment.

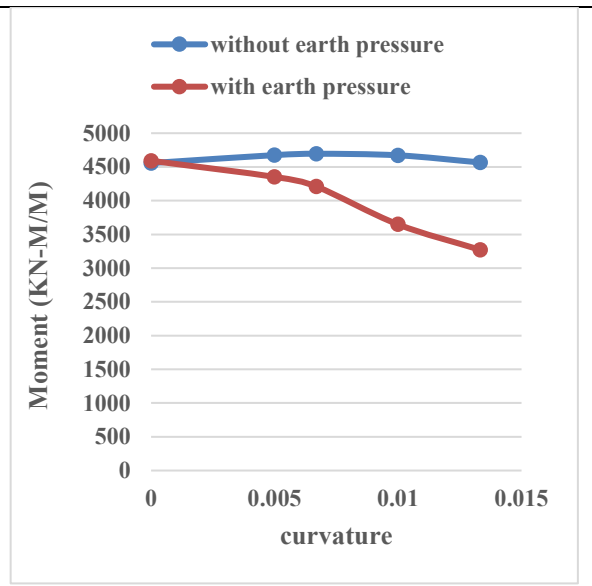


Graph 90. Variation of transverse moment at top of abutment w.r.t. skew with open foundation with or without earth behind abutment.

4.2.6.4 Variation of transverse moment at top of abutment with curvature in transverse seismic

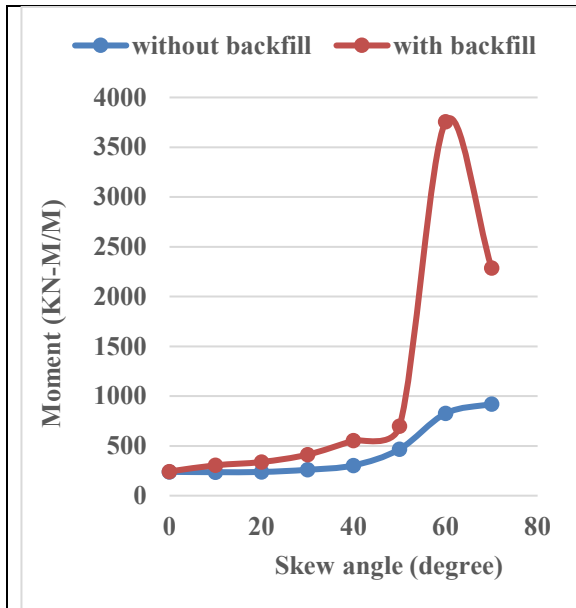


Graph 91. Variation of transverse moment at top of abutment w.r.t. curvature with pile foundation with or without earth behind abutment.

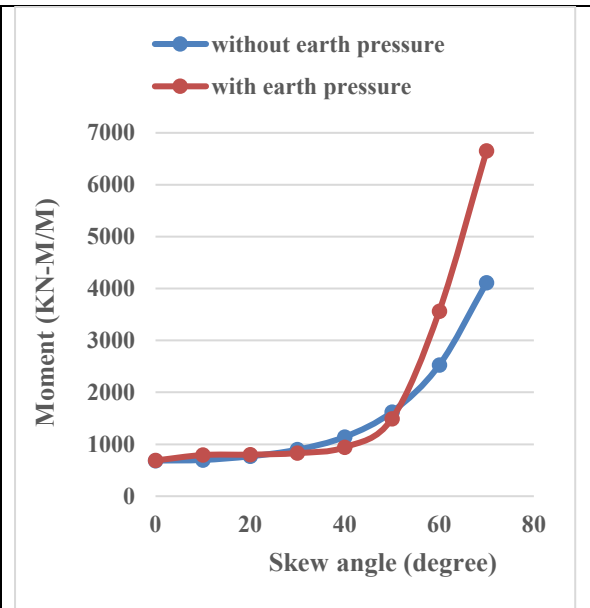


Graph 92. Variation of transverse moment at top of abutment w.r.t. curvature with open foundation with or without earth behind abutment.

4.2.6.5 Variation of torsional moment at top of abutment with skew angle in transverse seismic

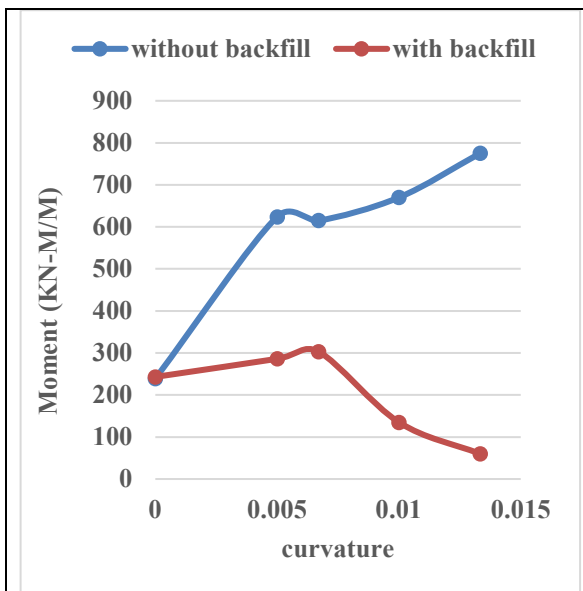


Graph 93. Variation of torsion at top of abutment w.r.t. skew with pile foundation with or without earth behind abutment.

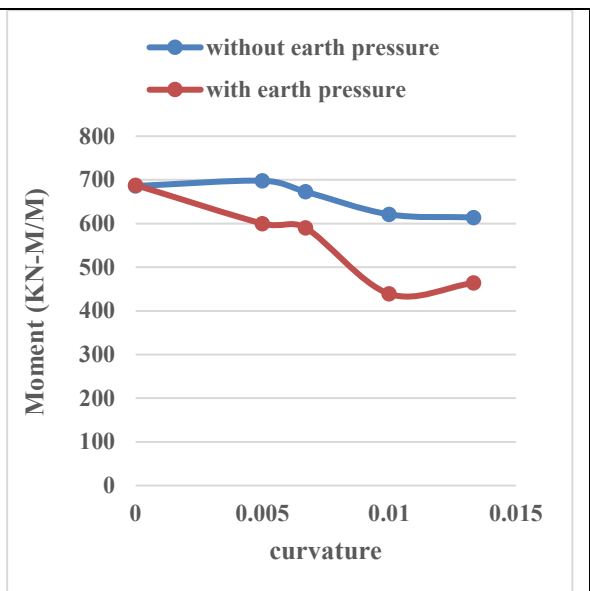


Graph 94. Variation of torsion at top of abutment w.r.t. skew with open foundation with or without earth behind abutment.

4.2.6.6 Variation of torsional moment at top of abutment with curvature in transverse seismic

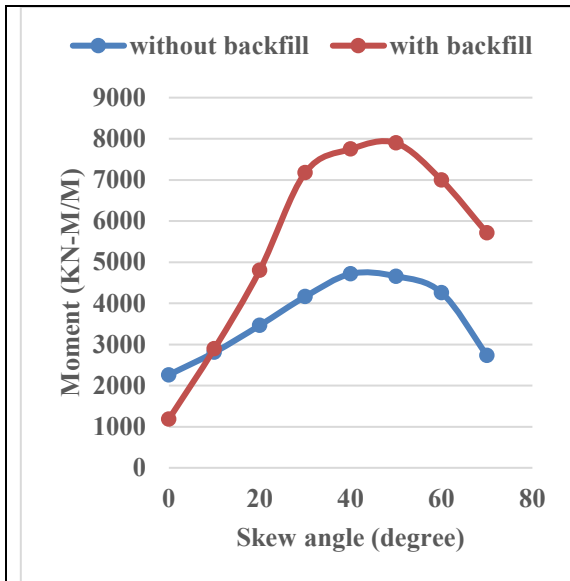


Graph 95. Variation of torsion at top of abutment w.r.t. curvature with pile foundation with or without earth behind abutment.

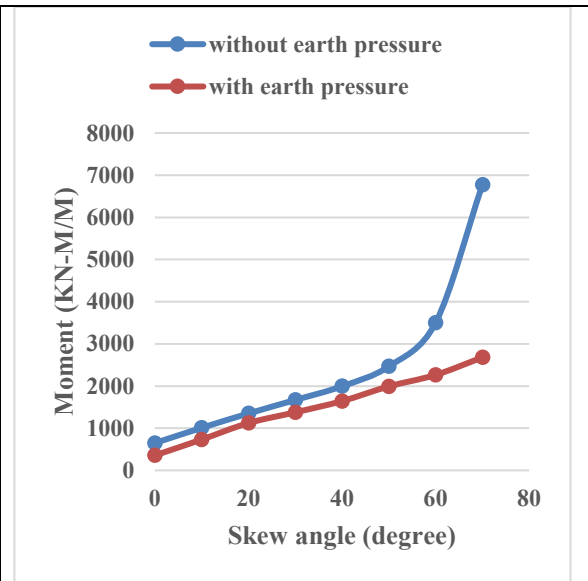


Graph 96. Variation of torsion at top of abutment w.r.t. curvature with open foundation with or without earth.

4.2.6.7 Variation of longitudinal moment at bottom of abutment with skew angle in transverse seismic

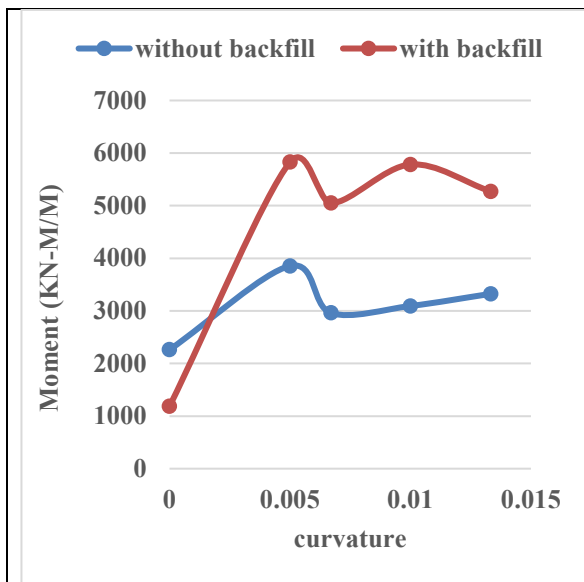


Graph 97. Variation of longitudinal moment at bottom of abutment w.r.t. skew with pile foundation with or without earth behind abutment.

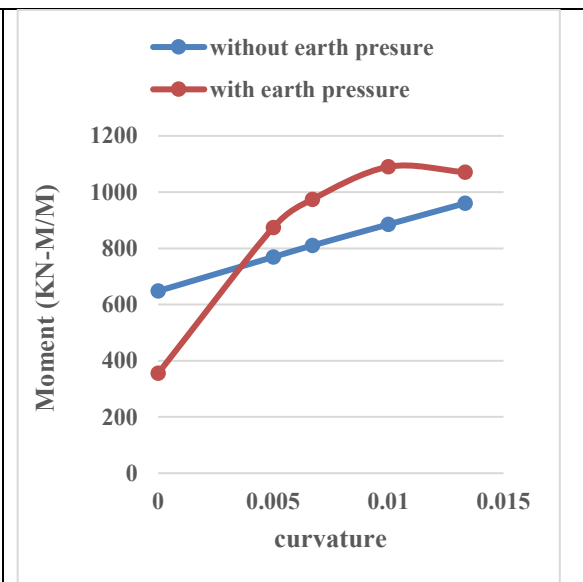


Graph 98. Variation of longitudinal moment at bottom of abutment w.r.t. skew with open foundation with or without earth behind abutment.

4.2.6.8 Variation of longitudinal moment at bottom of abutment with curvature in transverse seismic

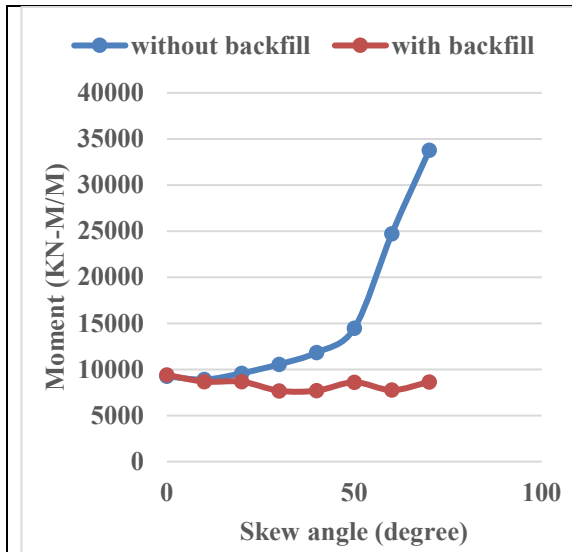


Graph 99. Variation of longitudinal moment at bottom of abutment w.r.t. curvature with pile foundation with or without earth behind abutment.

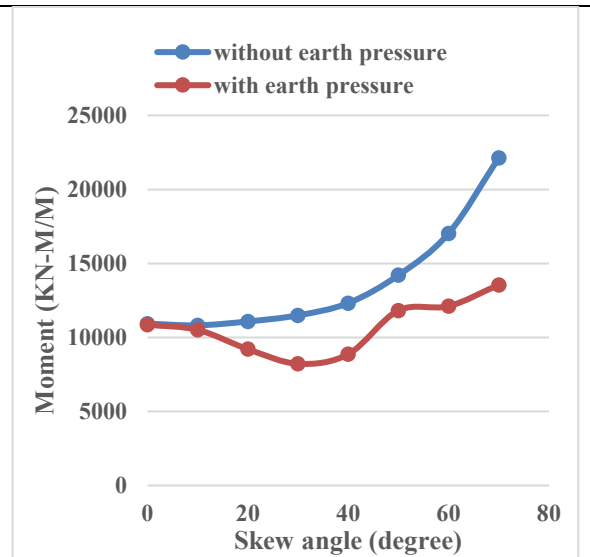


Graph 100. Variation of longitudinal moment at bottom of abutment w.r.t. curvature with open foundation with or without earth behind abutment.

4.2.6.9 Variation of transverse moment at bottom of abutment with skew angle in transverse seismic

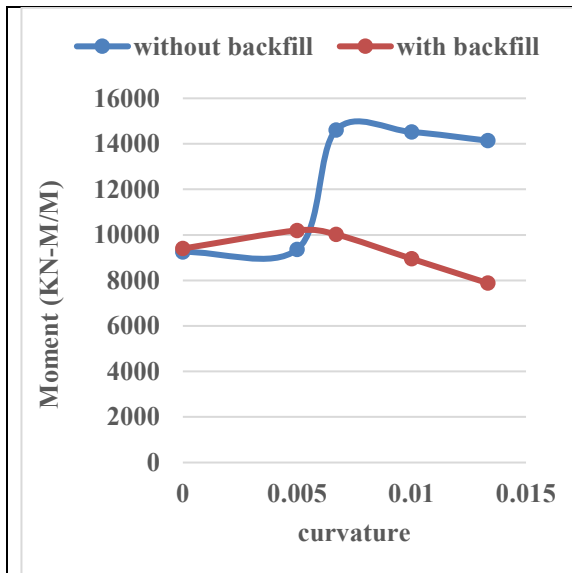


Graph 101. Variation of transverse moment at bottom of abutment w.r.t. skew with pile foundation with or without earth behind abutment.

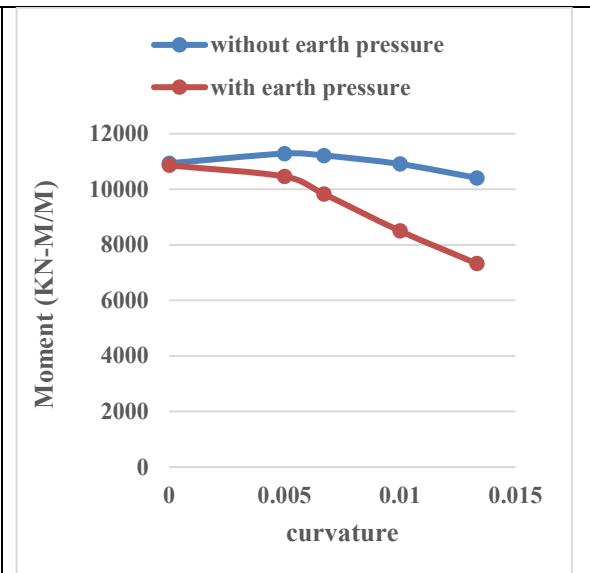


Graph 102. Variation of transverse moment at bottom of abutment w.r.t. skew with open foundation with or without earth behind abutment.

4.2.6.10 Variation of transverse moment at bottom of abutment with curvature in transverse seismic

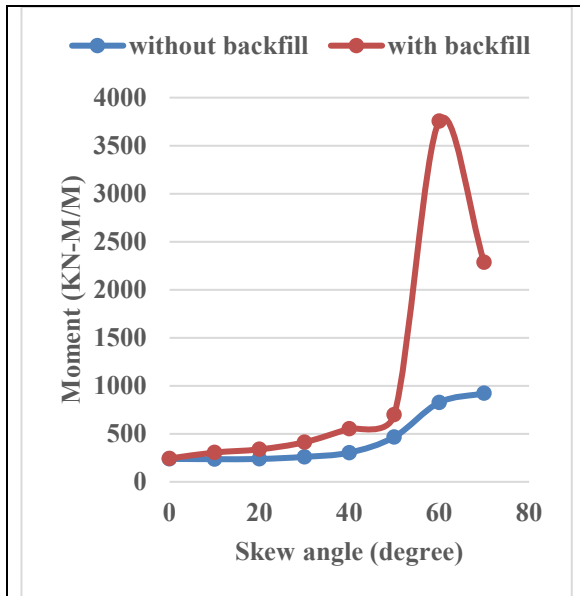


Graph 103. Variation of transverse moment at bottom of abutment w.r.t. curvature with pile foundation with or without earth behind abutment.

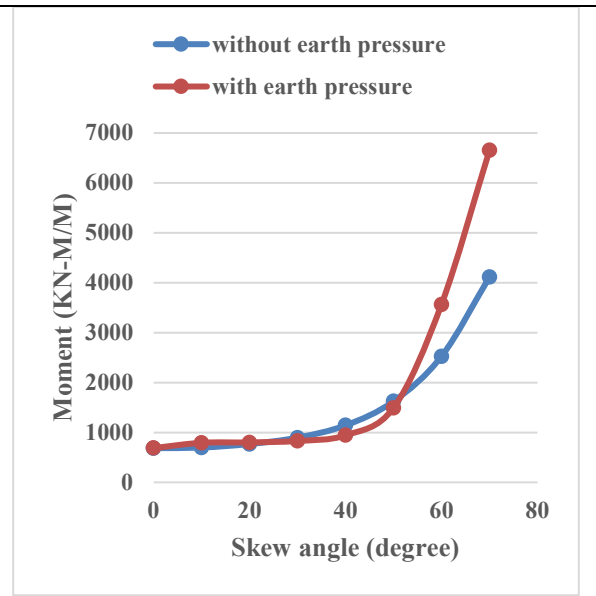


Graph 104. Variation of transverse moment at bottom of abutment w.r.t. curvature with open foundation with or without earth behind abutment.

4.2.6.11 Variation of torsional moment at bottom of abutment with skew angle in transverse seismic

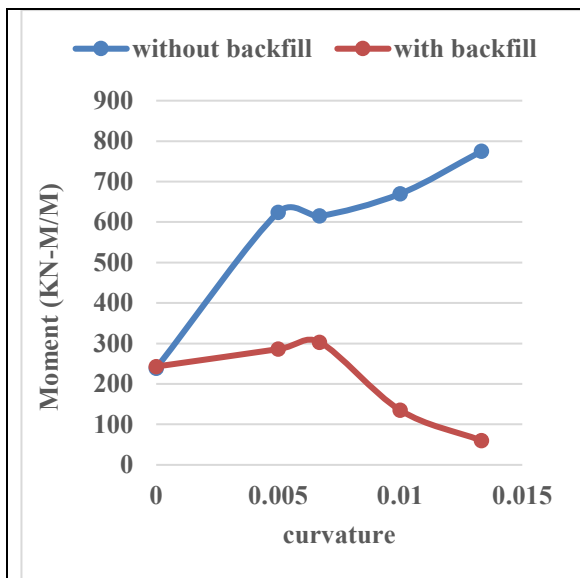


Graph 105. Variation of torsion at bottom of abutment w.r.t. skew with pile foundation with or without earth behind abutment.

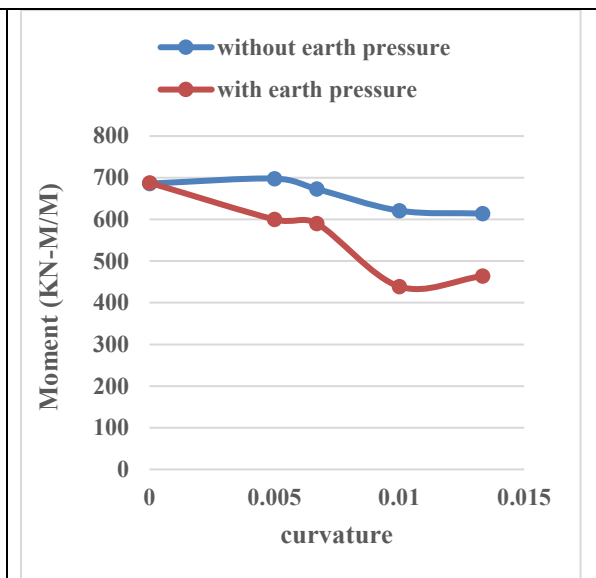


Graph 106. Variation of torsion at bottom of abutment w.r.t. skew with open foundation with or without earth behind abutment.

4.2.6.12 Variation of torsional moment at bottom of abutment with curvature in transverse seismic



Graph 107. Variation of torsion at bottom of abutment w.r.t. curvature with pile foundation with or without earth behind abutment.



Graph 108. Variation of torsion at bottom of abutment w.r.t. curvature with open foundation with or without earth behind abutment.

Based on the analysis of the provided data and graphs, the following observations can be made regarding the transverse seismic case:

- The longitudinal moment at the top of the abutment initially increases and then decreases with an increase in skew angle for both open and pile foundation configurations. The moment is higher for bridges without

backfill compared to those with backfill.

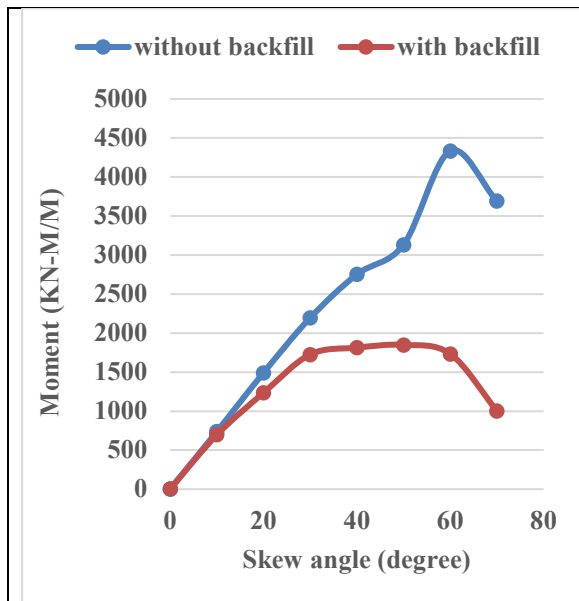
- The longitudinal moment at the top of the abutment increases with an increase in curvature for both open and pile foundation configurations.
- The transverse moment at the top of the abutment increases with an increase in skew angle for both open and pile foundation configurations.
- The transverse moment at the top of the abutment decreases with an increase in curvature for both open and pile foundation configurations, except for pile foundation without backfill.
- Torsion at the top of the abutment initially increases then decreases with an increase in skew angle for pile foundation with backfill, otherwise, it increases with an increase in skew angle.
- Torsion at the top of the abutment decreases with an increase in curvature for both open and pile foundations, except for pile foundations without backfill.

Regarding the observations for the bottom of the abutment:

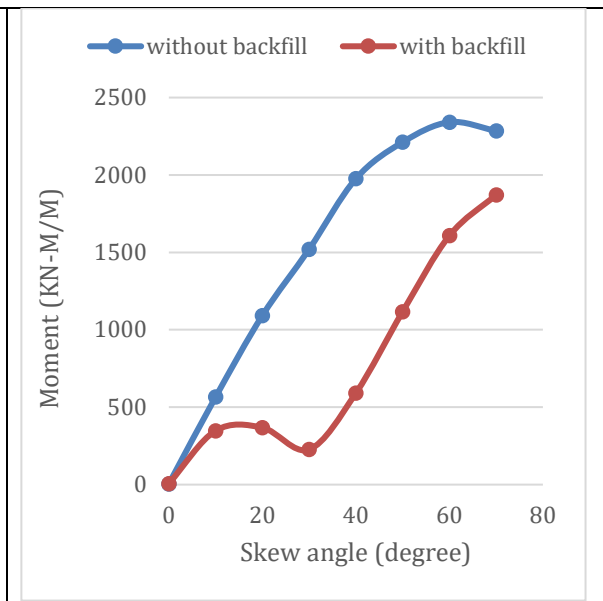
- The longitudinal moment initially increases then decreases with an increase in skew angle for pile foundations, while for open foundation configurations, it increases with an increase in skew angle.
- The longitudinal moment increases with an increase in curvature for both open and pile foundation configurations, with higher values observed for bridges with backfill and pile foundation.
- The transverse moment increases with an increase in skew angle.
- The transverse moment decreases with an increase in curvature.
- Torsion at the bottom of the abutment increases with an increase in skew angle and decreases with an increase in curvature.

4.2.7 Variation of the moment at bent columns in transverse seismic condition

4.2.7.1 Variation of longitudinal moment at top of bent columns with skew angle in transverse seismic

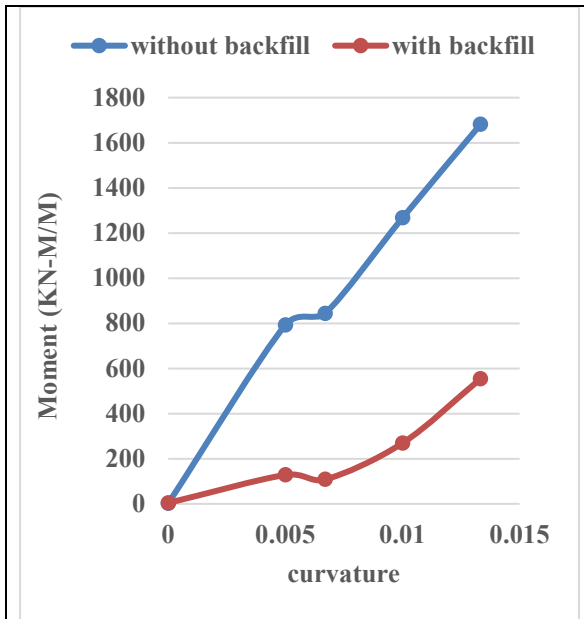


Graph 109. Variation of longitudinal moment at top of bent w.r.t. skew with pile foundation with or without earth behind abutment.

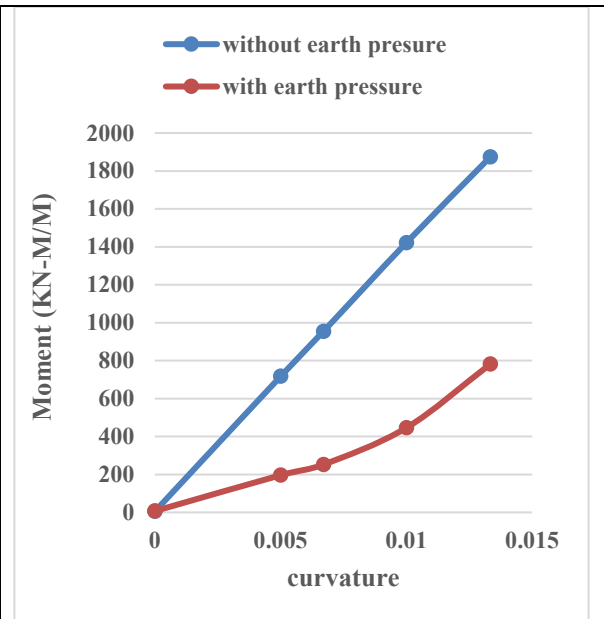


Graph 110. Variation of longitudinal moment at top of bent w.r.t. skew with open foundation with or without earth behind abutment.

4.2.7.2 Variation of longitudinal moment at top of bent columns with curvature in transverse seismic

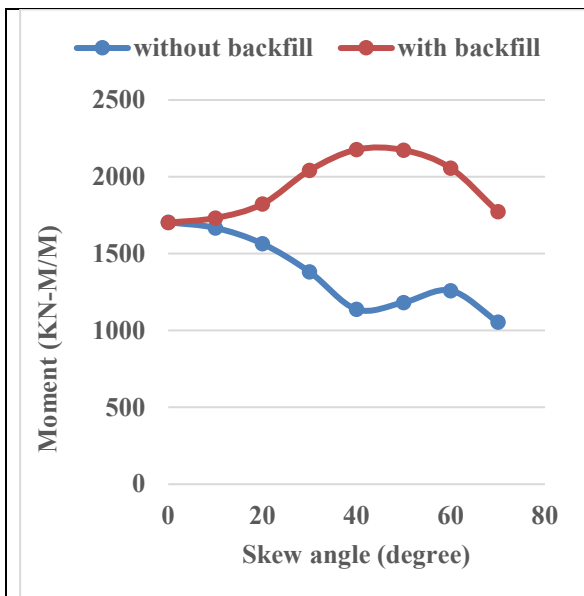


Graph 111. Variation of longitudinal moment at top of bent w.r.t. curvature with pile foundation with or without earth behind abutment.

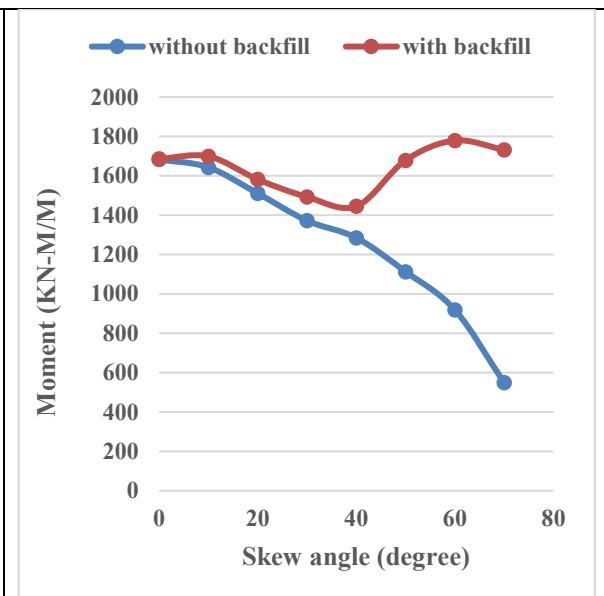


Graph 112. Variation of longitudinal moment at top of bent w.r.t. curvature with open foundation with or without earth behind abutment.

4.2.7.3 Variation of transverse moment at top of bent columns with skew angle in transverse seismic

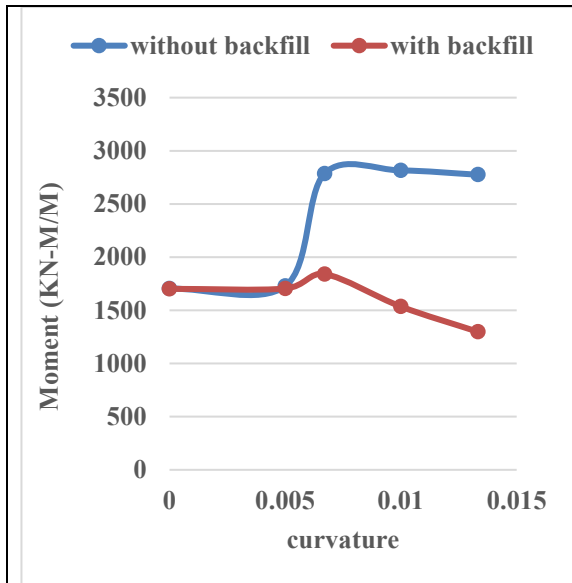


Graph 113. Variation of transverse moment at top of bent w.r.t. skew with pile foundation with or without earth behind abutment.

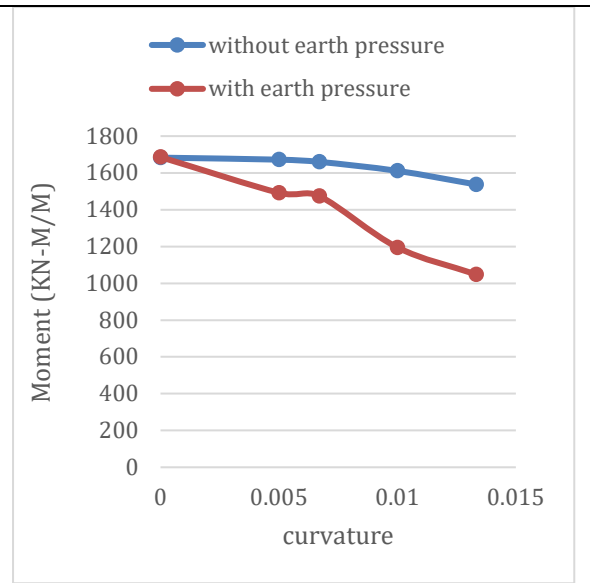


Graph 114. Variation of transverse moment at top of bent w.r.t. skew with open foundation with or without earth behind abutment.

4.2.7.4 Variation of transverse moment at top of bent columns with curvature in transverse seismic

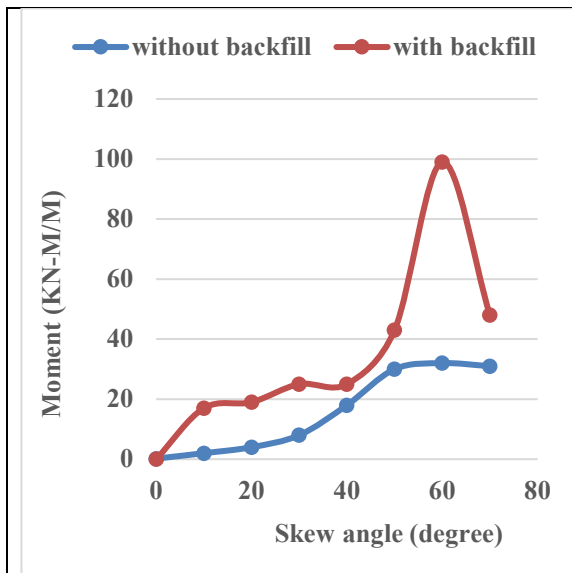


Graph 115. Variation of transverse moment at top of bent w.r.t. curvature with pile foundation with or without earth behind abutment.

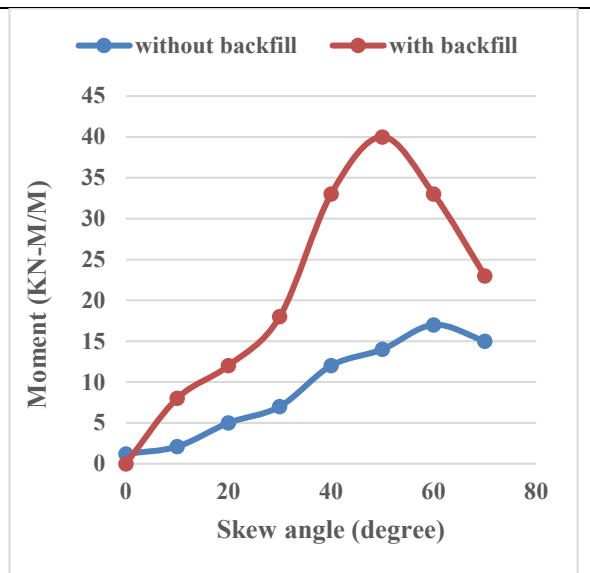


Graph 116. Variation of transverse moment at top of bent w.r.t. curvature with open foundation with or without earth behind abutment.

4.2.7.5 Variation of torsional moment at top of bent columns with skew angle in transverse seismic

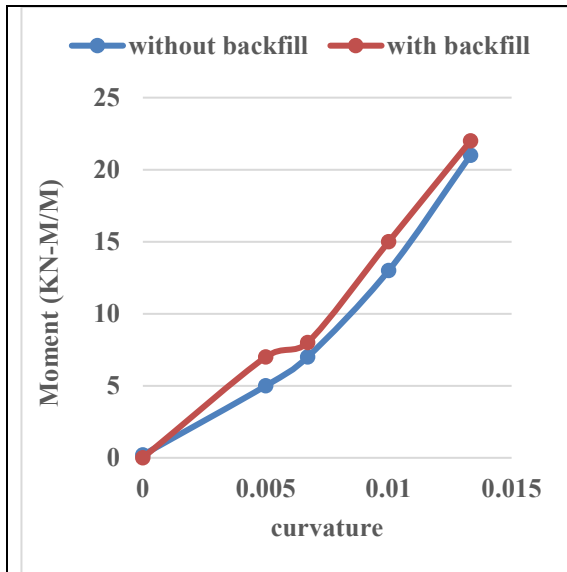


Graph 117. Variation of torsion at top of bent w.r.t. skew with pile foundation with or without earth behind abutment.

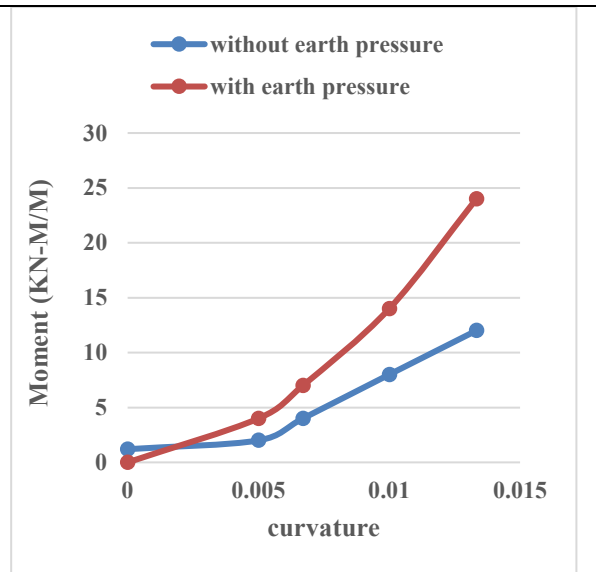


Graph 118. Variation of torsion at top of bent w.r.t. skew with open foundation with or without earth behind abutment.

4.2.7.6 Variation of torsional moment at top of bent columns with curvature in transverse seismic

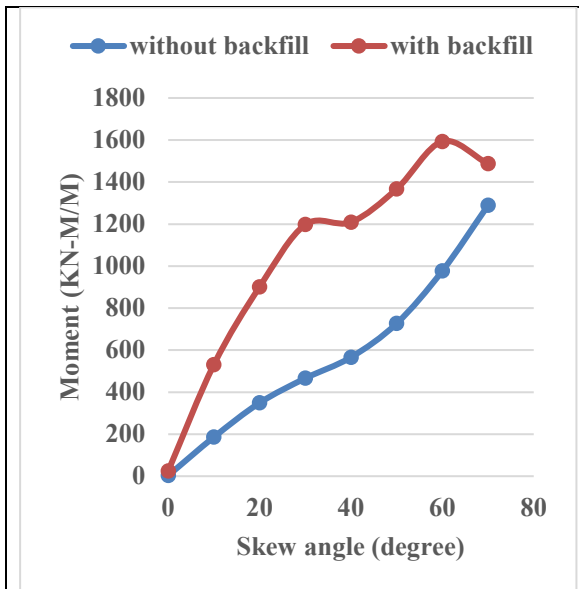


Graph 119. Variation of torsion at top of bent w.r.t. curvature with pile foundation with or without earth behind abutment.

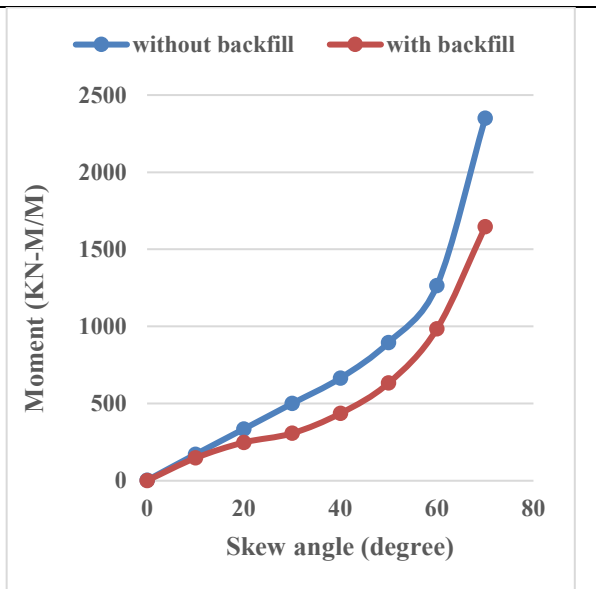


Graph 120. Variation of torsion at top of bent w.r.t. curvature with open foundation with or without earth behind abutment.

4.2.7.7 Variation of longitudinal moment at bottom of bent columns with skew angle in transverse seismic

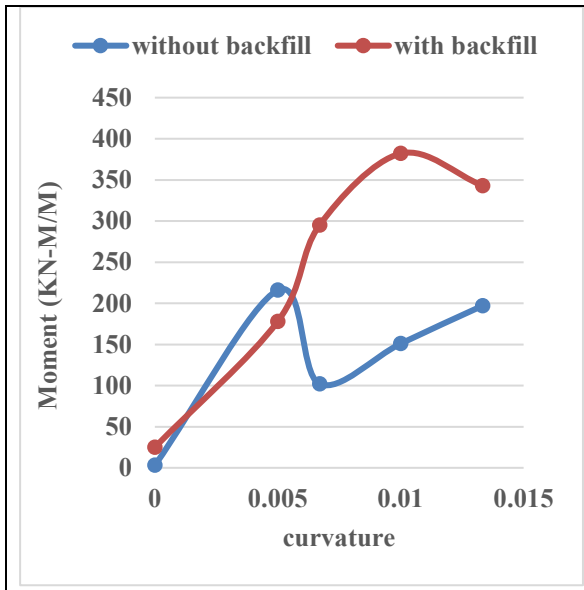


Graph 121. Variation of longitudinal moment at bottom of bent w.r.t. skew with pile foundation with or without earth behind abutment.

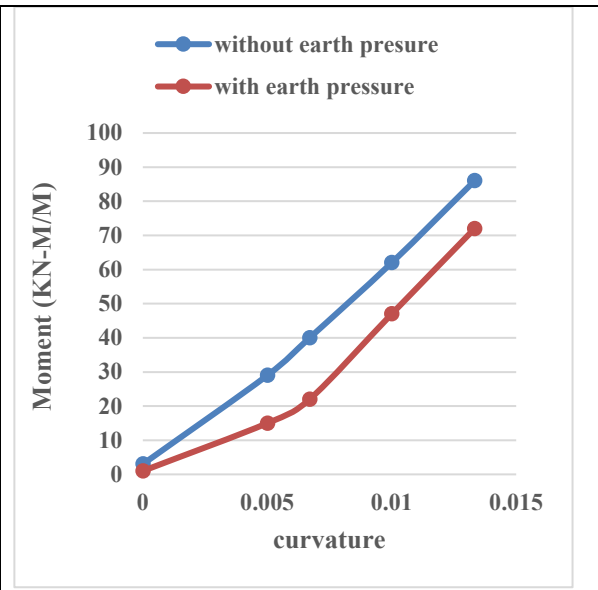


Graph 122. Variation of longitudinal moment at bottom of bent w.r.t. skew with open foundation with or without earth behind abutment.

4.2.7.8 Variation of longitudinal moment at bottom of bent columns with curvature in transverse seismic

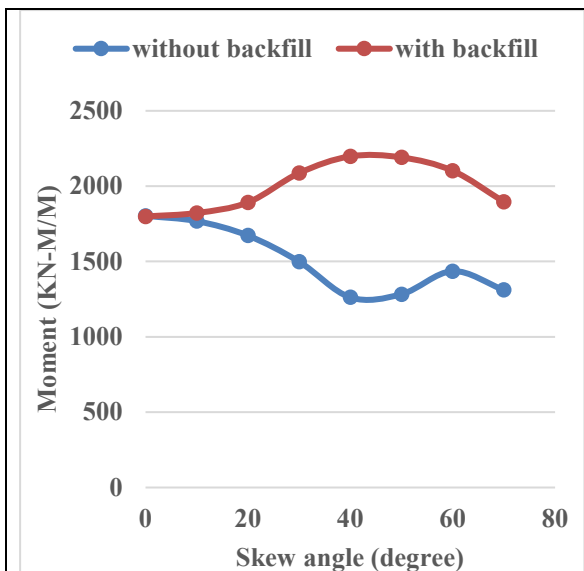


Graph 123. Variation of longitudinal moment at bottom of bent w.r.t. curvature with pile foundation with or without earth behind abutment.

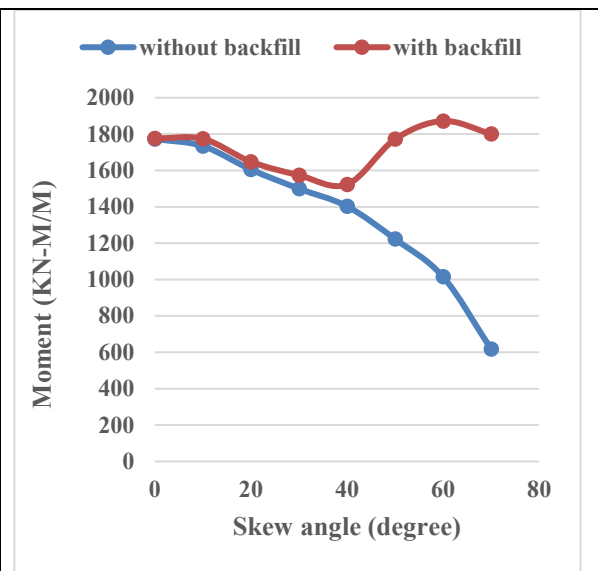


Graph 124. Variation of longitudinal moment at bottom of bent w.r.t. curvature with open foundation with or without earth behind abutment.

4.2.7.9 Variation of transverse moment at bottom of bent columns with skew angle in transverse seismic

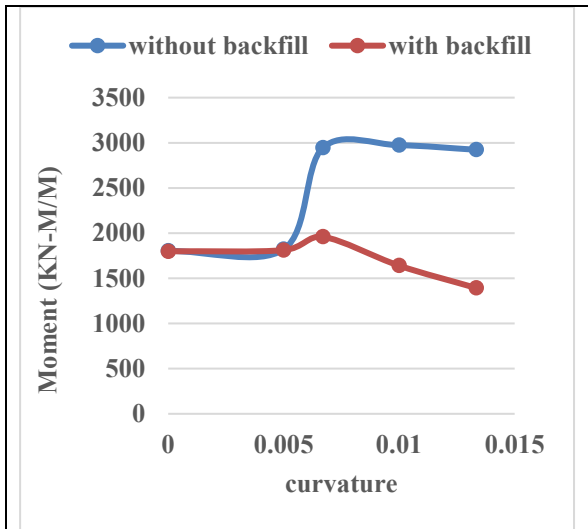


Graph 125. Variation of transverse moment at bottom of bent w.r.t. skew with pile foundation with or without earth behind abutment.

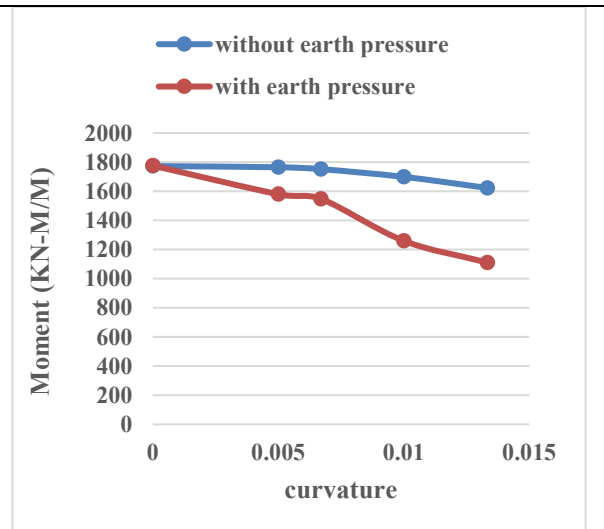


Graph 126. Variation of transverse moment at bottom of bent w.r.t. skew with open foundation with or without earth behind abutment.

4.2.7.10 Variation of transverse moment at bottom of bent columns with curvature in transverse seismic

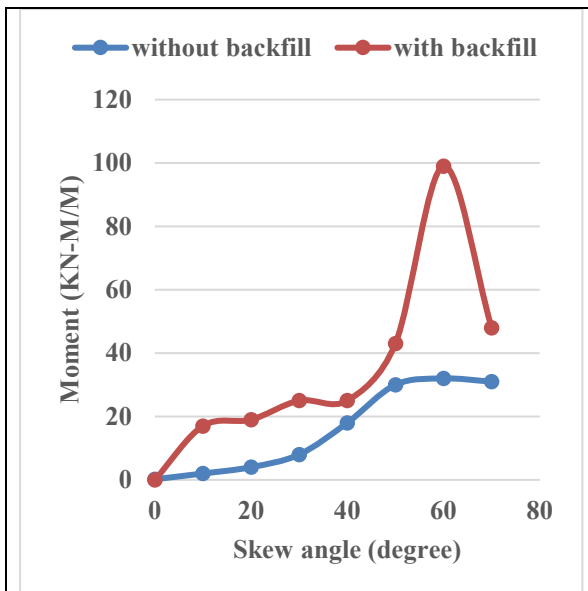


Graph 127. Variation of transverse moment at bottom of bent w.r.t. curvature with pile foundation with or without earth behind abutment.

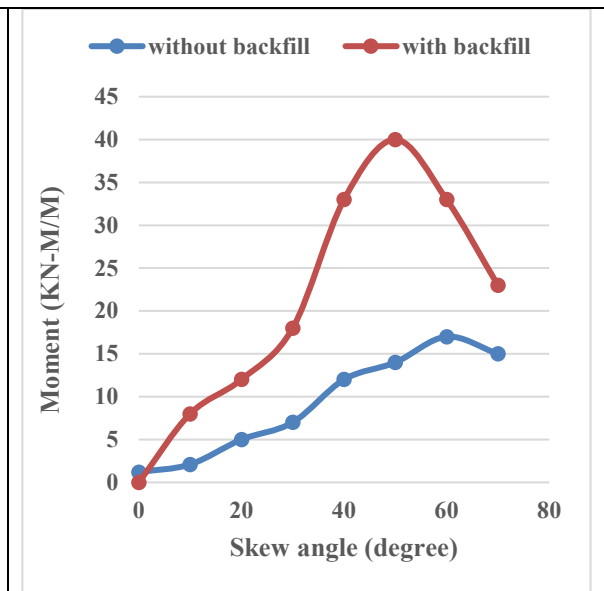


Graph 128. Variation of transverse moment at bottom of bent w.r.t. curvature with open foundation with or without earth behind abutment.

4.2.7.11 Variation of torsional moment at bottom of bent columns with skew angle in transverse seismic

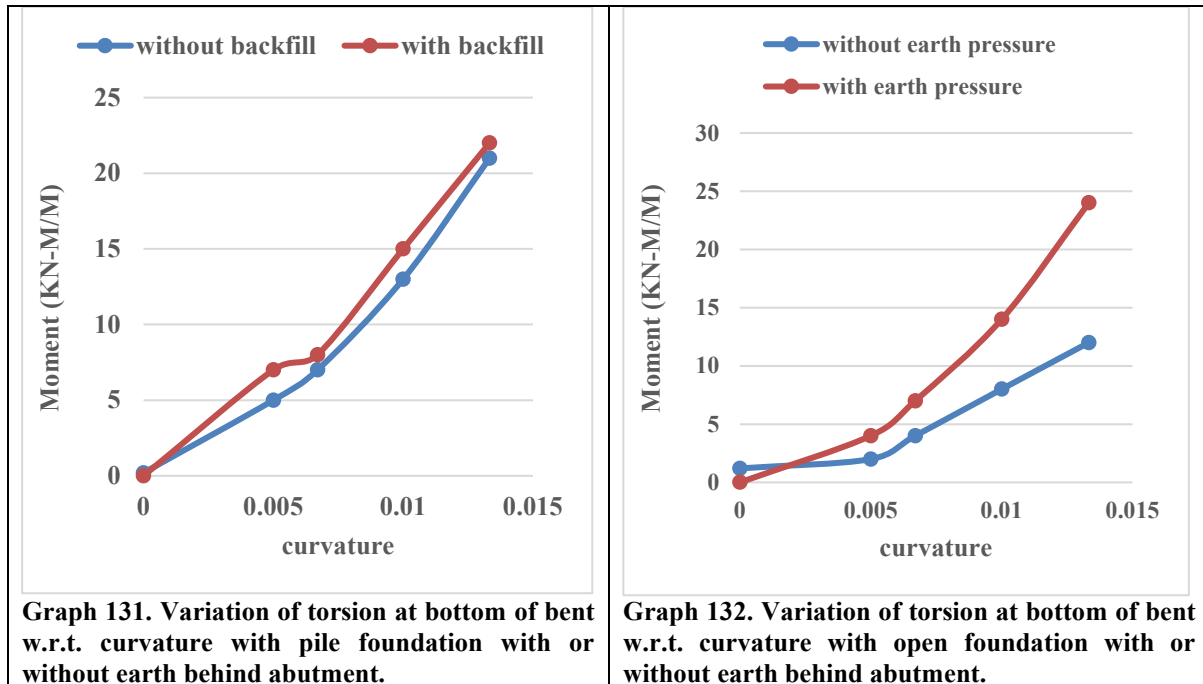


Graph 129. Variation of torsion at bottom of bent w.r.t. skew with pile foundation with or without earth behind abutment.



Graph 130. Variation of torsion at bottom of bent w.r.t. skew with open foundation with or without earth behind abutment.

4.2.7.12 Variation of torsional moment at bottom of bent columns with curvature in transverse seismic



Based on the analysis of the provided data and graphs, the following observations can be made regarding the transverse seismic case:

- The longitudinal moment at the top of the bent columns initially increases and then decreases with an increase in skew angle for both open and pile foundation configurations. The moment is higher for bridges without backfill compared to those with backfill.
- The longitudinal moment at the top of the bent columns increases with an increase in curvature.
- The transverse moment at the top of the bent columns initially increases then decreases with an increase in skew angle for pile foundation with backfill. Otherwise, it decreases.
- The transverse moment at the top of the bent columns decreases with an increase in curvature for both open and pile foundation configurations with backfill.
- Torsion at the top of the bent columns initially increases then decreases with an increase in skew angle.
- Torsion at the top of the bent columns increases with an increase in curvature.

Regarding the observations for the bottom of the bent columns:

- The longitudinal moment increases with an increase in skew angle for both open and pile foundations.
- The longitudinal moment increases and then decreases with an increase in curvature for pile foundation. Otherwise, it increases.
- The transverse moment initially increases and then decreases with an increase in skew angle only for pile foundation with backfill. Otherwise, it decreases.
- The transverse moment initially increases and then decreases with an increase in curvature only for pile foundation without backfill. Otherwise, it decreases.
- Torsion at the bottom of the bent columns initially increases then decreases with an increase in skew angle. It increases for bridges with all curvatures.

CONCLUSIONS

5.1 General

The present thesis delves into an examination of four distinct types of bridge responses, namely time period, base reaction, bending moment, and torsion, as outlined in Section 5.1. Additionally, Section 5.2 explores the prospective avenues for further research.

A comprehensive parametric analysis has been undertaken to assess the impact of curvature and skewness on various bridge responses of integral bridges. This involved conducting three-dimensional modeling and finite element analyses of bridges across a range of curvature and skewness combinations, utilizing the Midas Civil software package. The findings underscore a significant variation in bridge responses in relation to curvature and skewness.

Specifically, the study reveals a notable correlation between skew angle and dead load, with an observed increase in the latter as skew angle rises. Conversely, the effect of curvature on dead load remains consistent across different curvature values.

The graphical representations provided within this thesis offer valuable insights for designers, serving as crucial inputs for their endeavors. Furthermore, the analysis of the impact of curvature and angle variations on different design parameters of integral bridges aids practicing engineers in their decision-making processes.

Overall, this research contributes to a deeper understanding of integral bridge behavior and offers practical guidance for engineering design and decision-making processes in bridge construction projects.

5.1.1 Time period

The thesis focuses on investigating the time period of the first mode of vibration, exploring its variations in response to changes in skewness and curvature. The following conclusions have been drawn:

- Time period for first mode in pile foundation increases with skew angle, decreasing first with backfill.
- Open foundation's time period decreases with skew angle, more rapidly with backfill.
- Integral bridges with backfill exhibit rapid time period decrease with curvature, slower without backfill.
- Pile foundation bridges consistently have higher time periods than open foundation counterparts.

According to IRC: SP: 114-2018, the simplified formula for calculating the time period (T) is: $T = 2.0\sqrt{\frac{D}{1000F}}$

Where:

T = Fundamental natural period (in seconds)

D = Appropriate dead load of the superstructure and live load (in kN)

F = Horizontal force (in kN) required for one mm horizontal deflection at the top of the pier/abutment for earthquake in the transverse direction, or at the top of the bearings for earthquake in the longitudinal direction.

For bridges with pile foundations, the required horizontal force F is lower compared to bridges with open foundations due to the soil stiffness of the piles playing a significant role in deflection, thus necessitating less force.

Moreover, an increase in the skew angle of a bridge with backfill results in a longer backfill length, thereby increasing resistance to deflection and consequently decreasing the time period. Similarly, an increase in curvature enhances earth resistance, leading to a decrease in the time period. Consequently, bridges with backfill have shorter time periods compared to those without backfill due to increased resistance.

5.1.2 Base reaction

The study reveals significant variations in base reaction concerning changes in skew and curvature. As the skew angle increases, the dead load of the structure rises, consequently increasing the total base reaction. To discern the true impact of skewness, the variation of base shear/vertical reaction is compared, providing a clearer understanding of how skew and curvature affect the structure.

For longitudinal seismic case following observations can be made.

- Longitudinal base shear/vertical reaction increases with skew for pile foundation bridges, decreases initially for open foundation bridges with backfill before rising.
- Transverse base shear/vertical reaction rises then falls with skew, notably higher for bridges with backfill.
- Pile foundation bridges with backfill have higher longitudinal reactions.
- Longitudinal reaction increases slightly with curvature for bridges with backfill, remains constant without.
- Open foundation bridges generally exhibit higher longitudinal reactions.
- Transverse base shear is zero for bridges with no skew and all curvatures.

For transverse seismic case following observations can be made.

- Longitudinal base shear/vertical reaction initially rises with skew, higher for bridges with backfill and pile foundations.
- Transverse base shear/vertical reaction decreases with skew for bridges with backfill, increases without, higher for bridges with open foundations.
- Longitudinal base shear is nil for without skew bridges of all curvatures.
- Transverse/vertical reaction increases with curvature for pile foundations with backfill, decreases for open foundation configurations.

The effective seismic coefficient, A_h , derived from IRC: SP: 114-2018, is determined by the formula:

$$A_h = \frac{Z Sa}{\frac{2}{R} \frac{g}{I}}$$

Where:

Z = Zone factor

I = Importance factor

R = Response reduction factor

These factors remain consistent across all bridges. (S_a/g) is dependent on the time period, as per IRC: SP: 114-2018, illustrated in Fig. 23.

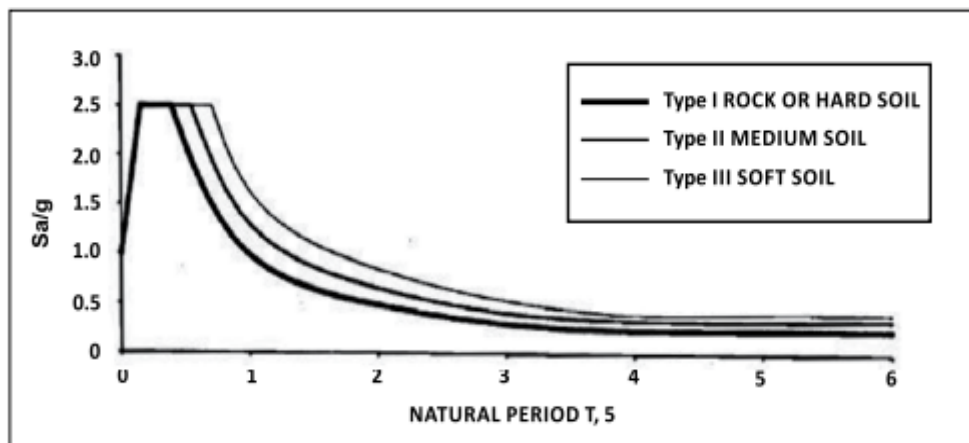


Fig. 23. Natural time period vs s_a/g

With increasing skew angle, the time period increases, resulting in a decrease in the ratio. Moreover, an increase in skew angle leads to a decrease in longitudinal force and an increase in transverse force. Consequently, in the longitudinal seismic case, the reaction in the longitudinal direction decreases while that in the transverse direction increases, and vice versa for the transverse seismic case.

Due to the shorter time period of open foundations compared to pile foundations, the ratio is higher for open foundations. Additionally, directional effects are absent for bridges with curvature, resulting in zero transverse reaction for longitudinal seismic cases and zero longitudinal reaction for transverse seismic cases.

5.1.3 Moment and torsion of abutment wall

During this study it is found that the moment and torsion of side wall varies with the variation of skew and curvature. The following conclusions can be made: -

Observations for Longitudinal Seismic Case-

- Longitudinal moment at the top of the abutment:
 - Decreases with increasing skew angle, higher for bridges without backfill, and for pile foundation structures.
 - Increases with curvature, particularly pronounced for bridges without backfill and open foundation structures.
- Transverse moment at the top of the abutment:
 - Increases with skew angle, especially for bridges without backfill, and higher for pile foundation structures.
 - Increases with curvature, with higher moments for bridges without backfill.
- Torsion at the top of the abutment:
 - Varied response with skew angle, increasing then decreasing for pile foundation configurations, consistently increasing for open foundation configurations.
 - Increases with curvature, notably for bridges with backfill.

Regarding the observations for the bottom of the abutment:

- Longitudinal moment:
 - Decreases with skew angle, more pronounced for bridges without backfill.
 - Increases with curvature for pile foundation structures.
- Transverse moment:
 - Increases with skew angle for bridges without backfill, variable for bridges with pile foundation and backfill.
 - Increases with curvature.
- Torsion:
 - Response varies with skew angle, generally increasing for bridges with open foundations and decreasing for those with pile foundations and backfill.
 - Increases with curvature, especially for bridges with pile foundations.

From the above observation the following conclusion may be drawn:-

The analysis of the longitudinal seismic case reveals distinct trends in the behavior of structural elements. Longitudinal moments at the top of the abutment decrease with increasing skew angle and increase with curvature, particularly notable in configurations without backfill and for pile foundation structures. Transverse moments follow a similar pattern, with increases observed with both skew angle and curvature, especially pronounced in bridges without backfill. Torsion at the top of the abutment exhibits varied responses to skew angle and consistently increases with curvature, particularly evident in configurations with backfill. At the bottom of the abutment, longitudinal moments decrease with skew angle and increase with curvature, while transverse moments generally increase with both skew angle and curvature. Torsion at the bottom of the abutment shows a diverse response to skew angle but increases uniformly with curvature, notably for bridges with pile foundations. These

observations underscore the importance of considering skew angle, curvature, and foundation type in the seismic design of bridge structures.

Observations for Transverse Seismic Case-

- Longitudinal moment at the top of the abutment:
 - Varied response with skew angle, initially increasing then decreasing, higher for bridges without backfill.
 - Increases with curvature for both open and pile foundation configurations.
- Transverse moment at the top of the abutment:
 - Increases with skew angle for both open and pile foundation configurations.
 - Decreases with curvature, except for pile foundation without backfill.
- Torsion at the top of the abutment:
 - Response varies with skew angle, initially increasing then decreasing for pile foundation with backfill, otherwise increasing.
 - Decreases with curvature for both open and pile foundations, except for pile foundations without backfill.

Regarding the observations for the bottom of the abutment:

- Longitudinal moment:
 - Varied response with skew angle, initially increasing then decreasing for pile foundations, while increasing for open foundation configurations.
 - Increases with curvature for both open and pile foundation configurations, particularly for bridges with backfill and pile foundation.
- Transverse moment:
 - Increases with skew angle.
 - Decreases with curvature.
- Torsion:
 - Increases with skew angle.
 - Decreases with curvature.

From the above observation the following conclusion may be drawn:-

The analysis of the transverse seismic case highlights notable trends in structural behavior. Longitudinal moments at the top of the abutment exhibit a complex response to skew angle, initially increasing then decreasing, with higher magnitudes for bridges without backfill. Additionally, they consistently increase with curvature for both open and pile foundation configurations. Transverse moments at the top of the abutment increase with skew angle but decrease with curvature, except for pile foundations without backfill. Torsion at the top of the abutment shows varied responses to skew angle, with a decrease in magnitude with curvature observed for both open and pile foundations, except for pile foundations without backfill. At the bottom of the abutment, longitudinal moments vary with skew angle, increasing then decreasing for pile foundations and increasing for open foundation configurations, while increasing with curvature for both types, notably for bridges with backfill and pile foundation. Transverse moments increase with skew angle and decrease with curvature, and torsion increases with skew angle but decreases with curvature. These findings underscore the importance of considering skew angle, curvature, and foundation characteristics in designing resilient bridge structures under transverse seismic loading.

5.1.4 Moment and torsion of bent columns

Observations for Longitudinal Seismic Case-

- Longitudinal moment at the top of the bent columns:
 - Decreases with skew angle for both open and pile foundation configurations, except for pile foundation with backfill.
 - Higher for bridges without backfill compared to those with backfill.

- Longitudinal moment remains almost the same with changing curvature for bridges without backfill, consistently higher than those with backfill.
- Transverse moment at the top of the bent columns:
 - Initially increases and then decreases with skew angle for open foundation configurations without backfill; otherwise, consistently increases.
 - Increases with changing curvature, higher for bridges without backfill.
- Torsion at the top of the bent columns:
 - Initially increases and then decreases with skew angle for both open and pile foundation configurations.
 - Increases with curvature, higher for bridges with and without backfill, and for bridges with pile foundations compared to those with open foundations.

Regarding the observations for the bottom of the bent columns:

- Longitudinal moment:
 - Increases with skew angle for both open and pile foundations, higher for bridges with pile foundations.
 - Initially increases then decreases with curvature for both open foundation and for pile foundation with backfill.
- Transverse moment:
 - Increases with skew angle.
 - Increases with curvature.
- Torsion:
 - Increases with skew angle for bridges without backfill.
 - Increases with curvature.

From the above observation the following conclusion may be drawn:-

The analysis of the longitudinal seismic case reveals significant trends in the behavior of bent columns. Longitudinal moments at the top of the columns decrease with skew angle, with exceptions noted for pile foundation configurations with backfill. Additionally, these moments are generally higher for bridges without backfill and remain relatively constant with changing curvature, consistently higher for configurations without backfill. Transverse moments exhibit varied responses to skew angle but consistently increase with curvature, particularly pronounced in bridges without backfill. Torsion at the top of the columns initially increases then decreases with skew angle, while increasing uniformly with curvature, notably for bridges with and without backfill, and for bridges with pile foundations compared to those with open foundations. At the bottom of the columns, longitudinal moments increase with skew angle, initially increase then decrease with curvature, and transverse moments increase with both skew angle and curvature. Torsion increases with skew angle for bridges without backfill and uniformly with curvature. These findings emphasize the importance of considering skew angle, curvature, and backfill conditions in designing resilient bent columns under longitudinal seismic loading.

Observations for Transverse Seismic Case-

- Longitudinal moment at the top of the bent columns:
 - Initially increases and then decreases with skew angle for both open and pile foundation configurations, higher for bridges without backfill.
 - Increases with curvature.
- Transverse moment at the top of the bent columns:
 - Initially increases then decreases with skew angle for pile foundation with backfill, otherwise decreases.
 - Decreases with an increase in curvature for both open and pile foundation configurations with backfill.
- Torsion at the top of the bent columns:
 - Initially increases then decreases with an increase in skew angle.

- Increases with an increase in curvature.

Regarding observations for the bottom of the bent columns:

- Longitudinal moment:
 - Increases with an increase in skew angle for both open and pile foundations.
 - Increases and then decreases with an increase in curvature for pile foundation, otherwise increases.
- Transverse moment:
 - Initially increases and then decreases with an increase in skew angle only for pile foundation with backfill, otherwise decreases.
 - Initially increases and then decreases with an increase in curvature only for pile foundation without backfill, otherwise decreases.
- Torsion:
 - Initially increases then decreases with an increase in skew angle, increases for bridges with all curvatures.

From the above observation the following conclusion may be drawn:-

The analysis of the transverse seismic case highlights distinct patterns in the behavior of bent columns. Longitudinal moments at the top of the columns initially increase and then decrease with skew angle, exhibiting higher magnitudes for bridges without backfill and increasing uniformly with curvature. Transverse moments at the top of the columns show varied responses to skew angle, with decreases observed for pile foundations with backfill and uniform decreases with curvature for both open and pile foundation configurations with backfill. Torsion at the top of the columns initially increases then decreases with skew angle and uniformly increases with curvature. At the bottom of the columns, longitudinal moments increase with skew angle and exhibit varied responses to curvature, while transverse moments initially increase then decrease with skew angle or curvature depending on the presence of backfill. Torsion initially increases then decreases with skew angle and uniformly increases with curvature. These findings underscore the importance of considering skew angle, curvature, and backfill conditions in designing resilient bent columns under transverse seismic loading.

5.2 Future scope of study

The critical discussion of the literature review in Chapter 2 underscores several areas requiring further investigation in integral bridge research. While the present thesis has focused on key responses such as time period, base reaction, bending moment, and torsion for skewed-curved integral slab bridges, numerous aspects remain unexplored. Future studies could encompass parametric analyses for different spans to enhance response coefficient accuracy, as well as explore integral bridges with alternative superstructures like T beams or composite girders to assess variations in moment, shear, and torsion. Additionally, investigations into the impact of earth behind abutments with varying abutment heights could provide valuable insights. Dynamic analyses, particularly focusing on the effect of response reduction due to integral action and backfill presence, represent crucial areas for exploration. Furthermore, studying these phenomena across different substructure types would contribute significantly to advancing understanding and design practices in integral bridge engineering.

References

1. Akib S, Moatasem Fayyadh M, Othman I, "Structural Behaviour of a Skewed Integral Bridge affected by Different Parameters", *The Baltic Journal of Road and Bridge Engineering* 2011, 6(2): 107–114.
2. Bardakis V J, Fardis M N, "Nonlinear Dynamic V Elastic Analysis for Seismic Deformation Demands in Concrete Bridges Having Deck Integral with The Piers", *Bull Earthquake Eng.* (2011) 9:519–535.
3. Bloodworth A G, Xu M, Banks J R, Clayton C R I, "Predicting the Earth Pressure on Integral Bridge Abutments", *15 Journal of Bridge Engineering, ASCE*, 2012.
4. Choi B H, Moreno L B, Lim C S, Nguyen D D, Lee T H, "Seismic Performance Evaluation of a Fully Integral Concrete Bridge with End-restraining Abutments", *Hindawi, Advances in Civil Engineering Volume 2019, Article ID 6873096.*
5. Civjan S, Lacroix J, Takeuchi A, Higgins K, "Curved Steel Girder Integral Abutment Bridges in Vermont, USA", *Civil Engineering Practice, Boston Society of Civil Engineers Section / ASCE ISSN: 0886-9685.*
6. Deng Y, Phares B M, Greimann L, Shryack G L, Hoffman J J, "Behavior of Curved and Skewed Bridges with Integral Abutments", *Journal of Constructional Steel Research* 109 (2015) 115–136,
7. Dicleli M, Erhan S, "Analysis of Effect of Modelling Simplifications on Nonlinear Seismic Analysis of Integral Bridges Including Dynamic Soil-Structure Interaction", *34th International Symposium on Bridge and Structural Engineering, Venice, 2010,*
8. Erhan S, Dicleli M, "Comparative assessment of the seismic performance of integral and conventional bridges with respect to the differences at the abutments", *Bull Earthquake Eng.* (2015) 13:653–677.
9. Far N E, Maleki S, Barghian M, "Design of integral abutment bridges for combined thermal and seismic loads", *The 2015 world congress on Advanced on Structural Engineering and Mechanics (ASEM15), Incheon Korea, August 25-29 2015,*
10. Faraji S, Ting J M, Crovo D S, and Ernst H, "Nonlinear Analysis of Integral Bridges: Finite-Element Model", *J. Geotech. Geoenviron. Eng.* 2001.127:454-461.
11. Fartaria C, "Soil-Structure Interaction in Integral Abutment Bridges", *Instituto Superior Técnico, Av. Rovisco Pais, 1,1049-001 Lisbon, Portugal.*
12. Greimann, L F, Wolde-Tinsae, A M, Yang P S, "Skewed Bridges with Integral Abutments", *62nd Annual Meeting of the Transportation Research Board, Washington District of Columbia, United States.*
13. Haymanmyintmaung, Kyawlinhtat, "Effect of Integral Bridge with Span Variation Under Dynamic Loading", *International Journal of Recent Advances in Engineering and Technology (IJRAET), ISSN (Online): 2347 - 2812, Volume-5, Issue-6, Aug.-2017.*
14. Haymanmyintmaung, Kyawlinhtat, "Investigation of Integral Bridge effect under dynamic loading", *International Journal of Advances in Mechanical and Civil Engineering, ISSN: 2250-3153, Volume-7, Issue-5, Aug.-2017*
15. Haymanmyintmaung, Kyawlinhtat, "Performance of skew integral bridge under dynamic loading", *International Journal of Advances in Mechanical and Civil Engineering, ISSN: 2394-2827, Volume-4, Issue-4, Aug.-2017.*
16. Ibrahim M K, Rahman A A, Ahmad B H, Abas F Z M, "Theoretical Modal Characteristics of Integral Abutment Bridge with Bored Piles Foundation:", *IOP Conf. Series: Materials Science and Engineering* 620 (2019) 012068J.
17. IndianHighways (2019). "Indian highways, october, 2019." S.K. Nirmal, Secretary General, IRC,270,IRC Bhawan, Kama Koti Marg, Sector-6, R.K. Puram, New Delhi-110 022.
18. Integral Bridge Function in Midas Civil at <https://www.midasbridge.com/en/blog/>
19. IRC:SP: 114: 2018: Guidelines for Seismic Design of Road Bridges.
20. IRC:SP: 115: 2018: Guidelines for Design of Integral Bridges.
21. Jayeshbhai D M, Sanghvi C S, "Review on Behavior of Curved Integral Bridges", *2020 JETIR July 2020, Volume 7, Issue 7.*
22. Joshi A, Patel R, "A Review on Analysis and Design of Integral Bridges for Different Type of Span using Finite Element.", *ISSN (Online): 2348-4098.*
23. Kalayci E, Breña S F, Civjan S A, "Curved Integral Abutment Bridges – Thermal Response Prediction through Finite Element Analysis", *Structures* 2009, *ASCE* 191 2015, 72-191.
24. Kalayci E, Civjan S A, Breña S F, "Parametric study on the thermal response of curved integral abutment bridges", *Engineering Structures* 43 (2012) 129–138.
25. Kataria N P, Jangid R S, "Seismic performance and effect of curved geometry on isolation system in horizontally curved", *The 2013 World Congress on Advances in Structural Engineering and Mechanics*

- (ASEM13), Jeju, Korea, September 8-12, 2013.
26. Kaviani P, Zareian F, Taciroglu E, Sarraf M, "Simplified Method for Seismic Performance Assessment of Skewed Bridges", COMPDYN 2011, 3rd ECCOMAS Thematic Conference on Computational Methods in Structural Dynamics and Earthquake Engineering, Greece, 25–28 May 2011.
 27. Kozak D L, LaFave J M, Fahnestoc L A, "Seismic modeling of integral abutment bridges in Illinois", *Engineering Structures* 165 (2018) 170-183.
 28. Mahjoubi, S, Maleki S, "Finite element modelling and seismic behaviour of integral abutment bridges considering soil– structure interaction", *European Journal of Environmental and Civil Engineering* 24, no. 6 (2020): 767-786.
 29. Malekjafarian A, Prendergast L J, O'Brien E J, "Use of mode shape ratios for pier scour monitoring in two-span integral bridges under changing environmental conditions.", *Canadian Journal of Civil Engineering* 47, no. 8 (2020): 962973.
 30. Mallick M, Raychowdhury P, "Seismic Analysis of Highway Skew Bridges with Nonlinear Soil–Pile Interaction", *Transportation Geotechnics* 3 (2015) 36–47.
 31. Masrilayanti M, "The Behaviour of Integral Bridges under Vertical and Horizontal Earthquake Ground Motion", School of Science, Computing and Engineering University of Salford, United Kingdom.
 32. Midas Civil user manual http://manual.midasuser.com/EN_Common/Civil/910/index.htm
 33. Mohtashami E, Shooshtari A, "Seismic Assessment of Integral Reinforced Concrete Bridges using adaptive Multi-Modal Pushover Analysis", 15 WCEE, LISBOA 2012.
 34. Muhammad A, Abdullah R, Hassan I O, "Long-Term Response Prediction of Skewed Integral Bridges under Creep Effects", *International Journal of Scientific Engineering and Technology*, Volume No.4 Issue No.1, pp : 20-23.
 35. Naji M, Firoozi A A, Firoozi A A, "A Review: Study of Integral Abutment Bridge with Consideration of Soil-Structure Interaction.", *Latin American Journal of Solids and Structures*, 2020, 17(2), e252.
 36. Oladele.O P, John W, "The Long Term Performance Of Skew Integral Bridges", *Journal of Multidisciplinary Engineering Science and Technology (JMEST)* ISSN: 3159-0040 Vol. 2 Issue 8, August – 2015.
 37. Panikkavettil K R, Raveendran K G, "Seismic Analysis of Integral Bridges Research", *International Journal of Scientific and Engineering Research* Volume 8, Issue 11, November-2017, ISSN 2229-5518.
 38. Parachos A, Made A, "Predrilled Holes for Pile Support of Skewed Integral Abutment Bridges", *Civil Engineering Practice*, ISSN: 0886-9685, Boston Society of Civil Engineers Section / ASCE.
 39. Peric´ D, Miletic´ M, Shah B R, Esmaeily A, Wang H, "Thermally induced soil structure interaction in the existing integral bridge", *Engineering Structures* 106 (2016) 484–494.
 40. Phares B M, "Field Monitoring of Curved Girder Bridges with Integral Abutments", Bridge Engineering Center, Iowa State University.
 41. Shilpa S, Thejashwini P T, Shruthi N P, "Seismic Analysis of Integral Bridges", *International Research Journal of Engineering and Technology (IRJET)*.
 42. Shreedhar R, Hosur V, "Soil-Pile Interaction for Integral Abutment Bridges", National Conference, NET-2011.
 43. Wood J H, "Earthquake Design of Bridges with Integral Abutments", 6th International Conference on Earthquake Geotechnical Engineering 1-4 November 2015 Christchurch, New Zealand.
 44. Wright B, LaFave J, Fahnestock L, Jarrett M, Riddle J, Svatora J S, "Field Monitoring of Skewed Integral Abutment Bridges", 6th International Conference on Advances in Experimental Structural Engineering, August 1-2, 2015, University of Illinois, Urbana-Champaign, United States.
 45. Zhao Q, Dong S, Wang Q, "Seismic Response of Skewed Integral Abutment Bridges under Near-Fault Ground Motions, Including Soil–Structure Interaction", *MDPI Applied science journal*.
 46. Zordan T, Briseghella B, Lan C, "Parametric and Pushover Analyses on Integral Abutment Bridge", *Engineering Structures* 33 (2011) 502–5151.